UNIVERSITAT POLITÈCNICA DE CATALUNYA
BARCELONATECH
Escola Superior d'Enginyeries Industrial, Aeroespacial i Audiovisual de Terrassa

Lightning Research Group

Design of a launch system for a scientific fix wing UAV without undercarriage

Document:

Report

Author:

Aleix Surroca Garcia

Director /Co-director:

Joan Montaña Puig / Montserrat Sánchez Romero

Degree:

Electrical + Mechanical engineering degree

Convocatory:

Spring

FINAL DEGREE PROJECT

Abstract

The general objective of this project is to design a vehicle ('dolly' type) for take-off of scientific fix wing UAV without undercarriage.

The Dolly has to ensure the integrity and stability of both, dolly and aircraft, during rolling-take-off while maintaining a fix heading. It will include a steering system to correct deviations, a propulsion system to provide additional acceleration during the take-off and breaking components to prevent possible accidents.

This work, in addition to showing the entire design and construction process as well as the analysis of alternatives and decision making, also aims to create a detailed final product with all the necessary drawings and references to easily reproduce the dolly as it's described.

The specific objectives are the following ones: study and definition of the mechanical specifications of the dolly (e.g. dimensions, weight, materials, wheelbase, track, center of gravity, wheels, operational lifetime, etc...) by using tools like Matlab/Simulink and Algodoo to simulate some physical phenomes and different situations in order to optimize the final model. The design and calculation of the mechanical structure and steering system of the dolly with SolidWorks, and the design of the propulsion and breaking system. Then, the production of the model, which parts will be majority printed with 3D materials, assembly and validation, in order to ensure the integrity of all components and a viable method of fabrication to be reproduced identically. We will use a programmable microcontroller called Arduino combined with different sensors, actuators and batteries to determinate the instantaneous direction relative to the North in degrees at every time, the determination of need and the type of the propulsion to provide the optimal push during take-off. And the description and specification of the breaking system to avoid crashes and accidents before and after of the take-off.

The final result of the project will consist on the one hand of all the documentation, studies and previous calculations, to carry out the 3D modeling and selection of the different components that make up the dolly, as well as the programming code to end up building a prototype that satisfies all the initial requirements.

Finally, the conclusions will explain the final results as well as notable data, the technical and economic feasibility of the project and possible problems that have arisen during the process.

Index

Tables Index

1. Introduction

1.1 Object

The final result that this work is intended to achieve consists of the creation of a technically and economically optimized Dolly type vehicle, to be able to take off a specific type of fixed-wing UAV without landing gear, used for scientific experiments in the *Lighting Research* Group of ESEIAAT School.

Thus, the main objective of the work could be summarized with the intention of creating a platform that in its latest model is autonomous in its operation, stable during acceleration and on take-off and capable of self-regulating the steering system to follow a fixed course, provide additional acceleration and stop when the plane is already flying. In addition to having a reproducible manufacturing system so that anyone with the necessary resources has the capacity, only with the text documents, plans and format files that are presented in this work, to reproduce the final model and assemble it to achieve a Dolly exactly as shown in the presentation of the work.

To achieve the main objectives mentioned, shorter-term secondary objectives appear, which together will ensure the integrity of the system.

1.2 Scope

The scope of the project includes:

- Review of existing models in order to examine their operation and acquire ideas for the first sketches.
- Exact definition of the UAV model for which the dolly will be destined.
- Studies of the different types of existing chassis and the feasibility of applying them in the design of the Dolly. General designs focused on the type of structure (chassis). The implementation of different types of materials for the construction of the model, as well as different manufacturing methods, will also be valued.
- Realization of the first detailed sketches, calculations and numerical simulations taking into account physical phenomena such as gravity, aerodynamic and friction coefficients, as well as the characteristics of the propulsion and steering systems.
- Definition of the parts and selection of components that will constitute the Dolly.
- Chassis modeling in SolidWorks.
- Study and simulation of structural loads applied to the previously designed model. Evaluation of results.
- Study, calculations and design of the steering system.
- Design of the rest of the components and selection of the standardized elements such as screws and bearings.
- Final assembly of all components in SolidWorks.
- Obtaining the detailed plans of all the non-standard elements, as well as the technical documents and format files necessary for the reproduction of the project.
- Manufacturing and validation process.
- Definition of the functions to be performed by the Dolly, choice and justification of the control system used and the components that will intervene in the process.
- Programming of the control system.
- Design of the electronic circuit.
- Validation of the control system.
- Assembly of the control system with the physical model and field tests for its validation.
- Modifications

1.3 Requirements

Dolly's final model must ensure the correct take-off of the plane. For this, it is necessary for it to be able to maintain its stability following a set course and correcting possible deviations that may occur, whether caused by wind, inclination on the take-off runway or any other factor. The steering system will be made using an Arduino, which as the company explain: "*is an open-source electronics platform based on easy-to-use hardware and software. Arduino boards are able to read inputs - light on a sensor, a finger on a button, or a Twitter message - and turn it into an output - activating a motor, turning on an LED, publishing something online. You can tell your board what to do by sending a set of instructions to the microcontroller on the board. To do so you use the Arduino programming language (based on Wiring), and the Arduino Software (IDE), based on Processing.*" - (*Arduino - Introduction*, n.d.). So we will program the Arduino microcontroller according with the selected elements in order to design steering system.

Another of the project's requirements consists of the contribution of acceleration through an additional propulsion system to reach the speed necessary to take off the plane from the ground as soon as possible. The type of additional propulsion used will be decided according to the appropriate criteria.

As mentioned, another of the main requirements is that the entire design, processing and programming process be documented and carried out in order to be easily reproduced by anyone on the planet who has the necessary resources. To ensure that, we will use the 3D SolidWorks design program in order to design all the components of the dolly considering the material and also to realize the assembly of the elements. Then, it will also be used to verify the integrity of the structure by performing a structural calculation by the finite element method. Finally, the SolidWorks program will be used to obtain the 2D drawings of all the parts and the materials list.

During the design and construction process of the project, the environmental aspect will also be considered, so that, in the selection of materials, manufacturing methods and other aspects that intervene in the project, the impact of the same on the environment.

As the final product is intended for use in a specific type of aircraft, which is the one used in scientific experiments, it is essential that the final dolly model is adapted to that particular aircraft. Regarding the operating mode of the Dolly and the type of communication with the user in order to manage the dolly, the use of the Dolly must be possible while operating the remote control of the aircraft, assuming that the user will have their hands full during take-off. Therefore, the Dolly functions must be able to perform an automatic way.

1.4 Justification

In recent decades, the drone market has exploded, largely due to advances in technology in terms of wireless communications, image quality and stability, batteries, and general electronics. These reasons have promoted its application, use and commercialization for very different areas.

Unfortunately, as shown in figure 1, its most widespread use continues to be in the military field, although it is increasingly used in other fields, to the point that today they have been able to replace humans in many tasks such as taking aerial images, where in addition to the cameraman they have also replaced the pilot and the helicopter, greatly reducing

expenses. Drones are also beginning to be used in many countries for fighting fires, as well as for laying power lines or simply for a recreational use.

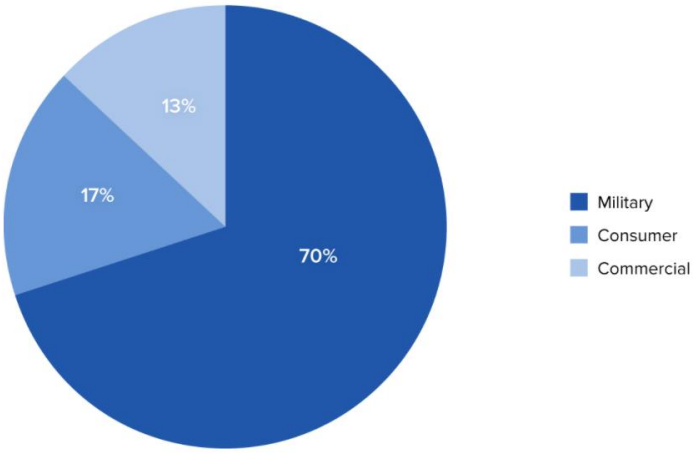

Figure 1. Drone market by sector. (Source: Goldman Sachs, Francesco Castellano. 2018 | Top Total)

Another of the most common uses that drones currently have are research and development tasks in the scientific field. In the particular case of this work, the drone that is intended to take off is intended for the investigation of an active load control system of a UAV, which is a replica of a real model. This active load control system is intended to match the potential of the aircraft with that of the environment in order to protect the aircraft from possible electrical discharges caused by lightning. Thus, it is intended to demonstrate the usefulness of this technology to later apply it to other types of aircraft.

The UAV used to carry out these tests is the Maja model from the German brand Bormatec (*Figure 2*).

Figure 2. Used UAV model Bormatec Maja (Source: *Bormatec* | *Ravensburg* | *Drohnen*, n.d.)

This particular model, like many other fixed-wing UAVs, does not have a landing gear, which makes the take-off maneuver complicated and even dangerous. For landing the problem is less since any plain surface with a minimum length so that the plane can glide and descend on it will be enough because the body of the plane is made mostly of expanded polypropylene that will avoid damage to it if the landing is not too abrubt.

On take-off, the operation is complicated since if no additional system is available, the user is forced to have to take off the plane by launching it with the hand while activating the engines with the remote control. Due to the large propeller and the great power of the brushless motor that the aircraft incorporates, makes this maneuver very dangerous for the user, as the propeller passes very close to their hand during launch. There are two popularized solutions to solve this problem, the first consists of taking off the UAV by using a shuttle like a slingshot that launches the plane with force into the air. The other method consists of the use of a carriage or rolling platform called a "dolly" that acts as the landing gear of the plane, providing it with a base with wheels in order to achieve the necessary speed for take-off. When the plane reaches this speed and takes flight, the dolly remains on the ground so that it can be used for the same purpose on future occasions.

Although the shuttle option seems that could be equally valid for the final objective of aircraft take-off, this type of device has been previously studied and built without success by the Lighting Research Group. The main problems encountered and why this other method of launching the aircraft was discarded are the following:

- Due to the high weight of the aircraft compared to other UAV models that do use this method for take-off, the catapult needed for the operation was too large and heavy to be practical and easy to transport and use.
- Also due to the heavy weight of the aircraft, the catapult had to exert a lot of force to provide the necessary acceleration for take-off, making it dangerous for people nearby at the time of take-off.

For this reason, the LRG rejected the catapult project. This project is based on the creation of the moving platform system and, therefore, will not focus on comparisons with the other system mentioned, since it was already rejected at the time.

2 Precedents

2.1 State of the art

It is well known, at the level of general culture, that all fixed-wing aircraft, except those that have a vertical take-off system, need a certain length of runway to achieve the necessary speed to take off. Thus, the plane will travel these meters of runway from when it is positioned to start the maneuver until it begins its flight, supported by the wheels. In the case of airplanes, these wheels do not provide tractive effort but only act as a point of contact or sliding with the ground. The objective of allowing the aircraft to glide by rolling in contact with the tarmac during take-off or to maneuver on the ground, is only the first of the different functions that the landing gear fulfills. Another of its main objectives is to brake the plane at the moment of landing. As the plane and the ground act as the only point of contact, the landing gear and especially the tires are heavily overloaded. Another of the main functions of the landing gears, perhaps not so well known, is the damping of the system at the moment in which the plane makes contact with the ground. If this system were not available, especially in large and heavy aircraft destined for commercial flights, the landing could lead to the loss of stability or even the breakage of some of the parts of the plane, leading to a tragic end.

There are 2 main types of landing gears, the fixed ones, which are those that do not have mobility and, as their name indicates, remain fixed at all times. This type of landing gear is used mainly in small, light airplanes that reach relatively low speeds, where the increase in

weight due to the installation of a retractable system would mean the loss of stability of the plane or even complications in takeoff. On the other hand, the retractable landing gear, more complex than the previous one and intended for larger, heavier or faster aircraft, consists of a system by which the landing gear engages with the aircraft, thus achieving a uniform surface in the airplanes. limits of the plane. The main objective of this type of landing gear is to improve the aerodynamics of the aircraft, reducing friction with the air and consequently increasing its stability. Another function of this type of system is to protect the landing gear from possible impacts with birds or other objects, since it is one of the most important safety elements of the aircraft and on which the safety of the aircraft's crew potentially depends. .

As for fixed-wing UAVs marketed in the current market, most are developed as replicas of real scale models. And although the latter, as has been seen, have the vast majority of landing gear, this is not such an essential element in the creation of unmanned aircraft since the safety of the crew is no longer a trivial issue in design. of the airplane. It is for this reason, coupled with the fact of lowering costs, that many manufacturers omit this element in the design of their unmanned aircraft. Consequently, due in large part to the fact that many of the models marketed within the UAV market do not have landing gear, not a few people have dedicated themselves to developing solutions for this problem. In some cases, these solutions have been achieved by following standardized design, construction, validation and marketing procedures by commercial companies, professionals to a greater or lesser extent. In other cases, however, these solutions have been achieved following non-standardized procedures rather in a domestic environment and for a private use.

2.2 Revision of existing models

Considering the general objective of the work to achieve a system to take off a UAV based on a rolling platform, the first efforts have focused on making a review of existing models (commercialized or prototypes) that perform a basic function equal to or very similar to the one used in this work. This will allow to acquire the initial ideas necessary to make the first design sketches of the dolly. In addition, it will also allow the dimensioning of the project and prevent possible failures and improvements in the final design.

2.2.1 Commercial dolly types

In this section, those existing dolly models that are patented or commercialized in the market will be considered, since regardless of their complexity and the functions they perform, they are considered as professionals because they are created by for-profit companies.

Figure 3 shows a patented dolly model that aims to perform, in general terms, the same function as the one to be achieved with this work. In this case we observe that the supporting structure is formed by a horizontal base body that joins two vertical walls that are in turn attached to the wheels. In turn, these two parallel vertical walls also serve to hold the aircraft, in this case by the wings. It is a relatively simple system since it does not offer the possibility of turning the wheels to compensate the deviation of the track or any other function that is intended to be covered in this project. From this model we can also visualize that the platform holds the plane very close to its front. As much as at first glance it may seem that

the plane could fall backwards, this is because the center of gravity of airplanes (also of scale UAVs) is located just below the wings so that the flight is stable. That is why the dolly must hold the plane at that point regardless of the overhang the tail of the plane is on.

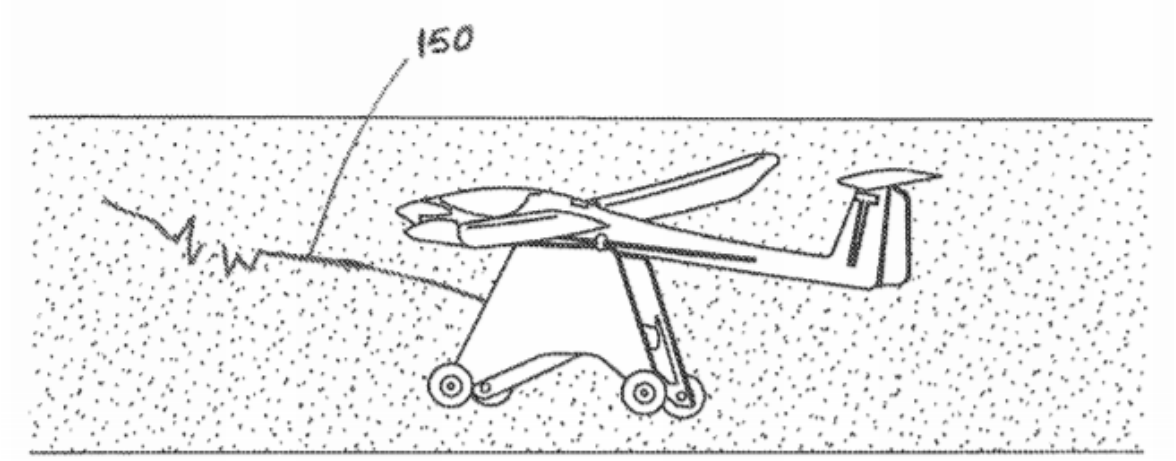

Figure 3. Current patent of dolly model. (Source: (US9708077B2 - UAV Take-off Method and Apparatus - Google Patents, n.d.)

The following model, shown in figure 4, is very similar to the previous one but incorporates some differences, especially the distance to the ground what in this case is shorter. It is a model commercialized by the company "A Lot of Hobbies". It can be purchased for $ 62.99.

As it's advertised by the seller: “the dolly is Designed for medium sport, large electric and scale sailplanes the Top Model Sailplane Take Off Dolly is a great alternative to launching from the ground. No more scarred wing tips and tails. The dolly provides better control, as it holds the aircraft straight and level during rollout.

It’s constructed from CNC routed plywood and supplied with 2 stainless steel axels and 4 six inch wheels. Adhesive backed foam is provided for the saddle area to protect the aircraft during rollout. The dolly is shipped flat pack style and requires assembly. Assembly is a simple, straight forward evening build.” - (*Top Model Sailplane Take-off Dolly 1*, n.d.).

Figure 4. Commercial dolly model 1 (Source: op Model Sailplane Take-off Dolly 1)

In figure 5, it’s possible to observe another dolly type. In this case, the structure is very similar to the others but there’s an important difference: all the body part of the dolly is made of PLA by using a 3D printer instead of wood like the other models. Despite of PLA

is not the most resistant material between the 3D printing materials, the fact of someone has built it in a 3D printer and has commercialized the final result, significate that it's possible and economically viable. This model costs 150$ and it's distributed in eBay.

Figure 5. Commercial dolly model 2 (Source: (RC Glider Sailplane Airplane Models TAKEOFF DOLLY 6" Wheels - NEW | EBay, n.d.))

2.2.2 Non-commercial dolly car types

If we refer to dolly's designed for non-commercial use, due and thanks to the internet, users of forums related to aeromodelling share their designs with others and everyone interested can see them. In the case shown in figure 6, a homemade and handmade dolly is observable, completely different from those seen so far. In this case it is a dolly with 3 trike-type wheels. It differs from the others both in its structure, much simpler and lighter, and in its wheels. It consists of 2 rear wheels much smaller than previous models and a front wheel with the ability to turn. Another important difference is the method of holding the plane, which in this case is not by the wings as in the previous ones. The plane is hold by the body until the plane takes flight. This fact in particular has been considered relevant since having obtained the information from a video, it has been possible to verify the effectiveness of the system.

Figure 6. Noncommercial dolly model.
(Source: https://www.youtube.com/watch?v=F1H-Nr)

The last existing model to review is the one manufactured by the Lightening Research Group of the ESEIAAT in order to obtain an effective way to take-off his scientific fic wing UAV. It is specifically designed and built with the same purpose as the one being worked on in this project, and it has also been designed for the same particular aircraft. We can say that it is the direct predecessor of the dolly that we are preparing, so that having been designed with the same particularities, functions and requirements, it will be the model in which we will focus the most when it comes to getting ideas. The fact that this model was built in the same school in which the work takes place, has allowed to have availability of the dolly. It should be noted that this project does not intend to improve an existing model such as the one shown in figure 7, but rather that the objective is the design, construction and validation of a new model with new and improved functionalities. The existing model before starting the work will only be considered to take ideas and test prototypes before the final design of the model under construction.

With a general view of the dolly, it is observed that it is more professional than the previous ones. It is constructed of mostly square aluminum tube, rather than the wood or PLA used in the other models. This makes it more resistant to impacts while being lightweight and durable. It also has PLA joints made on a 3D printer. Unlike the previous model seen in figure 5 (made entirely with 3D printing material), it only has a few joints made of PLA and the rest of the dolly body is made of aluminum. The next detail to comment is that it also has three wheels arranged in trike mode, with two rear wheels and a front wheel capable of turning. The most remarkable aspect with respect to the models seen above is that this model has a heading control system that aims to maintain a fixed direction to avoid deviations of the dolly-plane assembly during take-off. These deviations could be due to the slope of the runway, the wind or other factors that can affect the quality of the take-off.

During the tests carried out with the dolly created by the Lightening Research Group of the ESEIAAT, different failures were observed that made it impossible for it to carry out its main mission. The prototype lacked stability due in part to its weight distribution and three-wheel design. The wobbly of the moving parts of the model had also played an important role in the lack of stability. However, the main problem that the dolly suffered was the very abrupt movements caused by the heading control system when self-regulating to maintain a fixed direction, mainly due to the wobbly between parts of the steering system, and especially to the code used during the programming of the microcontroller. As a result of these sudden movements and his extremely sensitivity to the variation of the fixed direction, the dolly turned its front (directional) wheel excessively, causing an imbalance of the system as a whole and sometimes even accidents, which could cause damage to both the plane and on the dolly.

2.2.3 Conclusions about the existing models

After doing a general search of the main existing models, we can assure that the global market in this specific field of application is very small. In case of having a fixed wing UAV model without landing gear, the options available to buy a dolly that allows the plane to take off are very small and very similar to each other.

The market study and research task has served to acquire general and more specific ideas on the subject. It has also been possible to conclude that the existing models are mostly very simple and do not meet the requirements and objectives set out in this work. None of them have heading control except the one created in the school, and even this, did not work correctly. On the other hand, neither has an additional propulsion system. Furthermore, all

the structures seen so far are very simple and unstable. They will hardly allow a correct takeoff of the plane. Therefore, at this point, it can be said that the project covers a technological field very little worked on a commercial scale. After analyzing the different types of existing dolly designs that can be found online, it's easy to observe that most of them are built in a very similar way, with a ladder frame chassis which support to parallel walls that are destined to support the plane. It is probably the simplest and cheapest way to plan the design of a dolly for taking off a plane, and also a good way to produce and reproduce it for example by a 2D drawing document that can be easily shared and used to cut a PC or PMMA plate by laser or other method.

Despite the attributes mentioned, these models has a common problem, which is the low stability and heavy weight they have. In order to solve these problems and achieve a completely effective dolly, it has been decided to create a new model that offers greater stability, rigidity, lightness, acceleration, efficiency and, above all, easy to reproduce. The project design will be inspired in a real car chassis type and not a simply toy.

The main ideas acquired are the following:

- A tubular chassis like the one in the model in figure 7, whether made of aluminum or another material, provides rigidity and stability to the system while maintaining lightness.
- The dollies built with three wheels (trike-type) are not viable due to the lack of stability of the structure, but above all due to the sensitivity of the steering system.
- 3D printed parts are a good option to make the joints if they are not welded or screwed.
- A lower center of mass benefits the stability during the take-off acceleration.

3 General features

In order to achieve a satisfactory result, complying with the established objectives and requirements, it becomes a vital necessity to follow an established order during the development process. To do this, the chapters of this block will be structured in the same order as that followed during the design, manufacturing, assembly and validation process.

The first step, seen in the previous block, was to make a study of the existing models to help acquire the first ideas, which will be after developed. Said market study has made it possible to make a first analysis of benefits on the different forms, materials and systems used in the models seen. Although the study carried out on the existing models has led to the acquisition of general ideas about the design and construction of the model to be created, it is necessary to know the exact characteristics of the fix wing UAV to use to ensure physical and mechanical compatibility between both.

3.1 UAV definition

To ensure physical and functional compatibility between the dolly and the UAV, it's important to design the dolly considering the UAV already selected. For this reason, the different characteristics of the aircraft will be studied. This procedure is essential to size the dolly.

3.1.1 Definition of the compatibility criterial between the dolly and the UAV

The first objective to achieve an effective study will be to define which are the characteristics of the aircraft in particular in which we will have to focus more when designing the dolly, since these will be the ones that most affect compliance with the requirements and compatibility between both.

The aspects to take into account in the compatibility criterial definition between both are:

- The overall dimensions of the plane will be relevant because the dolly cannot be much bigger since it would cease to be practical to transport it, and it cannot be too small since that would lead to a lack of stability of the plane on the dolly at the time of the acceleration.

- Another important feature to take into account will be the weight of the plane as a whole, with the batteries included, as it will be the weight that the dolly will have to accelerate in addition to its own. This data will contribute to the definition of the weight of the dolly and the power that the propulsion system must provide.

- The speed necessary for the UAV to take off will be considered in reduced wind conditions, since as we see in figures 7 and 8 it can increase if the wind comes from the tail or decrease if the wind comes from the head. This is because the plane will experiment a high pressure under the wings with the wind coming from the head than if it's coming from the tail, for the same velocity. The speed necessary to take off the plane will be vital to dimension the weight-to-power ratio of the dolly, and the required stability as a whole. In addition to the sensitivity of the steering system since the more speed the more unstable it becomes.

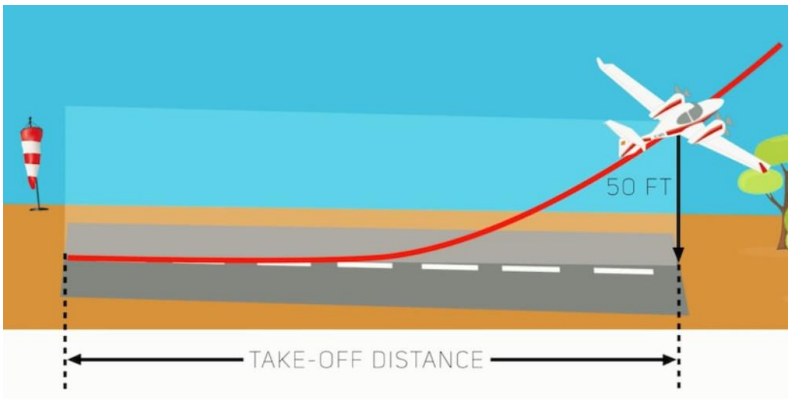

Figure 7. Take of distance without wind. *(Source :* One Air Company, n.d.)

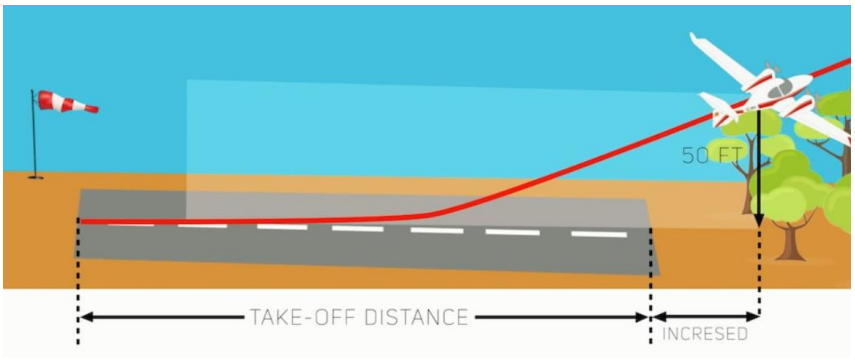

Figure 8. Take of distance with wind coming from the tail. (Source: One Air Company, n.d.*))*

- Another fundamental aspect to take into account will be the physical shape of the UAV because it has to be able to adapt a fastening system that fixes the UAV on the dolly during acceleration.

3.1.2 Main characteristics of the UAV

The first resource available for acquiring technical data regarding the aircraft is its technical data sheet. By consulting the manufacturer's website (https://www.bormatec.com/), the summarized information is obtained with the relevant data shown in table 1.

The table below shows general aircraft characteristics such as overall length, wing span, and total weight without battery. These values will help us to dimension the approximate size that the dolly should have. Below is data related to the battery. Of these, the most notable for the purpose of the work is its weight, which together with that of the plane will be the load that the dolly must accelerate, apart from its own weight. Next, the engine model and the rpm per volt ratio are defined. These data provide us with information about the propulsion capacity of the aircraft. If the UAV engine is very powerful, the additional propulsion system incorporated in the dolly may not be necessary, while if the motor is insufficient in relation to the force necessary to accelerate the dolly-plane assembly, it will be important to dimension a propulsion system additional suitable. Next, reference is made to the amperage of the aircraft engine controller, which will determine the maximum power that the engine can develop as a whole. Finally, it provides information on the propeller used, the number of blades, their diameter and their pitch.

GENERAL	Material	EPP and black Coroplast,
	Wings Span	180 cm
	Length	120 cm
	Weight Without Battery	3250 g
BATTERY	Battery Model	RC, LiPo 3S/8000
	Weight	234 g
	Flight Time	60 min.
MOTOR	Motor model	ROXXY C35-42-05
	Number of Motors	1
	KV (w/o torque)	1100 rpm/V
CONTROLLER	Controller Current	80A , 90A max.
PROPELLER	Type	APC Electric E
	Diameter	11 inch
	Pitch	10 inch
	Number of blades	2

Table 1. Bormatec Maja technical data. *(Traduced from - (Bormatec | Ravensburg | Drohnen, n.d.)*

Table 1 has provided very relevant information about the plane. This data can be used to calculate important parameters to consider in the design, such as the speed required to take off the aircraft (in reduced wind conditions). Even so, the calculations to be carried out are complex and extended, so the ECalc tool has been used to calculate these parameters.

3.1.3 ECalc simulation

The ECalc is an online tool, accessible on the website: *https://www.ecalc.ch/motorcalc.php - (ECalc-PropCalc-the Most Reliable Propeller Calculator on the Web, n.d.)* – that allows the realization of a detailed study of the different parameters and characteristics of the UAV. This tool is used by many users in order to make simulations on possible modifications in their model. Next, different images taken directly from the program will be shown to observe the entire simulation process and the interface between the tool and the user.. In addition, due to how well worked the tool is, it also offers a specific section for the interpretation of the results, which can be consulted in: *https://www.ecalc.ch/calcinclude/help/helicalchelp.htm#:~:text=mixed%20Flight%20Time%3A%20Expected%20Flight,difference%20from%20hover%20to%20max.)*

Figure 9 shows the entry data for the program. Most has been introduced from table 1.

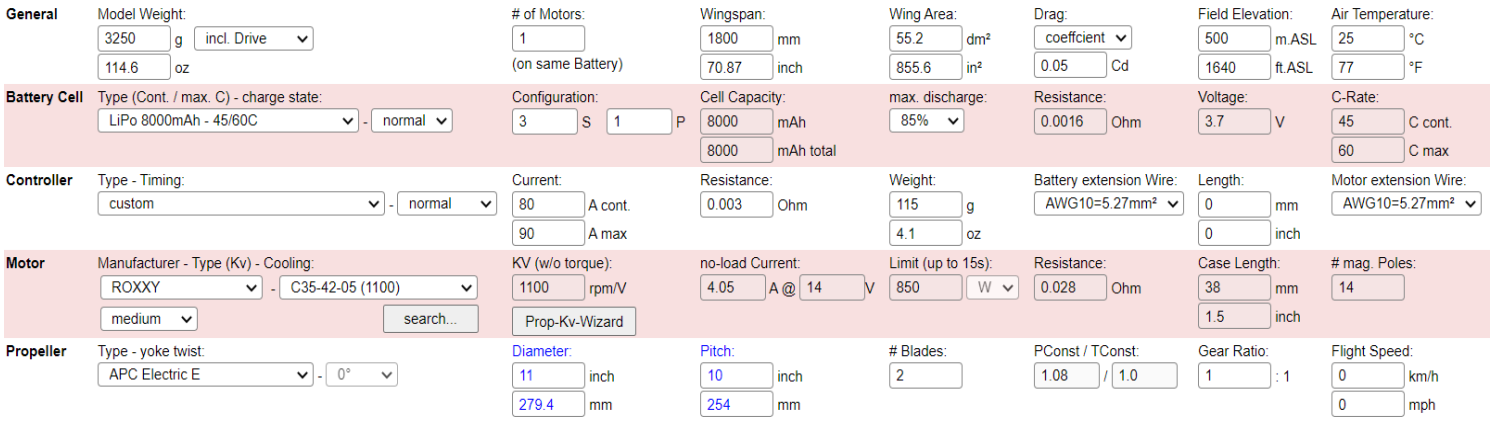

Figure 9. ECalc data entry form *(Source:* eCalc - propCalc - the most reliable Propeller Calculator on the Web. *(n.d.)*

The first results of the simulation are shown by the figure 10. It's possible to observe different graphics. Among them we can find the load of the UAV, the mixed time flight, which is " the Expected Flight Time based on all-up weight when moving based on max. discharge % of Battery, base is geometric mean value of current difference from hover to max.)" - (*ECalc - the Most Reliable RC Calculators on the Web for Electric Motors*, n.d.). The electric power, the est.Temperature, the thrust-weight ratio and the pitch speed. The most important for our project and the ones which will be considered is the electric power and Thurst-Weight ratio.

Figure 10. ECalc graphic results *(Source:* eCalc - propCalc - the most reliable Propeller Calculator on the Web. *(n.d.))*

Apart from graphical and numerical results, the program also provides additional comments on the study carried out. In this case they are the following:

Remarks:

- The airflow at the propeller blade will stall. Therefore, the static thrust and max. current may not be reached. On ground you will measure *Stall Thrust* as maximum.
- 74.0km/h / 46mph - above this airspeed stall at the propeller blade will have disappeared completely.
- Due propeller stall and low stall thrust a hand launch might become difficult.

It's important to pay important attention to the last remark. It says that due to the thrust lost the hand launch might become difficult. That's exactly the reason of making this project.

The program provides us with a long list of results that will be attached in the form of a report in the annexes. In this document, specifically in figure 11, only those directly related to the design of the dolly will be shown.

Airplane

All-up Weight:	3250 g
	114.6 oz
Wing Load:	59 g/dm²
	19.3 oz/ft²
Cubic Wing Load:	7.9
est. Stall Speed:	37 km/h

Figure 11. ECalc final results. *(Source:* eCalc - propCalc - the most reliable Propeller Calculator on the Web. *(n.d.))*

The most important information among all provided by the simulation report of the ECalc program, is the numerical value of the stall speed in [km / h]. "Stall speed refers to the minimum speed at which an airplane must fly to produce lift. Going back to the basics of aerospace dynamic, airplanes produce lift in response to the air moving over their wings. At high speeds, the fast-moving air "lifts" the airplane so that it doesn't fall to the ground. All airplanes have a specified stall speed. If an airplane drops below its specified stall speed, it will no longer produce lift. Stall speeds vary depending on many factors, some of which include the airplane's weight, dimensions, altitude and even the weather dimensions. Regardless, airplanes must fly faster than their respective stall speed to maintain lift." - *(What Is a Stall Speed and How Does It Affect Airplanes? – Monroe Aerospace News, n.d.)* So, knowing the UAV stall speed, it's easy to get an idea about the take-off speed needed because they both will be quite similar. Thanks to the study provided by the ECalc tool, it's known that the take-off speed will be around 40 [km/h]. It's important to apply a security factor to this value when dimensioning the dolly to ensure the correct operation. Finally, the simulation software provides the graph shown in figure 12, in which the different characteristics of the motor are represented at full throttle for different intensities in amperes. The most relevant data extracted from this graph is the power curve, since it allows us to acquire knowledge about how the plane will react when the current supplied increases and this will also help to size the propulsion system.

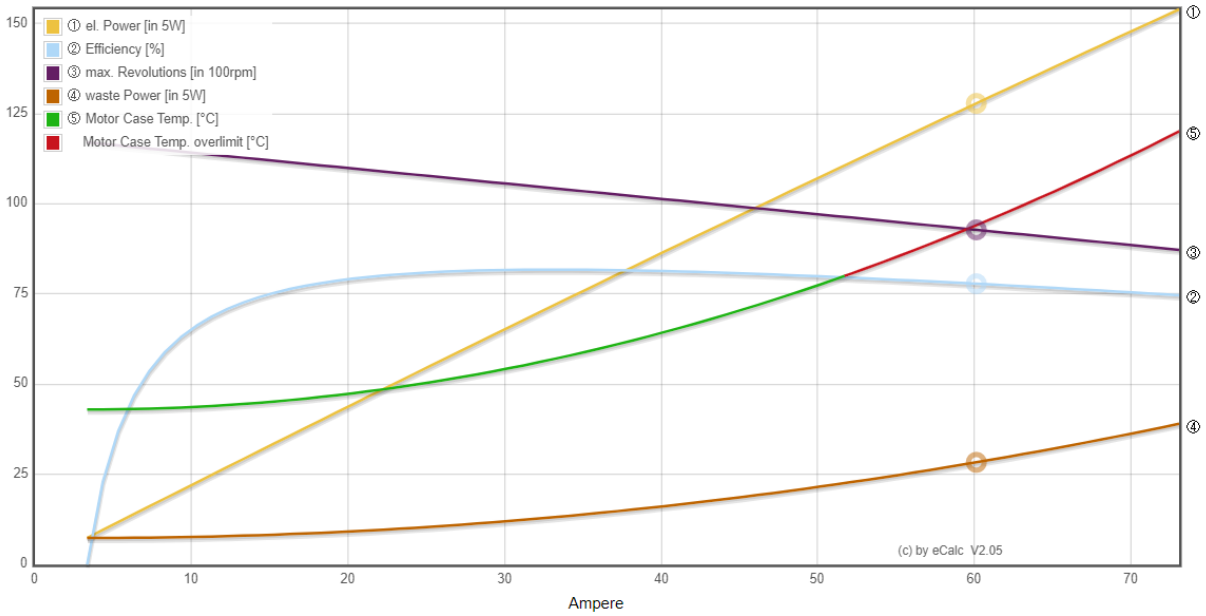

Figure 12. Motor Characteristic at full Throttle *(Source:* eCalc - propCalc - the most reliable Propeller Calculator on the Web. *(n.d.))*

3.1.4 UAV modelling in SolidWorks

In order to elaborate the dolly designs based on the physical form of the UAV with the SolidWorks 3D modeling program, a model of the airplane has been created. Using the program will allow to work with real measures and scales. In addition, the fact of having the 3D model of the plane will allow both dimensioning the dolly and promoting compatibility between the two by designing a structure that adapts to the shape of the UAV.

Finally, SolidWorks will allow to assign materials with their respective characteristics to the different parts to later carry out a detailed analytical study.

The first step in creating the 3D model has been the search of the 2D drawings, which by means of general and specific dimensions define the physical shape of the UAV. They have been created by "*DIY Drones*" and are shown in the annex.

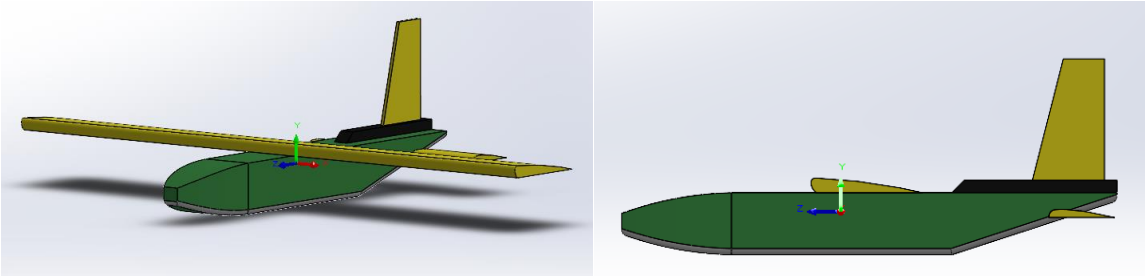

Figure 13. Fix wing UAV 3D model. *(Source: own elaboration)*

Figure 13 shows the UAV modeling that has been done using the SolidWorks program. It has remained practically the same as the real one, so that it will allow us to design on the UAV at scale. Even material and appearance have been assigned to the model. The results

of an analytical study applied to the model, also obtained using SolidWorks, are shown below:

Properties of Fix wing UAV

Mass = 3256.06(g)
Volume = 34407932.39 (mm^3)
Surface area = 1875620.49 (mm^2)

Center of mass: (mm)
X = 0.00
Y = 30.00
Z = 0.00

Principal inertial axis and principal momentum axis: ($g \cdot mm^2$)
Measured from the center of mass.

Ix = (1.00, 0.00, 0.00)	Px = 2200472039.49
Iy = (0.00, 0.04, -1.00)	Py = 2738757622.13
Iz = (0.00, 1.00, 0.04)	Pz = 4754008981.59

Although it is a detailed study and from which we could obtain more data, in the case of this work, the most relevant information provided that appears in it is the location of the center of mass. If the center of coordinates of the UAV marked in figure 14 is carefully observed, and considering the coordinates of the center of mass provided by the study, his location in the image of the figure can be determined. In general terms, the mass center of an aircraft must be in the center if the aircraft is being looked form the front, and it must be 30% from the leading edge of the wing when looked from the profile. If this theory is compared with the results obtained in the SolidWorks study, it can be stated that the center of mass seen from the profile coincides with 30% of the width of the wing with respect to the leading edge.

3.2 Car physics

In this chapter we will study different factors to take into account in relation to the general physics of the car. These factors are present in all types of vehicle and play an important role in the dolly design process. They will condition their behavior directly.

The factors that will be analyzed are the following:

- Track width
- Wheelbase
- The center of mass or center of gravity (CG)
- Size of the wheels

3.2.1 Wheelbase

"Wheelbase is the center distance between the front and the rear axle of the vehicle. It is one of the important dimensions of the vehicle that is specified by the vehicle manufacturers.

This term is applicable to bicycles, two-wheelers, four-wheelers, trucks etc." - (*Wheelbase: How Important Is It In Designing The Vehicle? - CarBikeTech*, n.d.)

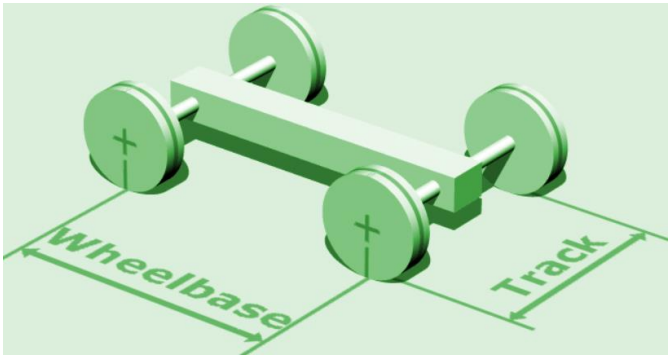

Figure 15. Wheelbase and track *(Source: Wheelbase: How Important Is It In Designing The Vehicle? - CarBikeTech)*

As mentioned, the wheelbase refers to the distance between the front and rear axle of the vehicle. This characteristic will sometimes be conditioned by the total length of the vehicle but it does not necessarily have to be this way.

The wheelbase plays a very important role in the behavior of the vehicle: a long wheelbase gives the vehicle more poise at high speeds, but less agility in twisty sections or tight corners. This, therefore, means that high-end vehicles designed to offer a high quality of ride have a longer wheelbase than normal.

Applying this information to the specific model of dolly in which you are working, it can be determined that since the main objective is to keep the vehicle in a straight line and the turns will be very small, the ability to take curves will not be relevant in the design. Therefore, the wheelbase will be dimensioned to be as long as possible following the criteria set by the UAV and the rest of the components.

3.2.2 Track width

"The track width is the width of the car, measured between the centers of the tire contact patches. The track width is important because it determines how much weight is transferred by the mass of the car in cornering." - (*Car Chassis Basics, How-To & Design Tips* , n.d.)

The track width increase for a longer distance between the right and left wheel. A bigger track width will provide more stability in straight roads and open curves roads, but it can difficult the cornering in close curves roads.

After reviewing the concept of track width and studying its effect on the behavior of the vehicle, it can be determined that its greater width will be beneficial and will be limited only by the design criteria, the UAV and the rest of the components of the dolly.

3.2.3 Center of gravity (CG)

"Center of gravity, also known as center of mass, is that point at which a system or body behaves as if all its mass were centered at that point. Where the weight, and also all accelerative forces of acceleration, braking and cornering act through it.

Center of gravity location can be defined as:

- The balance point of an object
- The point through which a force will cause pure translation
- The point about which gravity moments are balanced (see Figure 16)
- The point which if the body is hanged from it will stay balanced (leveled as it is on the ground)." - (*(The car tech)*, n.d.)

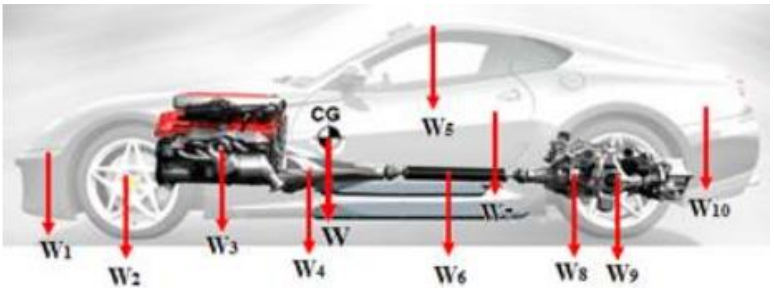

Figure 16. Summation of moments. *(Source:* North American International Auto Show (NAIAS),2018)

As the figure 15 shows, the summation of moments of all parts weights around any point is equal to the moment of the summation of weights around this point W. :

$X_{CG} = (W_1.X_1 + W_2.X_2 + W_3.X_3 + W_4.X_4 + W_5.X_5 + \ldots)$

$X_{CG} = \Sigma (W.X) / \Sigma (W)$, where X_i is the distance in x direction between the point "i"and the CG point.

"When making an analysis of the forces applied on the car, the CG is the point to place the car weight, and the centrifugal forces when the car is turning or when accelerating or decelerating. Any force that acts through the CG has no tendency to make the car rotate. The center of mass height, relative to the track, determines load transfer, (related to, but not exactly weight transfer), from side to side and causes body lean. When tires of a vehicle provide a centripetal force to pull it around a turn, the momentum of the vehicle actuates load transfer in a direction going from the vehicle's current position to a point on a path tangent to the vehicle's path. This load transfer presents itself in the form of body lean. Body lean can be controlled by lowering the center of weight or the widening the car track, it can also be controlled by the springs, anti-roll bars or the roll center heights. The center of mass height, relative to the wheelbase, determines load transfer between front and rear. The car's momentum acts at its center of mass to tilt the car forward or backward, respectively during braking and acceleration. Since it is only the downward force that changes and not the location of the center of mass, the effect on over/under steer is opposite to that of an actual change in the center of mass. A lower center of mass is a principal performance advantage of sports cars, compared to sedans and (especially) SUVs. Some cars have body panels made of lightweight materials partly for this reason." - (*(The car tech)*, n.d.)

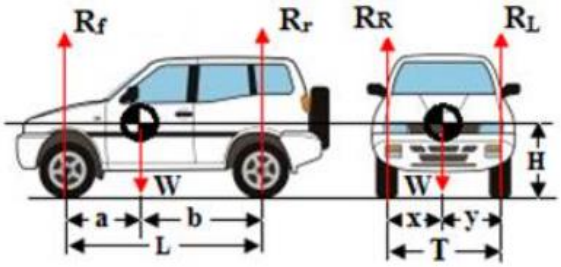

Figure 17. Location of the CG. *(Source:* North American International Auto Show (NAIAS),2018)

As seen in Figure 17, the center of gravity relative to the wheelbase is located in the center in all car models so that they are symmetrical in shape and mass when viewed from the front or rear. This is because otherwise the behavior of the vehicle would be asymmetric and differences would be noticed when taking curves to the right or left. In this sense, the dolly must be balanced so that its center of gravity is in the center (exactly in the middle point between the left and right wheel).

On the other hand, regarding the location of the CG referring to the track, there may be variations depending on the shape and characteristics of the vehicle being analyzed. Although it is true that its location cannot be centered in either of the two extremes, it must be rather centered, in this case it is possible that it is not exactly in the center but that it differs a little towards the front or rear of the vehicle. It is common especially in front-wheel drive vehicles for the center of gravity to be in front of the middle of the vehicle in order to compensate for the efforts exerted by the engine.

After reviewing the concept of the center of gravity, specific conclusions can be drawn about the application of this information in the specific area covered by the project. If we focus on the definition of the optimal location of the CG in the dolly model of the project:

- If we look at the model from the front, the CG should be found midway between the left and right wheels to ensure the longitudinal symmetry of the model. This particular factor is of vital importance since the dolly is designed to maintain a fixed direction in a straight line, any possible deviation in the balance of weights would cause an imbalance in the system directing the dolly towards the side that was closest to the CG.

- Looking at the Dolly in profile, the location of the CG should be centered, but as mentioned, as long as its position is not extreme towards the front or back, small variations can be tolerated since in this case it is not as critical as the previous. The factor that will most determine the position of the longitudinal CG will be the position in which the UAV is attached to the dolly. Since ideally the CG of the UAV, which is located under its wings, should be made to coincide with the CG of the dolly. This will avoid system instabilities during the acceleration maneuver.

- Finally, the height of the CG should be as close as possible to the ground to maintain stability when accelerating, braking and correcting the turn. The only limitation that this dimension has is the necessary height at which the plane must be positioned above the dolly, since as it forms a certain angle with respect to the ground when taking off, if it is located very close to the ground, the tail of the UAV could impact with the ground when starting the flight.

3.2.4 Study of the wheel parameters

The size of the dolly wheels is also a factor to consider as it will affect in its behavior. It should be noted that the size of the wheels does not have to be related to either the ground clearance or the total height that the dolly will have, since the first factor will be delimited by the height of the CG and the second by the height at the aircraft must be positioned to take off correctly without hitting the ground with the tail when performing the maneuver.

During the history of mankind and since the discovery of the wheel back in 3500 BC, many types of wheels have been designed, depending on the use and technology available at that time.

"Currently in the world most of the wheels intended for use in vehicles use a standardized code that provides the consumer about the wheel information. This code is made up of three terms, firstly the width of the rim expressed in millimeters, secondly the relationship between the height of the side wall and the width of the rim expressed as a percentage. Finally, the letter "R" which means "radial", accompanied by the diameter of the rim expressed in inches." - *(A Salute to the Wheel | Science | Smithsonian Magazine, n.d.)*

3.2.4.1 Wheel diameter

The total wheel diameter is considered as the length of the final reduction ratio of the transmission. Increasing the total wheel diameter will also increase the final reduction ratio and this has essentially two consequences: acceleration potential is decreased but a higher top speed can be reached. These changes are proportional to the variation of size. But there is another element to be taken into consideration: increasing the wheel diameter will also increase the axle weight as a whole. This will obviously increase inertia, cause further loss of acceleration and also lower cornering accuracy. The behavior of the car may also change: increasing the tire diameter for the same fixation point, will obviously raise the chassis height and the center of gravity as a consequence, with the direct effect of increasing roll and oscillations. And less stability, especially in corners. Another advantage of a large diameter is that apart from the higher inertia in the movement, more speed can be taken since the small bumps that the track may contain will be less significant in relation to the size of the wheel and therefore, they will slow down the dolly less, but above all they will make it more stable.

3.2.4.2 Tread width

The modification of the tread width will have consequences too; larger width will contribute to increasing friction. A positive effect of this is an increase in road holding and stability. But rolling resistance is also incremented at the same time.

3.2.4.3 *Wheel definition*

After reviewing the main characteristics of the wheel and how it effects on the car behavior it's possible to affirm the following:

- A larger diameter of the wheels will improve the stability of the dolly, the max velocity an it's capacity to go over obstacles. It will also increase the maximum load of the car. On the other hand, a larger diameter means that the wheel will be heavier and consequently acceleration will be slightly compromised (depending also on the torque. Braking will so take more time
- Smaller diameter allows for tighter turns.
- Wider wheel will increase the stability
- Shorter width will reduce the rolling resistance.

The table 2 shows the main consequences of modifying the diameter and width of the wheels and its consequences.

Measurements	Consequences	Results
Increasing the total wheel diameter	Increases the final reduction lenght	Dicreases aceleration
		Increases the top speed
	Increases the axle wheight as a whole (increasing the inertia)	Further loss of acceleration
		Lower cornering accuracy
	Increases the heigh of the chassis (increasing the center of gravity)	increase roll and oscillations
Increasing the tread width	Increases friction	increases road holding
		Increases rolling resistance

Table 2. Wheel diameter and width comparison.

In the particular case what is studied in this project, the dolly will maintain a fixed direction, that's why it is dimensioned to have the much stability as possible advancing in straight line and not for taking corners. Then, we will prefer a larger diameter of wheels and a larger width as possible, according with the rest of elements filled in the dolly.

4 Chassis design

After reviewing the existing dolly models in order to get ideas and examine in detail the characteristics of the aircraft, and reviewing the main physics phenomes and characteristics that affect the cars behavior, the next step is to determine the type of structural chassis that will be used, to start making the first designs.

The type of chassis chosen will be a crucial element that will largely determine the rest of the elements chosen. Many of the final characteristics of the dolly will depend directly on the chosen chassis. Therefore, it is of great importance to take the necessary time to study and compare the different possibilities.

The characteristics and factors of the final design that will depend directly on the type of chassis chosen are: rigidity and mechanical resistance, weight, free height from the ground, the height at which the UAV will be placed, its position and the type of fastening used. It will also influence the materials used and the manufacturing process.

4.1 Review of the existing chassis

Para asegurar una correcta elección del modelo de chasis con el objetivo de que el elegido sea la mejor opción disponible, se ha hecho una revisión de los modelos de chasis existentes y utilizados mayormente en la industria del automóvil.

There are multiple types of chassis but all of them can be classified into one of two approaches:

- Use lengths of round or square tubing, or other structural metal shapes to form the chassis structure (Space frame, multi-tube, ladder frame)

- Use joined panels to form the chassis structure (Monocoque, Unibody)

Both approaches can provide a structure capable of mounting other vehicle components, but each has its own advantages and disadvantages.

The main existing chassis types are the following ones:

4.1.1 Ladder frame chassis

This type of chassis is one of the oldest, the ladder chassis gets its name from it's shape which has the shape of a ladder. It has two long and heavy beams at the both sides, which are supported by two short beams at the front and the rear to provide rigidity and stability during driving. The main selling point of the ladder chassis what made it famous, was how easy it was to manufacture. Due to the lack of technology during the beginning of the automobile era, most of cars manufactured and produced in series were equipped with the ladder chassis because that way made it easier to mass-produce. The chassis also makes the car assembly easier just adding parts which were supported on the beams. The ladder chassis is quite heavy and thus still finds use in modern vehicles that need to tow heavy stuff around like heavyweight or agricultural machinery.

Advantages

- The assembly is quite easier because the parts are easily fixed to the chassis.
- The dimensions and the type of structure what it adopted makes it very resistant.
- Easier to repair as parts are not permanently attached and can be easily removed.
- The simplicity of the structure and the used materials makes it cheaper.

Disadvantages

- The ladder chassis has a weak torsional rigidity making it bad for cornering.
- Heavyweight makes it not ideal for sports cars or hatchbacks.
- The recent development of advanced technology in the automotive sector has allowed to appearing new types of chassis which has a better characteristic with a better manufacturing what permits the mass-produce, decreasing the total cost of the vehicle.

Figure 18. Ladder frame chassis. *(Source:* (Rangam Kartik, 2020) *Types Of Car Chassis Explained | From Ladder To Monocoque)*

"The Spaceframe chassis uses numerous cut and shaped pieces of structural metal tubing (usually steel) joined together to form a strong framework. That's why they are also called tubular chassis.

Tubular chassis were mainly used in race cars due to the unrivalled safety they provide. These were an upgrade from the ladder chassis as they were three dimensional and were stronger than ladder chassis. "- *(Car Chassis Basics, How-To & Design Tips , n.d.)*

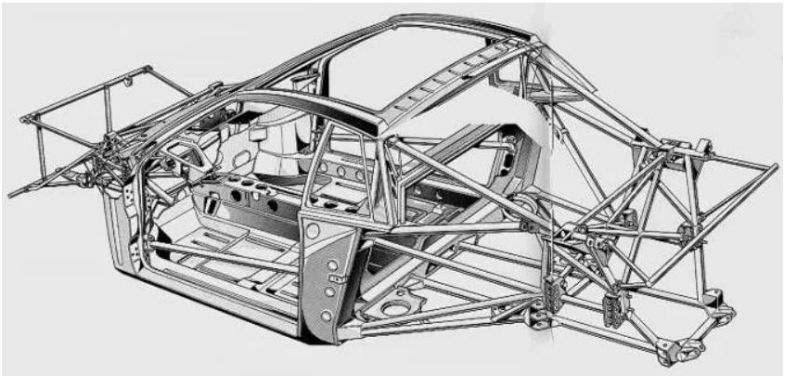

Figure 19. Spaceframe chassis. *(Source: Source:* (Rangam Kartik, 2020) *Types Of Car Chassis Explained | From Ladder To Monocoque)*

The principle of spaceframe design is to use triangulation of the tubes to create a rigid structure. Figures 21 and 22 below show how triangulation is used to rigidize a structure:

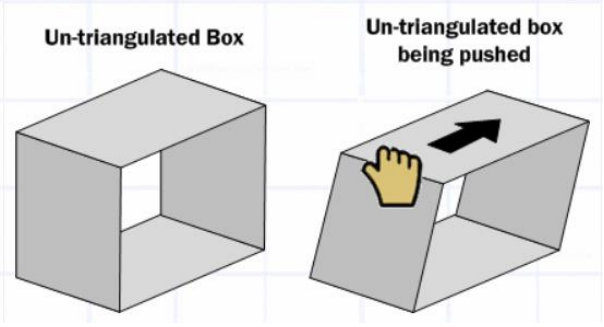

Figure 20. Un-triangulated box. *(Source:* (Build your own race car, 2018) | *Car Chassis Basics and How-To Design Tips)*

Figure 21 shows an un-triangulated box, what has very little strength. As the hand pushes against the corner of the box, the shape warps into a parallelogram modifying the momentum of the applicate force.

This will change by triangulating the box with a tube, the strength is greatly increased because the structure is not allowed to wrap into a parallelogram. With this modification (a box with a cross-member) the structure forms two triangles that's why is said to be triangulated. Now, as shows the figure 18, the force applied to the box is trying to pull the cross-member apart.

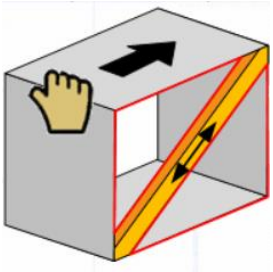

Figure 21. Triangulated box. *(Source:* (Build your own race car, 2018) | *Car Chassis Basics and How-To Design Tips)*

As it's observed in Figure 22, the bar in the mid is being pulled as if the corners of the box to where it is attached were trying to tear it apart. Thanks to the mid bar strength in tension, the box will not deform into the parallelogram as in figure 21.

Triangulation can also work in compression. However, the ideal design always has the member tubes working in tension because it provides superior strength than the tubes working in compression.

Advantages

- Better rigidity compared to other chassis in the same weight.
- Offers the best weight/rigidity ratio allowing the car to be lightweight while being strong.
- It has a better torsional rigidity which makes it better for cornering
- Due to his structure with a cage shape it is the most safety type of chassis.
- All the previous advantages make it the most used chassis on the race cars.

Disadvantages

- Tubular chassis are complex structures and cannot be made using autonomous methods.
- Tubular chassis are time-consuming to build and cannot be mass-produced.
- Not feasible to be used on passenger cars.
- The structure raises the door which makes it difficult to access the interior of the dolly.

4.1.2 Monocoque chassis

The Monocoque is described like a "unibody structure, it too gets its name from its structural look. Monocoque being French for 'single shell' or a 'single hull'. The monocoque was first used by ships and then by planes. It took quite some time to figure out that they can be used in cars as well. A monocoque is a shell around the car made by using both chassis as the frame in a single construction. This is the most commonly used chassis right now due to the number of advantages of has over the other two chassis." - *(Types Of Car Chassis Explained | From Ladder To Monocoque!, n.d.)*

"The monocoque chassis is technically an improvement over the spaceframe chassis". - *(Car Chassis Basics, How-To & Design Tips , n.d.)*

Advantages:

- It is very safe due to its cage-like construction.
- The chassis is also easy to repair.
- It has a good torsional rigidity, that allows a better cornering.
- Currently, it is the most used chassis in vehicles, due to its ability to be serial-produced. It is also the most economical type of chassis on a large scale due to its manufacturing method intended for mass production.

Disadvantages:

- The chassis is obviously heavy as it's both the frame and chassis as one single entity.
- In the manufacturing model that the automotive sector has nowadays of massive productions, it results economical, but producing it in small quantities is not financially feasible and thus it cannot be used for cars that are not mass-produced. It's because the complexity of the cage-like structure of the monocoque requires of an specific and expensive molds.

Figure 22. Monocoque chassis. *(Source:* (Rangam Kartik, 2020) *Types Of Car Chassis Explained | From Ladder To Monocoque)*

4.2 Chassis comparison

After reviewing the different existing types of chassis, in order to compare the characteristics of the different models and choose the one that best suits the specific requirements of the project, the Pugh matrix will be used.

4.2.1 Pugh matrix definition

"The decision-matrix method, also called Pugh method or Pugh concept selection, invented by Stuart Pugh, is a qualitative technique used to rank the multi-dimensional options of an option set. It is frequently used in engineering for making design decisions but can also be used to rank investment options, vendor options, product options or any other set of multidimensional entities."- *(Decision-Matrix Method - Wikipedia, n.d.)*

To use this method, it's necessary to identify the evaluation criteria of the product (usually the product requirements), and then assign to each of them a value of importance. In this way, It'is possible to give more relevance to the more critical criteria for the achievement of the product against those who are not. It is also necessary to define the possible design alternatives. Once this has been determined, the method allows each of the criteria to be evaluated numerically for each alternative. Finally, a row or column is added to the matrix in which the total sum of the criteria for each alternative. As expected, the one that obtains the higher score is the best option to be elected.

4.2.1.1 Evaluation criteria

The different evaluation criteria that will be taken into account to determine the chassis to use are mentioned below:

- Rigidity of the system: The type of chassis created must be sufficiently rigid to maintain the stability of the system and not give way or have wobbly when different forces are applied.

- Lightness: The type of chassis cannot be very heavy since this will make it difficult for the whole to accelerate and will make it necessary to have a more powerful additional propulsion system.

- Accuracy and stability in curves: Although the dolly is designed to maintain a fixed direction in a straight line, it must make small variations in trajectory to correct possible deviations. It is important that the dolly maintain stability at all times.

- Ease of assembly and simplicity: The simpler the procedure for the same end result, the better the model will be, as it will save design and construction time.

- Mechanical resistance: The chosen chassis model must have enought mechanical resistance to withstand the plane's load.

- Cost: As in most projects, the economic factor plays a very important role. Faced with two alternatives that fulfill the same function with similar efficiency, the most economical one will always be chosen.

- Ability to fix the UAV to the dolly: Since the ultimate goal of the dolly is to take off the UAV, it will be important that the chosen chassis allows the design of the aircraft restraint.

In order to make the chassis election considering the importance of the previous criteria, the table 3 was made. It shows the importance that has been assigned to each of the criteria.

For this, each of them has been assigned a value from 1 to 5, such that:

1. Meeting the criteria is very unimportant for the achievement of the objectives.
2. Meeting the criteria is unimportant for the achievement of the objectives.
3. Meeting the criteria is important to the achievement of the objectives.
4. Meeting the criteria is quite important to the achievement of the objectives.
5. Meeting the criteria is very important to the achievement of the objectives.

CRITERIA	IMPORTANCE
Rigidity	4
Lightness	3
Stability while cornering	2
Simplicity (during design and construction	5
Mechanical resistance	4
Cost (for one unit)	5
Ease of holding the UAV	4

Table 3. Importance assigned to the chassis election criteria

4.2.1.2 Options

The alternatives for the election are the chassis type mentioned above.

- Ladder frame chassis
- Spaceframe chassis
- Monocoque chassis

4.2.1.3 Final election

Finally, the assessment of compliance with each of the criteria has been carried out by assigning, to each alternative, a value from 1 to 5 so that:

1. The alternative does not satisfy the criteria.
2. The alternative meets the criteria poorly.
3. The alternative satisfies the criterion.
4. The alternative meets the criteria well.
5. The alternative meets the criteria very well.

The results obtained after applying Pugh's method are shown below:

	Importance	Ladder	Spaceframe	Monocoque
Rigidity	4	4	5	4
Lightness	3	2	4	4
Cornering stability	2	2	5	4
Simplicity	5	5	3	1
Mechanical resistance	4	4	5	3
Cost	5	5	3	1
Ease of holding UAV	4	4	3	3
TOTAL		108	104	70

Table 4. Pugh matrix comparison

Finally, as table 4 shows, the most favorable chassis type, determined with the Pugh matrix, is the Ladder type chassis. Even so, the Spaceframe chassis has obtained an almost equal score, which means that it is also a very good option to consider. On the other hand, the Monocoque chassis, although in the real application of mass production of automobiles it would be the best option, in the specific case that is dealt with in this project, it would undoubtedly be a mistake to select this chassis.

The final decision regarding the chassis design will be a mix between the ladder type and the spaceframe. Since both have proven to be the most recommended.

4.3 Introducing to SolidWorks simulation

After having made a detailed review of the characteristics of the UAV and having studied and compared the different types of existing chassis to end up choosing the most convenient one, we have all the ingredients to make the first chassis designs.

In this section the first designs of the dolly chassis will be shown. To carry them out, the previously used program, SolidWorks, will be used again. The main objective of this task will be to define the final chassis design that will incorporate the dolly. To do this, various different models will be designed, their physical properties will be studied using the SolidWorks Simulation tool, which includes the same 3D CAD program, and the results will be compared from an analytical point of view considering the relevant factors.

For the moment, the chassis joints will not be considered, but only the shape of its structure.

Thus, in the pre-design process, different simple structures will be proposed, with different shapes, measures and triangulations. A study will be carried out with the design program and finally the results will be analyzed taking into account the simplicity, lightness and mechanical resistance of each structure as criteria.

For the design of the different structures, the same tube profile, thickness and dimensions will be used and the same loads will be applied in the position in which the plane will be placed on top of the dolly. To compare the structures on equal terms and simulate the point of application of the force that the UAV will exert on the model.

The simulation studies that will be carried out to contribute to the choice of a certain type of structure or another are the following:

- Study of tensions and deformations: It will show graphically by means of a color code the deformation suffered by each point of the structure. This study will also allow to know which is the critical point subjected to more deformation and its value.

- Study of the safety factor: It will allow us by means of a color code to know the safety factor with which we work at each point of the structure. It will serve to know if the mechanical resistance of the structure is within the working ranges ($FS \in \{1.8, 2.4\}$), if it will break, or if on the contrary it is oversized. The latter is not a problem at the operational level, but it means that more money has been spent on material than necessary.

It should be noted that this study is not real or definitive and will only serve to determine the best structure, comparing different types subjected to the same conditions. To carry out the

study, a distributed mass of 1000kg will be applied on the beams that will hold the base where the aircraft will be housed.

The simulation study will also help us to determine the material with which the chassis will be built since the tool allows the selection of the material and takes into account its physical properties in its internal calculations. For this, the procedure to follow will be as follows: First, the possible materials to be compared will be defined, based on their optimal physical properties. Next, different types of structures will be designed to which a distributed load of 1000kg will be applied and each will be assigned 3 different materials. The simulation will be carried out with the program and the results will be analyzed in search of the best structure and the best material.

4.4 Pre-Selection of the chassis material

To make a definitive comparison of the potentially effective material, and not have to do excessive simulations with many different types of materials, a first filter of materials has been carried out following the following criteria:

- The material must be accessible to anyone. Special, limited, or expensive materials are not contemplated.
- The material must have a good weight-mechanical resistance ratio.
- It must be found on the market in the form of a tube, since one of the conclusions that has been determined previously is that the chassis will be formed by a tubular structure.
- Has to be resistant to atmospheric phenomena as well as oxidation.

Following the mentioned criteria, the 3 possible materials chosen are the following: stainless steel, carbon fiber and aluminum.

For aluminum, the 6063 T6 alloy will be chosen as it has good mechanical properties since it has an elastic module of 69,5 GPa and a mass density of 2700 kg / m ^ 3. In addition, it is abundant in the global market in the form of a square profile.

In the annex its complete datasheet is attached. Its price is quite cheap, depending on the manufacturer you can find already processed aluminum in the form of a 15 x 15 mm ^ 2 profile and 1.5 m thick for about € 7.5 / m, price at which it is sold at: <https://www.bauhaus.es >.

As for carbon fiber, Thornel Mat VMA has been chosen. This type of fiber has an elastic modulus of 170 GPa and a density of 2001 kg / m ^ 3. As can be seen, its mechanical properties are better than those of the aluminum, but on the other hand its price is much higher. Currently it is around € 100 / kg.

It is also available in the global market in the form of a hollow square profile. It can be found at <https://www.castrocompositesshop.com > for a price of 43 € / m.

Regarding stainless steel, the standard AISI 304 alloy has been chosen since “it is an austenitic stainless steel for general use with a face-centered cubic structure. It is

essentially non-magnetic in the annealed state and can only be cold hardened. Its low carbon content compared to alloy 302 provides better resistance to corrosion in welded structures. "- *(Acero Inoxidable - AISI 304 - Catalogo En Linea - Materiales En Pequenas Cantidades Para El Diseno - Goodfellow, n.d.)*

After reviewing its properties attached in the annex, it can be concluded that AISI 304 stainless steel could be a good option, since it has good weldability and very high mechanical resistance. It can be found in the form of a square aluminum profile for a price of 20 [€ / m].

4.5 SolidWorks simulation

In this section, the simulations corresponding to each of the types of structure designed will be carried out. Next, the result for each one of them will be analyzed and finally the best type of structure will be chosen. To perform the task correctly and with objective criteria, the simulations corresponding to each type of structure will be subject to the same conditions: a distributed load of 100 kg and 6063 T6 aluminum as the specified material. It has an elastic limit of $2{,}15 * 10^8 \left[\frac{\mathrm{N}}{\mathrm{mm}^2}\right]$

The structure of the analysis will be as follows: first, the proposed design will be presented and the study of its mass and center of mass will be carried out, then the simulations of stresses and safety factor will be shown. Finally, when the study of all the proposals has been presented, a comparative table will be made in which the results will be analyzed. When the type of suitable structure has been decided, the type of material to be used will be analyzed.

4.5.1 Structure A

The first structure proposal is presented in the figure 24 below. The general measurements have been considered based on the size of the plane and the characteristics studied in previous sections. In this case the triangulations have been omitted, only the minimum bars necessary for the integrity of the structure are shown.

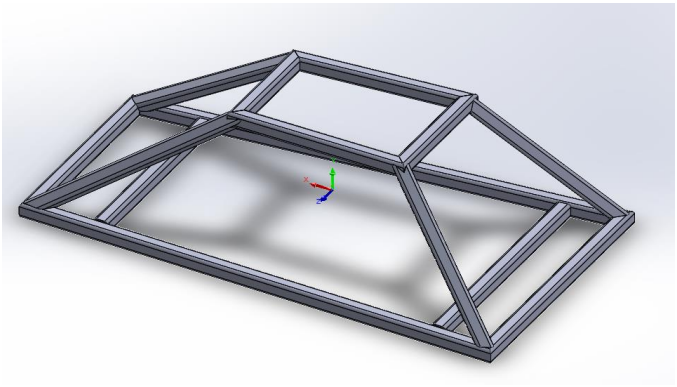

Figure 23. Structure A design *(Source: own elaboration)*

Mass = 1645.54 (grams)
Volume = 609459.03 (mm^3)
Surface Area = 615144.71 (mm^2)
Center of mass: (mm)
X = 24.34
Y = 53.18
Z = 0.0

Stress Simulation

Maximum axial stress = 1,631*10^8 [$\frac{N}{m^2}$]

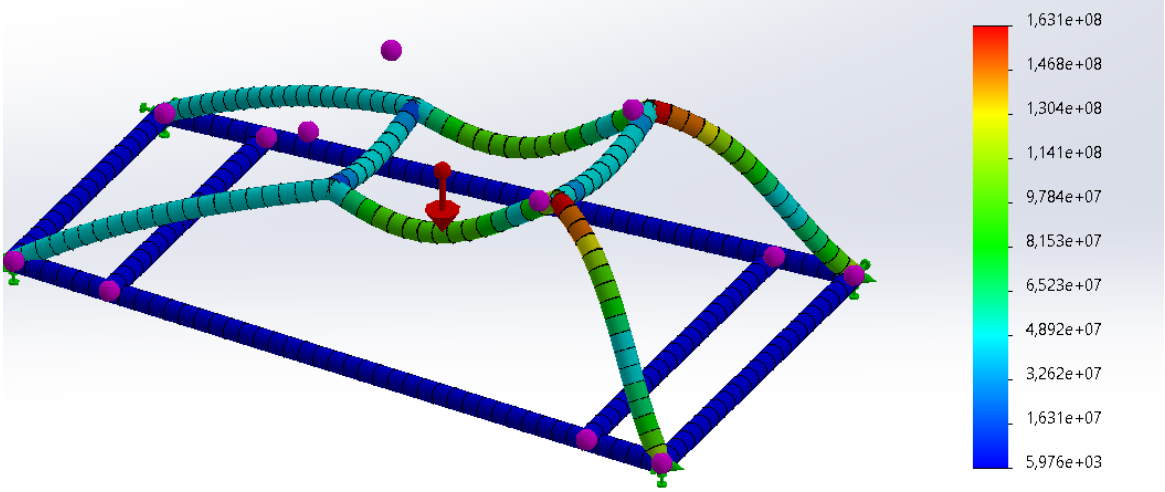

Figure 24. Structure A: Stress study *(Source: own elaboration)*

Safety Factor

Minimum Safety factor = 1,32

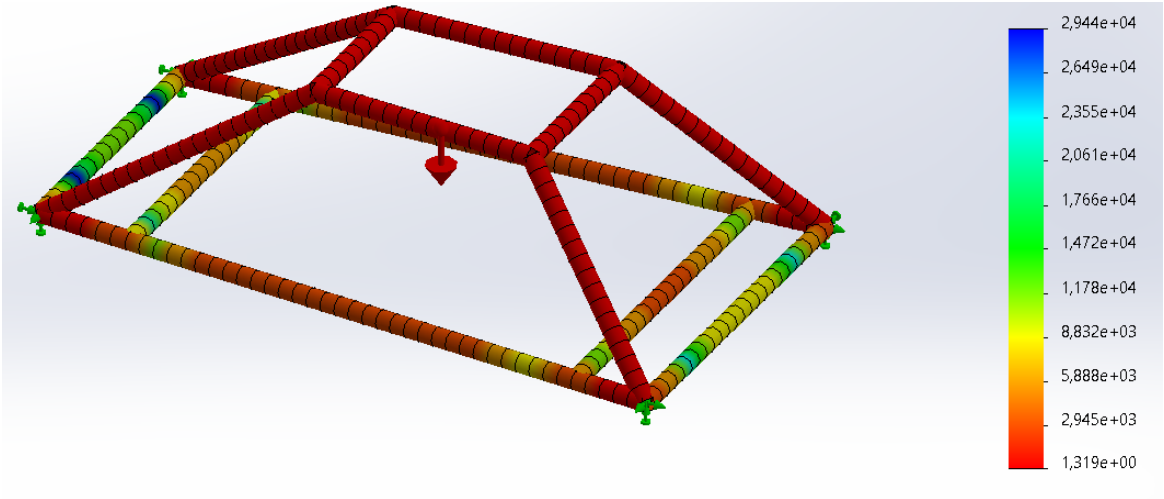

Figure 25. Structure A: Safety Factor *(Source: own elaboration)*

4.5.2 Structure B

After carrying out the first simulation study in structure A, which did not integrate any triangulation, it was possible to observe the critical points where the stress was higher and the safety factor was lower. In this structure B it is intended to carry out a redesign of structure A, adding triangulations at critical points.

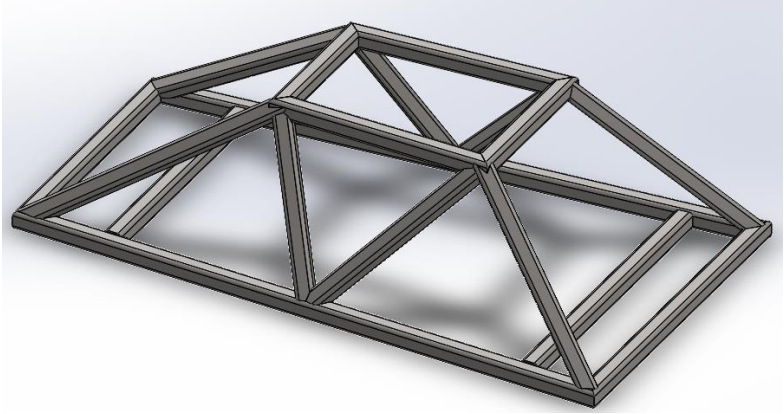

Figure 26. Structure B Design *(Source: own elaboration)*

Mass = 1941.75 (g)
Volume = 719166.61 (mm^3)
Surface area = 726663.00 (mm^2)
Center of mass: (mm)
X = 25.77
Y = 58.42
Z = 0.01

Stress Simulation

Maximum axial stress = 9,185*10^7 [$\frac{N}{mm^2}$]

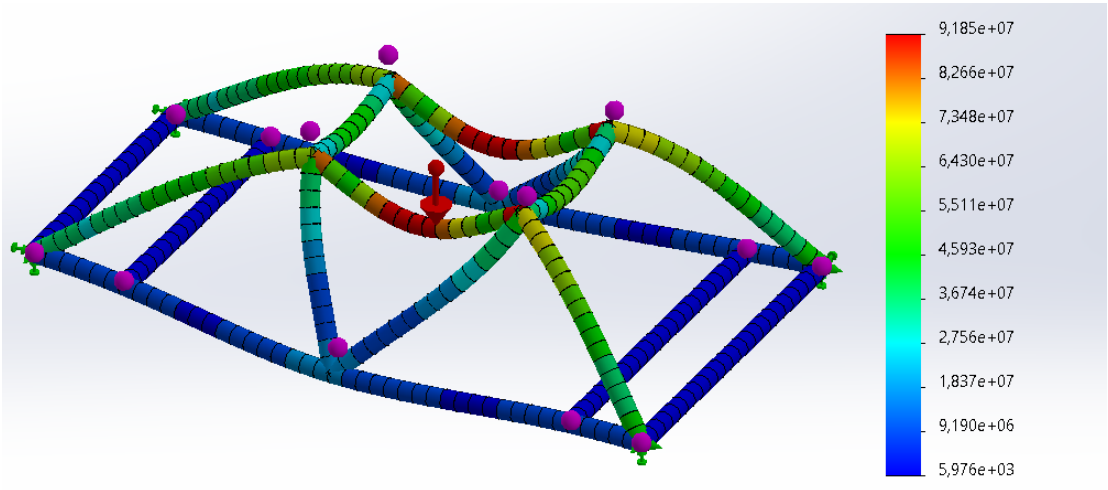

Figure 27. Structure B: Stress Study *(Source: own elaboration)*

Safety Factor

Minimum SF = 2,34

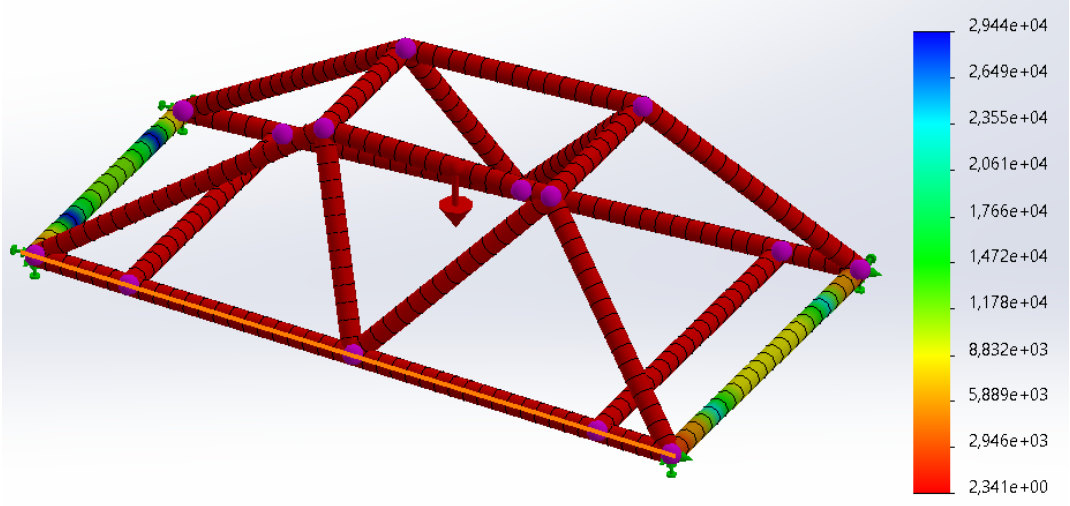

Figure 28. Structure B: Safety Factor Study *(Source: own elaboration)*

4.5.3 Structure C

In this case, another variant proposal of structure A with a different type of triangulation will be presented. While in the previous model a triangulation was proposed in which 2 bars were added on each side, here a new triangulation with a single bar on each side will be presented in order to lighten weight.

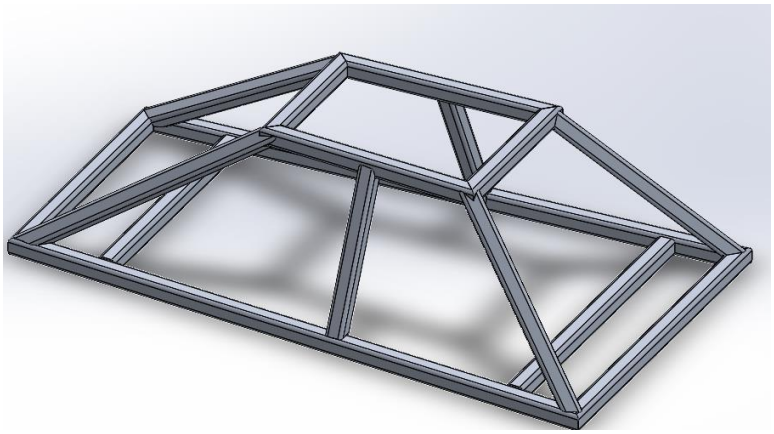

Figure 29. Structure C: Design *(Source: own elaboration)*

Mass = 1773.91 (g)
Volume = 657004.92 (mm^3)
Surface area = 663545.78 (mm^2)
Center of mass: (mm)
X = 26.21
Y = 55.67
Z = 0.00

Stress Simulation

Maximum axial stress = 1,275*10^8 $[\mathrm{N/m^2}]$

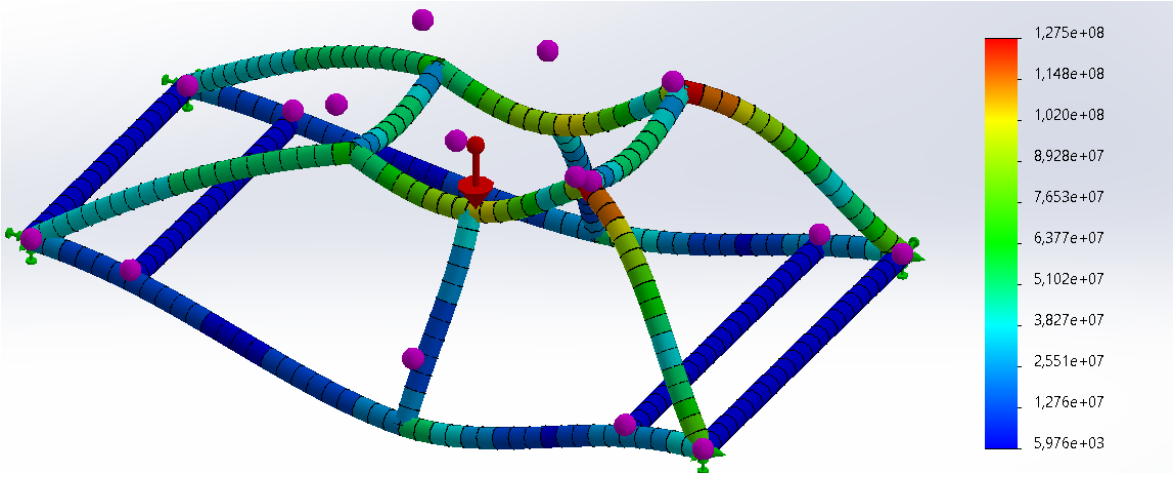

Figure 30. Structure C: Stress study *(Source: own elaboration)*

Safety Factor

Minimum SF = 1,69

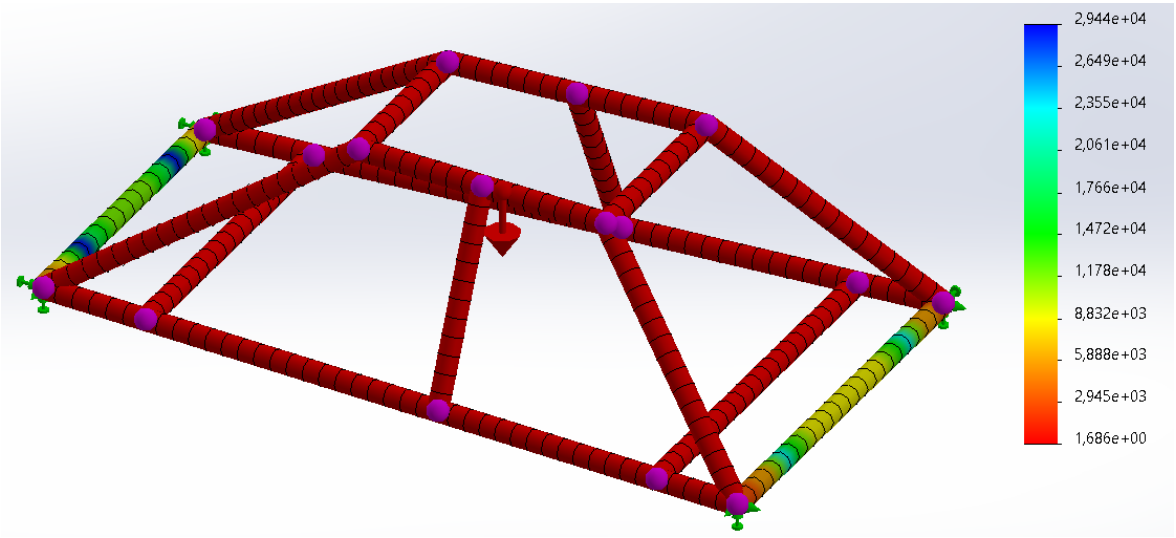

Figure 31. Structure C: Safety factor study *(Source: own elaboration)*

4.5.4 Structure D

Finally, a structure which is triangulated only from the back will be analyzed. In this model, the maximum weight reduction is sought while reinforcing the critical point of structure A (Figure 25). For this, there will be a single bar that will join the base of the chassis with the base on which the aircraft will be supported.

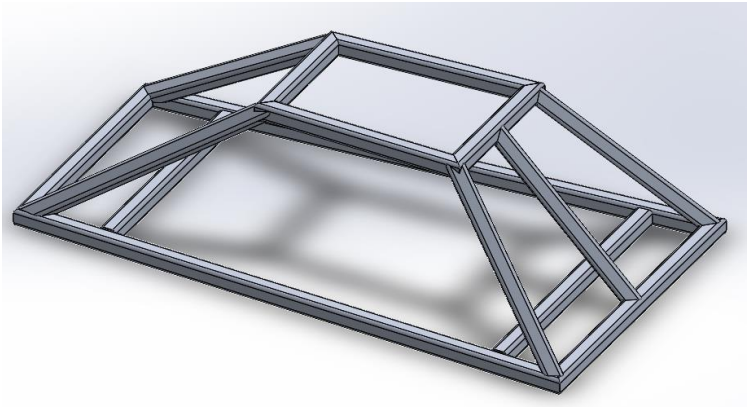

Figure 32. Structure D: Design *(Source: own elaboration)*

Mass = 1729.13 (g)
Volume = 640418.28 (mm^3)
Surface area = 646492.99 (mm^2)
Center of mass: (mm)
X = 35.60
Y = 54.84
Z = 0.00

Stress Simulation

Maximum axial stress = $1{,}452 * 10^8$ [$\frac{N}{m^2}$]

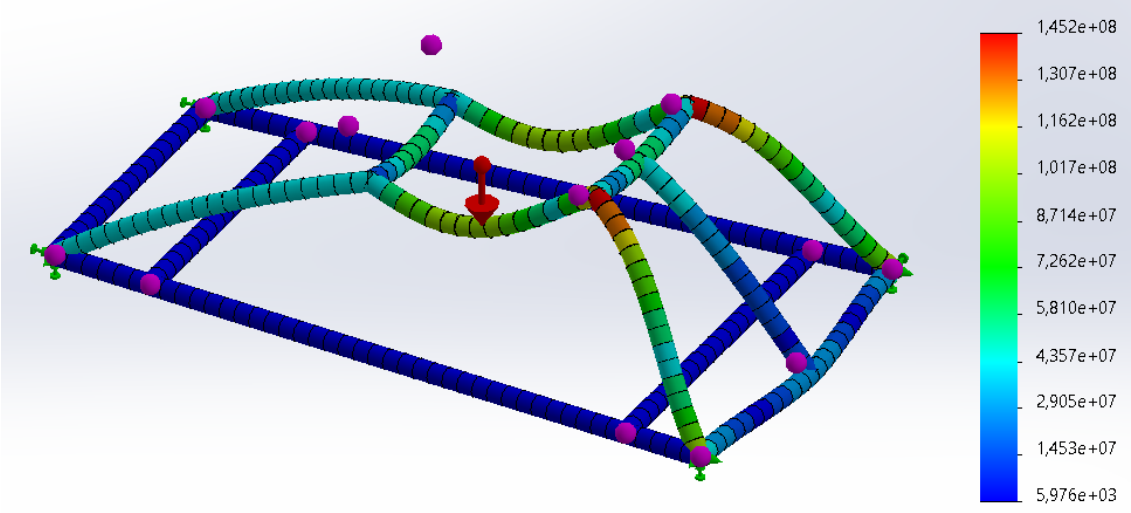

Figure 33. Structure D: Stress study *(Source: own elaboration)*

Minimum SF =1,48

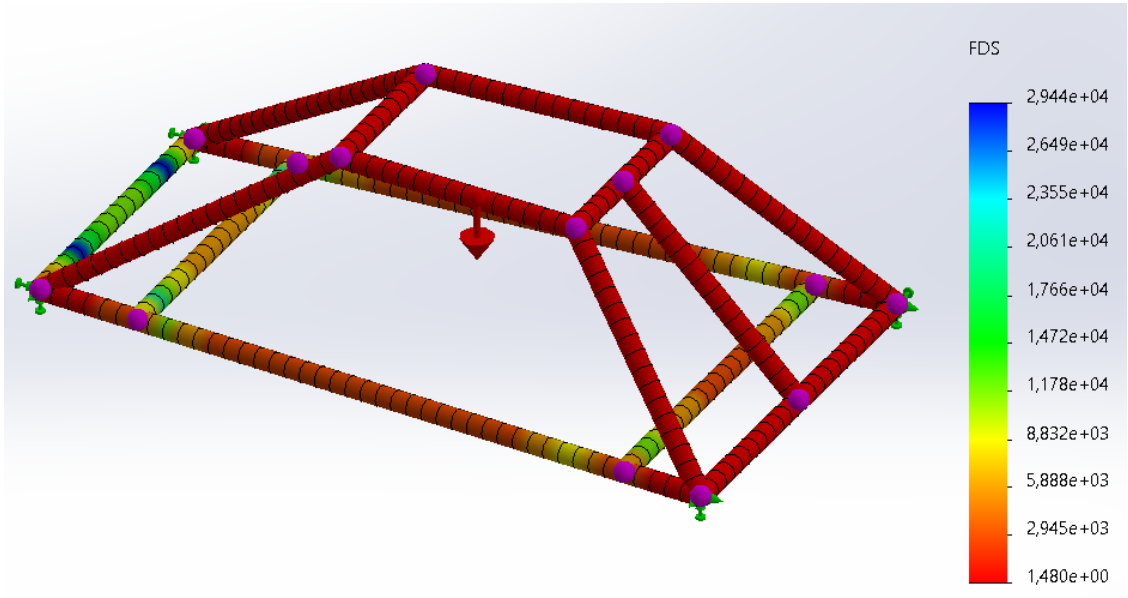

Figure 34. Structure D: Safety Factor study *(Source: own elaboration)*

4.6 Structure Determination

After reviewing and simulating the different chassis models, enough information has been obtained to perform a detailed analysis of the previous simulations.

As previously mentioned, for the results to be valid, the different structures had to be subjected to the same conditions during the simulation, so that they have been carried out by applying 100 kg of mass distributed on the beams that support the plane and defining aluminum as the material. 6063 T6.

For the analysis of results we will focus on 5 fundamental factors that will be key to the study of the structure.

- Mass: it will be the first factor to consider and will determine the lightness of the dolly as a whole. The smaller the better since in this way a smaller dimensioning is required in the propulsion system to achieve the same acceleration.

- CG height: As seen in previous chapters, the height of the center of gravity will largely determine the behavior of the dolly. The lower the CG is, the more stability and drag the dolly will have.

- Max. Stress: It refers to the maximum value of the applied voltage that occurs at the critical point. It will help us, on the one hand, to determine the point subjected to greater axial forces and, on the other hand, to know if the value of the stress at that point is within the permissible limit.

- Min. SF: It refers to the minimum safety factor that will be located at the most critical point of the chassis. The value of SF at the most critical point is obtained by dividing the elastic limit value of the material, in this case aluminum, by the maximum value of the stress at the critical point. This will be the most determining factor when comparing simulation results. In most projects that do not involve especially people's safety (as is the case), the safety factor is usually between {1.2, 1.5}. If the safety factor is placed below this range of values, it could lead to damage to the project. On the other hand, a SF that is too high would mean that the project is oversized and could make it cheaper to maintain its function.

Structure	A	B	C	D
Mass (g)	1645,54	1941,75	1773,91	1729,13
CG height (mm)	53,18	58,42	55,67	54,84
Max. Stress(N/m^2)	1,631*10^8	9,185*10^7	1,275*10^8	1,458*10^8
Min. SF	1,32	2,34	1,69	1,48

Table 5. Chassis Pre-Design

Table 5 shows how the structures behave depending on their level of triangulation. Being "A" the basic structure formed by trapezoids without any triangulation, structure "B" the most triangulated and from here the level of triangulation descends to structure “D”.

As a structure is more triangulated, the trend is as follows:

- The total mass of the chassis increases
- In this case, with the proposed triangulations, the height of the center of gravity also increases.
- Decreases the maximum stress to in the critical point.
- Increases the safety factor by decreasing the maximum applied stress.

On the basis that the safety factor in a project like this must be between 1.2 and 1.5 in order not to under-dimension or oversize the model, the alternatives “B” and “C” are discarded since their SF are above the desired ranges. So the mechanical resistance they provide is not really necessary since the model would be oversized, the only thing that it would do is adding more weight.

Choosing then between options "A" and "D", since they are the only ones that meet all the desired requirements, we will stick with structure "A", since it is lighter and simpler since it includes one bar and two joints fewer, its center of gravity is lower and its safety factor is in the middle of the desired range (which makes it optimal).

On the other hand, it should be noted that since the simulation is being carried out with a supposed load of 100 kg, and the actual load that the plane will suppose does not even reach 10% of it, therefore, all the structures including "A" are oversized because it is not the definitive simulation. The chassis with the structure "A" will be the chosen.

4.7 Material Determination

After confirming with the previous study with aluminum as the assigned material, that the structure is oversized, since it has an SF of 1.3 for a load of 100 kg, it has been decided to eliminate mechanical resistance from the list of characteristics to have into account when choosing the material. This has already been done because of the three possible materials proposed (carbon fiber, stainless steel and aluminum), aluminum, which is the one with which the tests have been carried out, is also the one with the lowest mechanical resistance.

The criteria to be followed for the definition of the material is the one included in table 6.

Material	Aluminum	Carbon fiber	Stainless steel
Technical name	Al. 6063 T6	Thornel mat VMA	AISI 304
Density [kg/m3]	2700	2001	7900
Prize[€/m]	7,5	43	19,35

Table 6. Comparison of the chassis materials

Although stainless steel has good and simple weldability, which would greatly simplify the joining of the bars and would allow the adoption of an identical structure to the one designed without any type of joint, comparing the data in the table, is possible to observe that, its density is excessive in comparison with the other two materials. This would mean a significant increase in the total mass of the dolly and therefore, it is the first material to be discarded.

From here it only remains to choose between carbon fiber and aluminum. Regarding the density of both, carbon fiber has a lower density, but even so, the reduction in mass that would imply adopting carbon fiber as a material instead of aluminum is not significant considering the purposes of this project. If the price of both materials is compared, the price of aluminum is significantly lower. The selection of this material instead of carbon fiber will mean a substantial reduction in the total cost of the project. Therefore, aluminum is the chosen material.

4.8 Types of Joints

In the previous section, the structure and material of the chassis was determined through a detailed study. In this section, the chosen model will be developed to finish designing the final chassis model that will incorporate the dolly. Although the material and shape of the structure to be used has already been decided, there is still a determining factor to consider when making a detailed design of the dolly chassis. This corresponds to the determination of the joints that will join the chassis beams.

The joints that will join the chassis beams has a big importance since the greater axial stress applied to the structure will fall on them. If Figure 25 is reviewed, corresponding to the stress study of structure "A" chosen as the chassis model, it can be seen that it is precisely in the two upper rear joints where the greatest stress is applied, with a value of 1.631*10^8 [N/m^2]. Although this value has been obtained by carrying out a simulation with 100 kg of distributed mass applied on the surface of the dolly at its upper base, an unreal mass value considering the purposes of the project, it is true that the critical point, although on a smaller scale, will be on the rear upper joints.

The types of joints that will be considered for its application in the chassis are the following:

- Permanent joints
- Removable joints

4.8.1 Permanent joints

Fixed joints are those that are designed for those joints in which it is intended to maintain the joint between different elements indefinitely, making disassembly impossible without damaging the joint.

Although there are different types of permanent joints, the most common and used are riveting and welding.

4.8.1.1 Riveting

Firstly, the riveting will be studied, which "is a permanent mechanical fastener. Before being installed, a rivet consists of a smooth cylindrical shaft with a head on one end. The end opposite to the head is called the tail. On installation, the rivet is placed in a punched or drilled hole, and the tail is upset, or bucked (i.e., deformed), so that it expands to about 1.5 times the original shaft diameter, holding the rivet in place. In other words, the pounding or pulling creates a new "head" on the tail end by smashing the "tail" material flatter, resulting in a rivet that is roughly a dumbbell shape. To distinguish between the two ends of the rivet, the original head is called the factory head and the deformed end is called the shop head or buck-tail.

Because there is effectively a head on each end of an installed rivet, it can support tension loads. However, it is much more capable of supporting shear loads (loads perpendicular to the axis of the shaft). " *(Rivet - Wikipedia, n.d.)*

Although the rivet has been the most widely used permanent joining method for much of human history, today due to the increasing application of detachable joints and the

continuous development of advanced welding methods, it only has a reason to be in some specific applications. Some of its main advantages are its simplicity and speed and cadence of application. On the other hand, its main disadvantages as a permanent joint compared to welding is its lack of mechanical resistance. This is due to the fact that in the case of riveting, the joint is made cold and does not involve the fusion of the filler material with the base material. Another of its disadvantages is that due to the movement and vibrations that the dolly joints will suffer under normal conditions during their normal operation, the joints can become wobbly, leading to a lack of stability and resistance of the structure.

For the specific solution that requires the determination of the joints that will join the beams that form the chassis of the dolly, riveting is ruled out as a possible joining method.

4.8.1.2 Welding

The second permanent fixing method is the welding. "Welded joints result in a rigid joint between two or more components. Normally the joining process is carried out by applying heat to two components of the same or similar materials, in addition, material can be applied to the joint or not. The heat causes the materials to melt, joining the different parts and resulting in a weld bead. The thickness of the bead will depend on the thicknesses of the components being joined. During the execution process the materials must be protected from atmospheric gases. There are different types of welding depending on how the materials fuse.

The main welded joints used in the industrial sector are:

- Arc welding.
- Power welding.
- Gas welding.
- Spot welding." - *(CLASSES OF MECHANICAL JOINTS - Bearcat, n.d.)*

The method and therefore the simplicity of the welding operation can vary greatly depending on the material and the conditions. As previously the material and the type of tube of the chassis beams have been defined, we will start from these data to study the appropriate welding method and its feasibility.

The beams defined in the previous section will be made of 6063 T6 aluminum square tube with a dimensions of 15mm x 15mm x 1.5mm. Therefore, we will focus on existing aluminum welding methods. Making a general review of the methods and ease of aluminum welding, we can determine that it is not an easy task. "Since aluminum has a higher thermal conductivity and a low melting point of (650ºC), it has a smaller window of workability than other metals and can easily lead to burn through. This, in combination with it being harder to indicate weld progress and quality, can make aluminum a difficult material to work with.

In sum, here are some of the most common factors that make aluminum challenging to weld:

- Oxidation: On top of aluminum sits an aluminum oxide layer, which melts at a significantly higher temperature than aluminum (1370 ºC). Melting through this layer requires high heat, however, the welder must be careful to not burn holes in the aluminum underneath.

- Porousness: In its molten state, aluminum absorbs hydrogen quicker the more it heats up. This hydrogen separates out as the metal returns to a solid form, which can leave behind bubbles in the material, causing the metal to become porous and weak.

- Impurities: As aluminum is very sensitive, there are several ways it can become contaminated by dirt, air and water during the welding process. Aluminum can become contaminated by air that reaches the weld because of poor shielding or excessively long arcs. Oxygen can reduce aluminum's strength, ductility and cause an oxide formation on aluminum welds, which affects its appearance and complicates multi-pass welding. Hydrogen can come from many sources, such as moisture in electrode fluxes, humid air, damp weld joints and more. For all of these reasons, it's important to clean aluminum thoroughly and store it correctly prior to welding.

- Thickness: Welding aluminum involves working with different material thicknesses. Welders must know how to avoid burning through thinner material while also penetrating thick material enough to create a strong weld." - *(How to Weld Aluminum: The Beginner's Guide, n.d.)*

The difficulties of aluminum welding are increased by the low thickness of the beams that make up the chassis.

Another drawback of welding will be the difficulty of replicating the different chassis units that will be built even using molds. As one of the main requirements of the project is the simplicity and ability of anyone to be able to produce a dolly model with few resources, the welding was discarded as a joining method for the chassis joints.

4.8.2 Non-permanent joints

As its name indicates, non-permanent joints are intended for those joints in which a possible disassembly is provided, either for maintenance, to better transport the object or for any other purpose. These joints will allow the assembly and disassembly of the structure repeatedly without compromising its structural integrity. The most notable are the bolted joints, although there are also other possibilities, as well as staples, clamps, flanges or many others.

4.8.2.1 Bolted joints

"Bolted joints are one of the most common elements in construction and machine design. They consist of fasteners that capture and join other parts, and are secured with the mating of screw threads.

There are two main types of bolted joint designs: tension joints and shear joints.

- In the tension joint, the bolt and clamped components of the joint are designed to transfer ok an applied tension load through the joint by way of the clamped components by the design of a proper balance of joint and bolt stiffness. The joint should be designed such that the clamp load is never overcome by the external tension forces acting to separate the joint. If the external tension forces

overcome the clamp load (bolt preload) the clamped joint components will separate, allowing relative motion of the components.

- The second type of bolted joint transfers the applied load in shear of the bolt shank and relies on the shear strength of the bolt. Tension loads on such a joint are only incidental. A preload is still applied but consideration of joint flexibility is not as critical as in the case where loads are transmitted through the joint in tension. Other such shear joints do not employ a preload on the bolt as they are designed to allow rotation of the joint about the bolt but use other methods of maintaining bolt/joint integrity. Joints that allow rotation include clevis linkages, and rely on a locking mechanism (like lock washers, thread adhesives, and lock nuts)." *(Bolted Joint - Wikipedia, n.d.)*

The optimal option among non-permanent joints is to use bolted joints, since, having all the necessary hardware (nuts and bolts), they allow easy assembly and disassembly of the structure. This will facilitate maintenance or repair of damaged parts easily. On the other hand, complying with one of the job requirements which says that the dolly model in its whole has to be easily reproduced, the use of threaded joints which will follow a normalized standardization, will allow the hardware used to be found in any location. In addition, while with other methods such as manual welding, the final model could vary from one unit to another, with this type of joints the standardization of the model is ensured. Assuming the use of threaded joints, a piece would be necessary to act as a joint between the beams. This is due to the fact that in all the nodes of the structure three bars are joined, therefore, it would be three bars that would have to be screwed to achieve the union. This would imply a significant increase in the total weight because having to use very long screws to cover the thickness of three of the beams at each of the joints. In addition, it would also lead to problems of wobbly between bars since with the vibrations it could become unscrewed.

4.9 Introducing to 3D printing

In order to solve this problem, the proposal made by the Lightening Research Group of the ESEIAAT is to build the parts that will used as joints for the chassis beams with a 3D printer.

The "3D printing, or additive manufacturing, is the construction of a three-dimensional object from a CAD model or a digital 3D model. The term "3D printing" can refer to a variety of processes in which material is deposited, joined or solidified under computer control to create a three-dimensional object, with material being added together (such as plastics, liquids or powder grains being fused together), typically layer by layer."- *(3D Printing - Wikipedia, n.d.)*

The Lightening Research Group of ESEIAAT have provided the 3D printer which is placed in the electrical machines laboratory, as a resource for carrying out the project. The printer used is a Creator 3 model, from the Chinese brand Flashforge established in 2011. It's shown in figure 36.

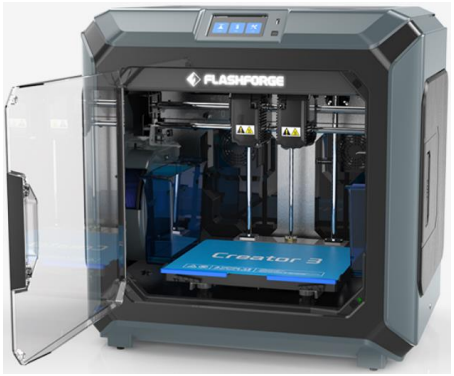

Figure 35. Flashforge Creator 3. *(Source:* (FlashForge Creator 3, 2018)*)*

There are so many types of 3D printer in order to satisfy the following considerations: print quality, print speed, printer cost, practicality, printer capability and user expectations. The nine most commune types are:

1. Stereo-lithography (SLA)
2. Digital Light Processing (DLP)
3. Fused deposition Modeling (FDM)
4. Selective Laser Sintering (SLS)
5. Selective Laser Melting (SLM)
6. Electronic Beam Melting (EBM)
7. Laminated Object Manufacturing (LOM)
8. Binder Jetting (BJ)
9. Material Jetting (MJ)

The one provided by the LRG is a 3D printer which uses the Fused Deposition Modeling (FDM) as a technique to realize the printing job.

The FDM "uses production grade thermal plastic materials to print its 3D objects. It's popular for producing functional prototypes, concept models, and manufacturing aids. It's a technology that can create accurate details and boasts an exceptional strength to weight ratio. Before the FDM printing process begins, the user has to slice the 3D CAD data (the 3D model) into multiple layers using special software. The sliced CAD data goes to the printer which then builds the object layer at a time on the build platform. It does this simply by heating and then extruding the thermoplastic filament through the nozzle and onto the base. The printer can also extrude various support materials as well as the thermoplastic. For example, as a way to support upper layers, the printer can add special support material underneath, which then dissolves after the printing process. As with all 3D printers, the time it takes to print all depends on the objects size and its complexity." - *(Types of 3D Printers: Complete Guide - SLA, DLP, FDM, SLS, SLM, EBM, LOM, BJ, MJ Printing, n.d.)*

As we can see in the datasheet shown in figure 37, the Creator 3 has two independent extrudes which can use a lot of types of support filament like PLA/ ABS / PVA / PETG / WOOD… So it would be a future task to select the 3D printing material. On the other hand, it's also important to notice that the printer has a 4,5-inch touch screen which we will use to carry out the different actions. The printer also has a camera to observe de printing remotely and different communications like Wi-Fi or Ethernet.

Print	
Extruder Number	2, Independent
Extruder Diameter	0.4 mm
Maximum Set Temp. of Extruder	300 ℃
Maximum Set Temp. of Platform	120 ℃
Print Speed	10-150 mm/s
Support Filament	PLA / ABS / PVA / PETG / HIPS / PA PC / WOOD / ASA / PA-CF / PA-GF
Print Volume	300*250*200 mm
Layer Resolution	0.05-0.4 mm
Print Resolution	±0.2 mm

Device	
Device Measure	627*485*615 mm
Screen	4.5-inch Touch Screen
Net Weight	40 kg
Gross Weight	52 kg
Input	100-240 VAC, 48-63Hz
Output	24 V, 20.8 A
Power	500 W
Internal Storage	8 G
Spool	48 mm
Contain Spool Diameter	53*200d*69h
Internal Storage	8G

Software/Communication	
Data Transmission	USB stick, Wi-Fi, Ethernet FlashCloud
Software	FlashPrint
Input	33mf / stl / obj / fpp / bmp / png jpg / jpeg files
Output	gx/g files
Output	Win 7/8/10, Mac OS, Linux

Others	
Camera	1
Filter Fan	1
Guider IIs High Temp. Version	Nozzle 300
Noise	55 dB
Working Environment	18-30 ℃

Figure 36. Flashforge Creator 3 datasheet. *(Source:* (FlashForge Creator 3, 2018)*)*

4.10 Material selection

As shown in figure 37, the printer is capable of printing with 10 different types of material. For the selection of the material, a comparative table has been studied, in which the relevant characteristics of the main possible materials to be used are summarized in the figure 38. Its datasheet are attached in the annex.

Filament Material	Super Power	Best Suited For	Printing Temp	Heated Bed	Strength 1-5	Durability	Flexibility	Ease of printing	Price (approx)
PLA	All-natural and Biodegradable	Prototypes and products	180-210°C	20-45°C	3	2	1	5	£31.96/KG
ABS	Strong and durable	End-use parts and casings	230-250°C	90-95°C	3	3	1	3	£31.96/KG
PLA Plus +	Very durable biopolymer	Vibration absorbing and less brittle version of PLA	220-240°C	50-60°C	3	3	2	4	£36.95/KG
Nylon	Extremely durable and flexible, low friction.	High impact or high stress parts – fantastic all-rounder	255-275°C	100-110°C	4	5	3	3	£37.96/0.5KG
PETG	Extremely durable and flexible	High impact or high stress parts	220-245°C	70-80°C	4	4	3	4	£39.95/KG
ASA	Strong, UV resistant alternative to ABS	Outside casings, covers and devices.	230-250°C	90-100°C	4	3	1	3	£42.95/KG

Figure 37. Filament comparison *(Source: (Rigid Ink | 3D filament comparison, 2019)*

As we can see, figure 38 offers us a comparative table of the different properties of the main materials for 3D printing. The table is made up of different columns corresponding to the element to be studied. First, the material to be treated is described, then its special property or its most outstanding characteristic is discussed. Its main use is mentioned in the next column, then the printing temperature of the extruder and the base is specified. Strength, durability, flexibility, and printability properties are then scored on a scale of 1 to 5, with one representing the minimum value and five the maximum value. Finally, the price in pounds / kilogram of each of the materials is compared. For a correct determination of the material to be analyzed, a detailed study of the properties and requirements of each of the possible materials has been necessary. As before, the Pugh matrix will be used for material determination. First, the importance scale of each of the factors to be analyzed will be determined, as shown in table 7.

Criteria	Importance
Printing T	1
Strength	5
Durability	4
Flexibility	4
Ease of printing	3
Price	2
Eco-Friendly	5

Table 7. Importance of each criteria in filament selection.

In the specific case of this project, regarding the factors that are analyzed, the following can be determined:

- Regarding the printing temperature and the base, we want it to be as low as possible since fewer requirements will be demanded from the printer. Although it will not be a determining factor since all the temperatures of the above materials are within the working ranges of the printer.

- The mechanical resistance will be the most determining factor, since, as has been seen previously, the greatest tensile stresses are located in the joints. We will be interested in a material with high mechanical resistance.

- Like resistance, durability and elasticity will also be physical factors of great importance for the integrity of the structure

- The ease of printing is also an important factor to consider since, not having experience in 3D printing, it will be interesting to choose a material that is easy to print, so as not to waste a lot of time in the production of the components.

- The price is very similar between the different materials, so it will not be one of the important criteria to take into account, since at the scale of the project, the difference is not significant.

- Another factor to take into account that was not shown in figure 38 is the impact on the environment that the studied materials may have. As the environmental problem is a global problem that is becoming more and more present, a five-point importance has been given to the environmental criterion. So the material that scores 5 on this criterion means that it is completely recyclable.

Although the printer is capable of printing many types of materials, we will be based on the most basic and used in the world of 3D printing such as PLA, ABS and PETG. This is because there is much more information about the use of these materials as well as support guides. But above all, because they are the easiest filament materials to find worldwide.

Starting from the defined criteria of more and less important factors for the selection of the material defined previously, we will now focus on the comparison matrix or Pugh matrix that is shown in table 8..

The scoring scale from one to five of each of the factors to be considered is multiplied by the importance of each factor (also on a scale of one to five) in relation to the selection criteria. When the scores for each of the materials have been calculated, a comparison will be made between those that have obtained a similar score to end up choosing the final material for the chassis joints. The datasheet of the materials used in order to determine the punctuation of each of them are attached in the annex.

Criteria	Importance	PLA	ABS	PETG
Printing Tº	1	5	2	4
Strength	5	3	3	4
Durability	4	2	3	4
Flexibility	4	1	1	3
Ease of printing	2	5	3	4
Price	1	5	5	2
Eco-Friendly	5	5	2	3
RESULTS	-	72	58	77

Table 8. Comparison matrix of the chassis material

As shown in table 8, the comparison between the possible materials has been favorable for PETG, highlighting above all its mechanical properties like the resistance, durability and elasticity. Although PETG is the most favorable according to the table, PLA has been very close, standing out above all in its ease of printing and its respect for the environment as it is completely recyclable.

Therefore, although PETG will be used in the manufacture of the joints, the use of PLA in other parts is not ruled out.

4.11 Joint Design

Now that the PETG has been determined as the material to be used, we will proceed to the SolidWorks design of the parts that will join the chassis beams.

The only criteria to take into account during the design is to ensure adequate mechanical resistance and functionality, trying not to oversize the part so as not to waste material, reduce costs, lighten the dolly and above all to reduce the printing times of the 3D printer.

In reference to the design and functionality of the joint, the proposal made consists of a type of joint with the same shape as the beams used. The joint has been designed as a node, so that each of them will join three bars that will be coupled inside the joint. To ensure the union, a through bolt with a nut at the other end for each beam will be provided, which will connect each of the three bars to the joint. In addition, to ensure that there is no wobbly between the join part and the chassis beams, the inside hole of the joint will be the same dimensions as the beam, plus a tolerance of 0.15mm to facilitate mounting. This tolerance has been determined since it is the average value of distortion that PETG undergoes when printed in 3D.

As each joint joins three bars with different angles, a different part will have to be made for each of the dolly joints, the right and left profile of the dolly being symmetrical, if we look at the dolly from the front.

The detailed design of each one of them will be attached in the annex, with the corresponding manufacturing plans and files, but in this document as a memory only the upper rear joints will be studied, as seen in image 25, which showed the stress study of the

chosen structure "A", it is where the critical point with the highest tension of the chassis is applied.

Figures 39 and 40 show the proposal for the upper rear joints, which as mentioned, are the ones that are subjected to the greatest tension. In the following images, the one on the left side is specifically shown. The one on the right side will be symmetrical to the one shown, regarding to the central profile of the dolly.

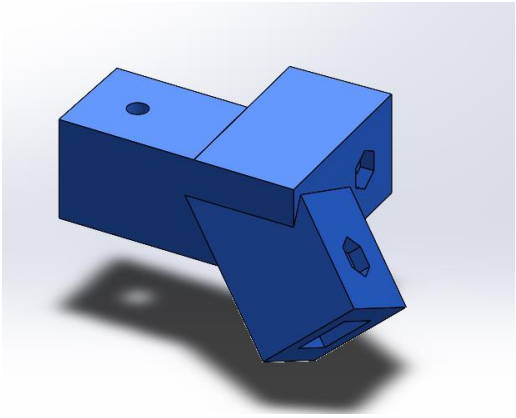

Figure 38. Joint design view 1 *(Source: own elaboration)*

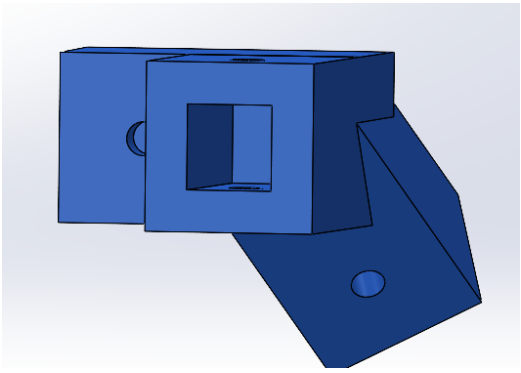

Figure 39. Joint design view 2 *(Source: own elaboration)*

In the previous figures, the design proposed for the joints between beams that as a whole will form the chassis is shown. Even so, to validate the design, a structural study of the part will be carried out with SolidWorks Simulation used previously.

4.12 Study and validation of the joint

In order to validate the design made and to be able to follow with the development of the project, it is necessary to determine that the resistance offered by the designed part will be sufficient to withstand the loads applied during its operation, thus ensuring the integrity of the structure. For this, a structural study has been carried out using the finite element

method that has been carried out as well as before with the used software, SolidWorks Simulation.

To determine the load to which the part will be subjected, since not all the weight of the plane will fall on it, it is difficult to study the distribution of loads that will act on each joint without having the final model defined. In addition, another factor to take into account is that in the simulation a completely solid piece is considered while in reality the piece will be formed by a structure with a percentage and a specific type of filling, which leaves empty spaces to lighten weight and reduce the printing time compared to a completely solid piece. Depending on the results obtained in the simulation, the percentage of filling of the piece will be chosen, as well as the type of structure.

Regarding the parameters of the simulation, the following criteria will be followed: the material specified for the part will be the PETG since it was the chosen material according with the material study. For the definition of the fasteners which will fix part during the simulation, it has been chosen to fix the three bottoms of the interior hole of the joint, leaving the three beams that the joint joins cantilevered as if the lateral and upper walls of each of the grooves were not supported by the beam that goes inside.

For the simulation, three key factors will be studied: first, a stress and safety factor analysis will be carried out, as was done previously. In addition, in this case, a study of the displacements suffered by the part will also be carried out to simulate the deviations that may occur and which points are the most susceptible to it.

Finally, comment that two simulations will be carried out, defined below:

4.12.1 Simulation 1

In the first case, the real weight on the joint will be simulated, taking into account that it is a solid part and therefore it will be more resistant than the final one, which will not be fully solid, these results are only indicative and cannot be taken as definitive since the final result will be less resistant than the one studied.

Since the airplane will rest on a base and this in turn will rest on the 4 upper joints, to determine the load that the weight of the airplane will carry out on only one of the joints, the mass of the airplane has been divided by four and has added an additional 15% mass, as a safety factor, as the design is not yet fully defined.

$$m_{UAV} = 3{,}250\ kg$$

$$15\%\ of\ m_{UAV} = 0{,}4875\ kg$$

$$m_{SF} = 3{,}25 + 0{,}4875 = 3{,}7375\ kg$$

$$m_{gasket} = \frac{3{,}7375}{4} = 0{,}934375\ kg \quad \rightarrow \quad F_{gasket} = 9{,}166\ N$$

If we apply a distributed load of 9.166 N on the upper surface of the part, the results obtained for Von Misses stress $\left[\frac{N}{m^2}\right]$, displacements [mm] and safety factor, are shown in figures 41, 42 and 43.

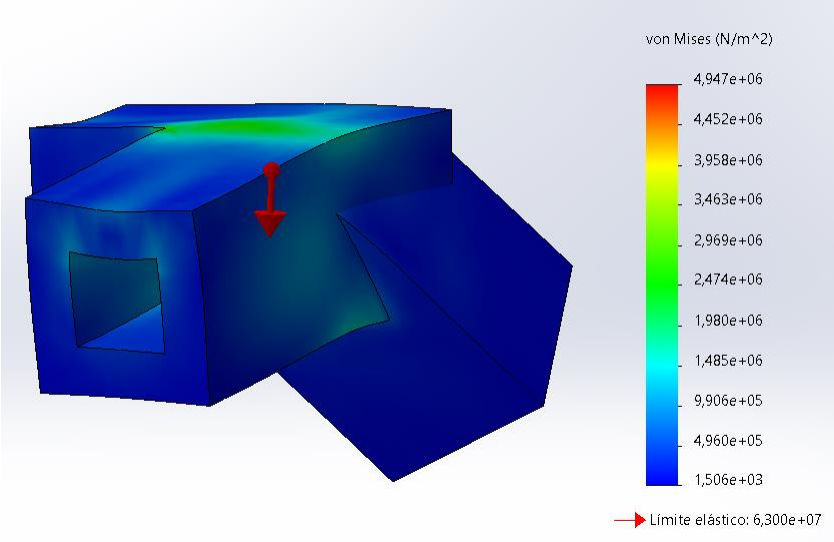

Figure 40. Simulation1: Von Misses stress study *(Source: own elaboration)*

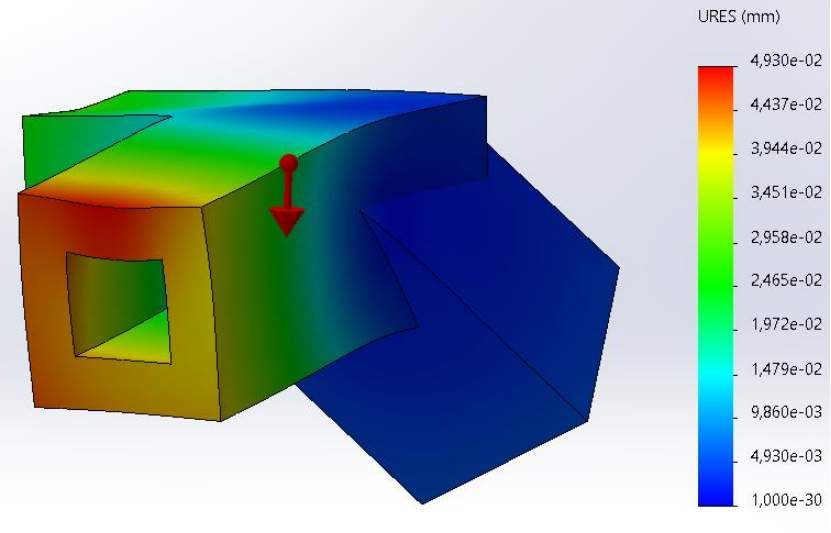

Figure 41. Simulation 1: displacements *(Source: own elaboration)*

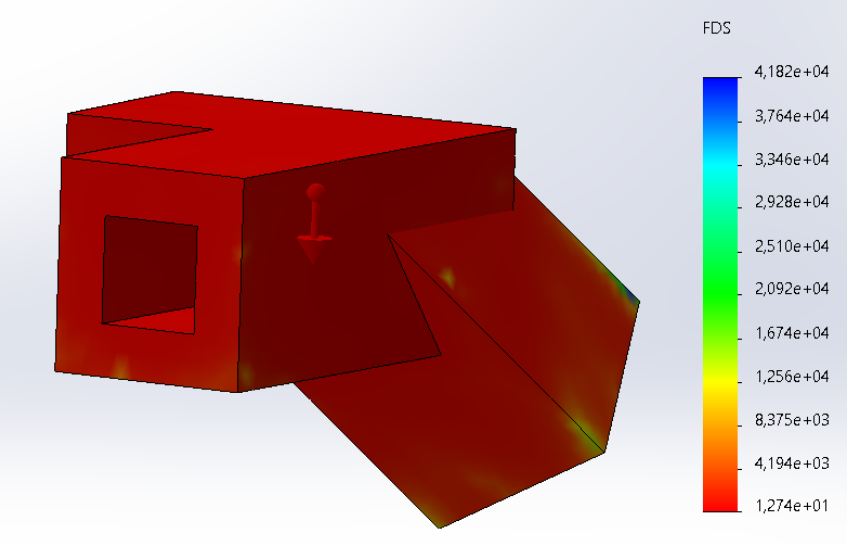

Figure 42. Simulation 1: safety factor *(Source: own elaboration)*

As can be seen in the previous figures following the color code, the part is very oversized for the applied distributed load, this is because, as mentioned, the simulation has been carried out considering a solid part while the actual 3D printed part will have a certain fill percentage and a specific structure to be determined later.

Still we can draw conclusions from this simulation. In the first place, it can be observed in figure 41 that the point subjected to the most tension is concentrated in the central part of the joint, where the longitudinal axes of the three beams would meet. On the other hand, in figure 42 we can see that the maximum displacement will occur at the cantilevered end of one of the three grooves. The fact that it occurs in this one in particular and not in the others, is that it is the longest of the three, therefore the bending moment of this one will be higher. Even so it is very small and insignificant. Finally, looking at figure 43, we can determine that the minimum SF will be 12,7 with the distributed load of 9.166 N. The oversizing of the part for this load can be clearly seen.

4.12.2 Simulation 2

For this second simulation, it has been decided to gradually increase the distributed load to which the part will be subjected in order to analyze how many [N / m ^ 2] will be necessary to achieve a safety factor between 1.2 and 1.3. All this taking into account that a completely solid piece of PETG is being considered.

After performing various simulations, it has been determined that the distributed load applied to the upper surface, necessary to obtain an SF of 1,275, is 735.75 N, the equivalent of 75 kg of distributed mass. This makes us appreciate the very high mechanical performance that this material provides.

The fixations and material have remained the same as in simulation 1. The results are shown below:

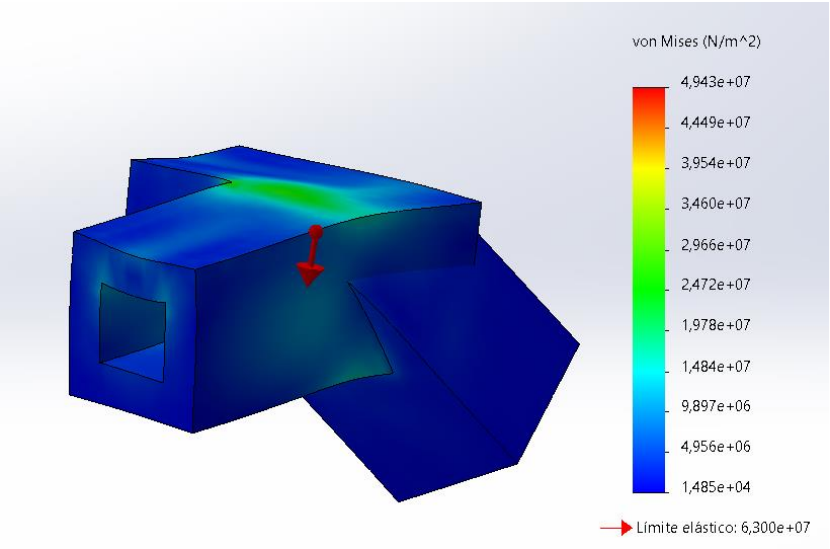

Figure 43. Simulation2: Von Misses stress study *(Source: own elaboration)*

From the study of Von Misses stresses shown in figure 44, we can determine that the most affected area, as in simulation 1, is the one comprised in the midpoint of the three grooves. As the applied load has increased, the maximum stress value for that point has also increased, which in this case is 49 MPa while the elastic limit of the material is 63 MPa.

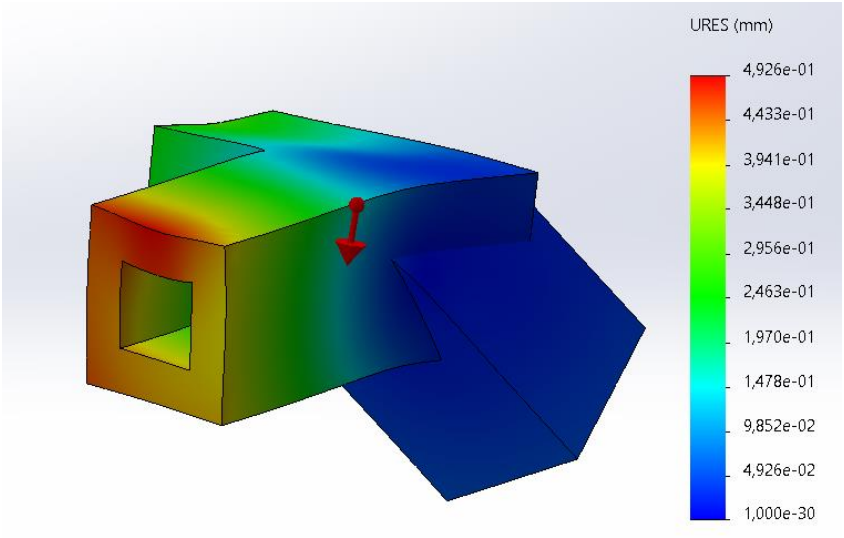

Figure 44. Simulation 1: displacements *(Source: own elaboration)*

In the displacement simulation, the most affected area also coincides with that of simulation 1. In this case, the maximum displacement value is 0.5 mm. It is within the allowed range.

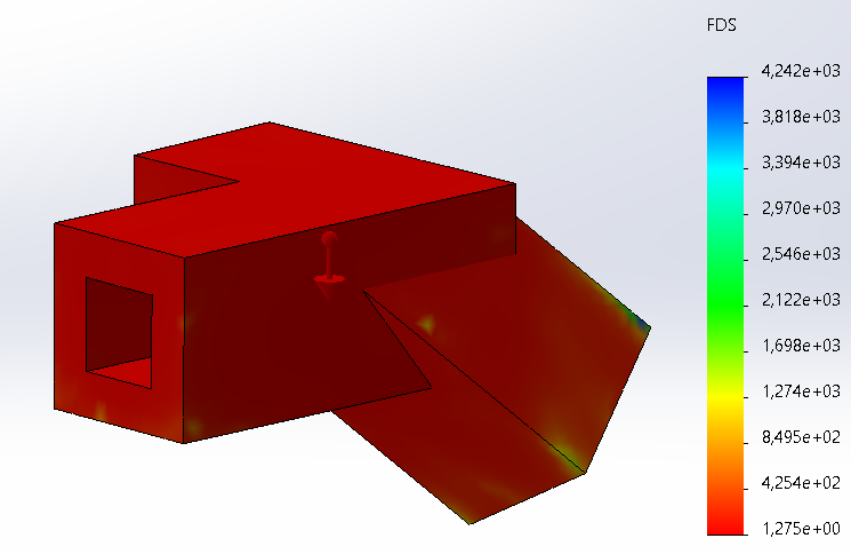

Figure 45. Simulation 1: safety factor *(Source: own elaboration)*

As shown in the previous results, following the color code, we can see that the most affected areas coincide with those of simulation 1, because the working conditions are identical except for the applied load, which is now higher. For this reason, the values of the simulation results are also higher.

The study of simulation 2 has served above all to make a dimensioning of the structure pattern and the amount of filling that will be necessary for the elaboration of the pieces.

As the SolidWorks program does not allow the consideration of partially hollow parts or with a certain pattern of internal structure, simulation 2 has been carried out to check what would be the distributed mass with which the part would be working with an SF within the stipulated ranges, in the event that the joint was solid. It has been concluded that if the joint were solid, it could support 75 kg of distributed mass working with a safety factor within the stipulated margin.

Extrapolating these results to a partially hollow part, we know that if it had a 100% fill it would be able to work in the previous conditions, much higher than those required in the project.

4.13 Printing Parameters Specification

As mentioned above, in the parts created with a 3D printer, a fill percentage must be defined, as well as the internal structural pattern. The mechanical strength and lightness of the final piece will depend on these characteristics, as well as the printing time necessary to make it. To determine the structural pattern and the filling percentage of the piece, it is only a matter of finding the balance between the desired resistance on one side and the mass and printing speed on the other. The more we want to increase the first, the more the other two properties will decrease.

4.13.1 Internal structure pattern

"In addition to filling the empty space, the filling in 3D printing will define the resistance of the part in question. Depending on the type of filling and its density, we will have a different resistance, which can be customized for our application in question. The creation of the fill type is carried out by the software itself (or Slicer). So as a user, you simply have to select the desired type. Another detail to take into account is the printing time. Depending on the shape of the filling, it can vary considerably. A complex 3D printing fill will take more time than a simple one." *(Traduced from) - (Rellenos En Impresión 3D. Definen Estructura, Resistencia y Peso., n.d.)*

The existing infill patterns are shown in figure 47.

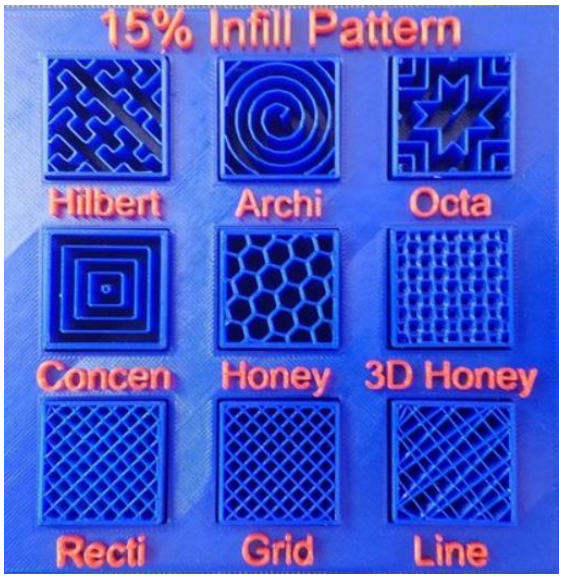

Figure 46. Infill patterns *(Source: (*Starffin Peter, 2019) | *3D printing infill patterns)*

Since not all 3D printers are capable of printing all the infill patterns seen in the previous figure, only the main and most used ones will be studied. These are the following patterns:

- Rectangular or rectilinear fill: this type of filling is the most used today, since it is configured by default in almost all 3D printing software. Offers good resistance in any direction and its printing speed is high.

- Triangular or diagonal fill: this filling is usually used when we need more resistance in the walls of the piece. It is also recommended for long and thin pieces.

- Honey: it is another type of widely used filler. It gives a fairly high resistance in all directions of the piece. Of course, the printing speed is somewhat lower than a triangular or rectangular filling.

For the purposes of this project and after having analyzed the simulation studies, it has been determined that the best structural pattern is honey since, although the printing time increases a little, it is the one that offers the most resistance in all directions.

4.13.2 Infill density

As discussed, the fill density will greatly affect the strength, density and printing time of the part. The higher the fill percentage, the more resistant the piece will be, but on the other hand, the heavier it will be and the longer it will take to print. In the picture 48 below it's possible to see the differences between infill density, applied to the honey pattern.

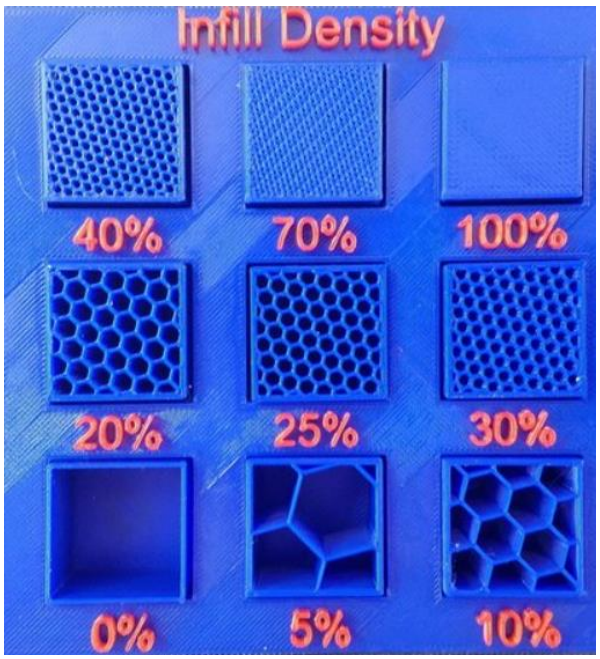

Figure 47. Infill density. *(Source: (*Starffin Peter, 2019) | *3D printing infill patterns)*

After studying the advantages and disadvantages of increasing or decreasing the filling density, it was compared with the simulation graph obtained in figure 46. In this simulation, the safety factor of the part was analyzed with an infill density of 100% and it was determined that it was possible to work with up to 75 kg of distributed mass within the desired ranges. As the actual mass that the part will have to support in normal operation will not exceed 1 kg, it has been determined that a fill density of 25% will be used. Surely less could be used, but to prepare for the stresses that will be applied during assembly, which will be greater than those applied in normal use, that will be the chosen fill density.

4.14 Chassis final design

After the study and subsequent analysis of all the elements that comprise it, the final chassis model that will be used for the dolly has finally been obtained.

As can be seen in figure 49, many elements still need to be added, such as the wheels, the steering system, the motor, the battery, the microcontroller ... Even so, the base to which all the components will be assembled already has been designed.

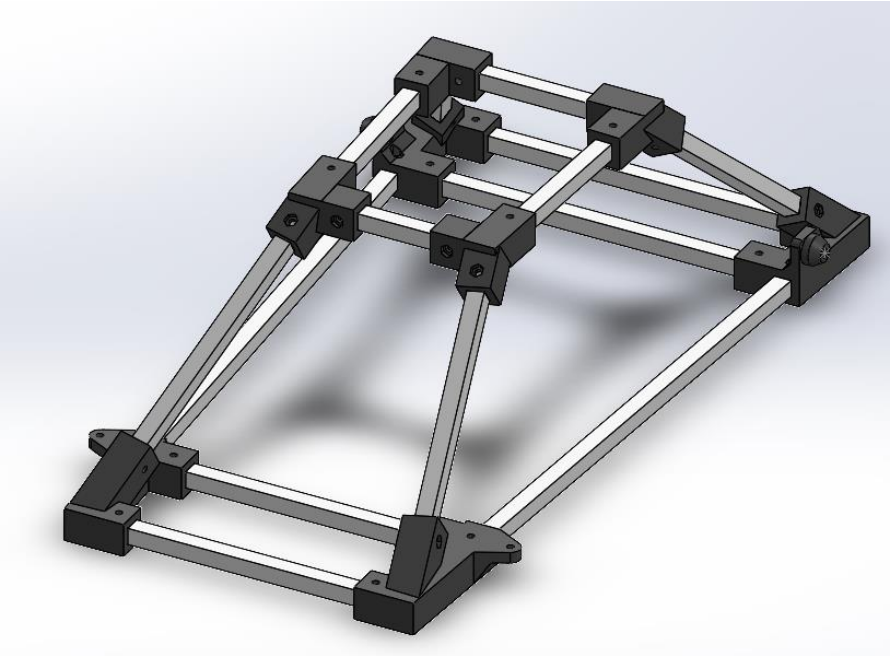

Figure 48. Final chassis design *(Source: own elaboration)*

As shown in the image above and as determined throughout this chapter, the main structure of the chassis will consist of eight joints made of PETG with a honey infill pattern and a density of 25%. On the other hand, the structure will also have fourteen 15mm x 15mm hollow square bars, with a thickness of 1.5 mm on each side. The material for the bars that will serve as the chassis structure will be aluminum 6063 T6.

5 Mechanical Design of the Steering System

With the final chassis model defined, work can begin on the next step, which will be the definition of the steering system. Following the requirements and objectives of the project, the steering system will serve to compensate possible deviations caused by unevenness or irregularities on the track or by the action of external phenomena. The steering system must be able to ensure the correct operation of the system, ensuring stability and integrity between the dolly-UAV assembly.

Although the steering system in its entirety will also consist of a heading control system which, through the use of electronic components and proper programming, will regulate the system to maintain a fixed direction, in this chapter we will focus exclusively on the steering system design of the mechanical parts that will physically allow the rotation and turning of the wheels.

For the complete definition of the steering system, a specific structure will be followed, with the aim of analyzing the phenomena and physical principles that take part with their respective simulations, as well as carrying out the pertinent calculations to conclude on the 3D design of the parts. that will constitute the system.

5.1 Study of the steering principles

Before starting with the study and design of the different components that will make up the steering system, it is necessary to review the physical principles involved in the steering maneuver.

In an ordinary car, “the steering system converts the rotation of the steering wheel into a swiveling movement of the road wheels in such a way that the steering-wheel rim turns a long way to move the road wheels a short way.”-*(How the Steering System Works | How a Car Works, n.d.).* In this project, this will not be the case, since the steering wheel will not be involved, but by means of another elements,the system it will be able to regulate itself. Even so, the principle of operation of the steering system will be the same as that of any vehicle.

5.1.1 Ackermann principle

The principle by which absolutely all well-designed steering systems are governed, in vehicles with 2 or more steer wheels, is the Ackermann principle.

In general termns, the “Ackermann steering geometry is a geometric arrangement of linkages in the steering of a car or other vehicle designed to solve the problem of wheels on the inside and outside of a turn needing to trace out circles of different radius.”-*(Ackermann Steering Geometry - Wikipedia, n.d.)*

Thus, Ackermann's principle is nothing more than the geometric principle that defines that for the performance of a smooth and effective steering system that prevents the steering wheels from slipping, the outer wheel when turning will always have a lower angle than the inner wheel, since the circumferential radius that the outer wheel will draw will be greater

than that of the inner wheel. In case this is not fulfilled and the wheels are parallel during the turn, their trajectories will coincide at one point, losing stability and causing the front axle of the vehicle to slide. To avoid this, as shown in the figure 50, the instantaneous geometric center of the turn, in which the centers of the circumferences described by both wheels will coincide, must always be located at some point along the rear axle of the vehicle.

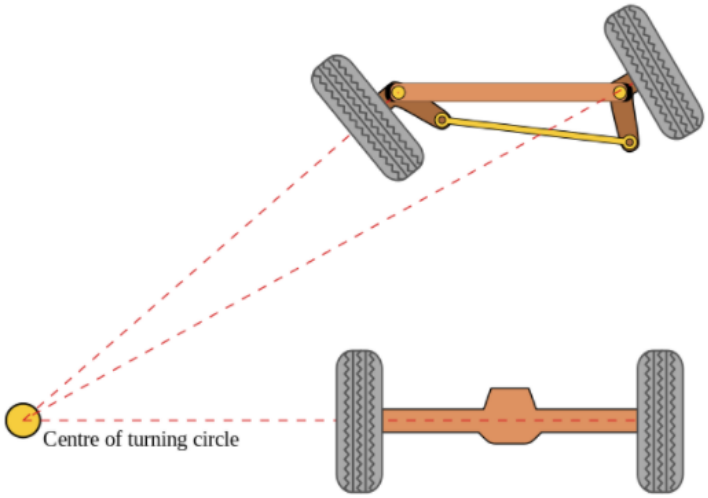

Figure 49. Ackermann principle 1. *(Source:* (*Ackermann Steering Geometry - Wikipedia*, Szakács, 2010)

As shown in figure 51, the way to achieve this type of geometry in which the centers of the circumferences traced by the displacement of the wheels during the turn coincide at a point aligned with the rear axle of the vehicle, is to design the steering levers at an angle such that the extension of it coincides in the center of the rear axle, with the wheels completely straight.

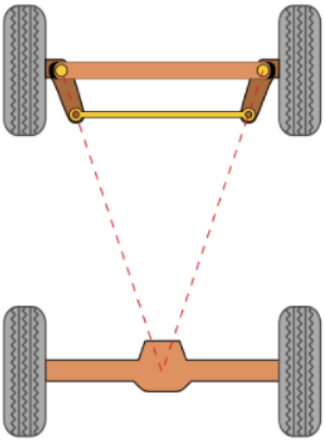

Figure 50. Ackermann principle 2. ((Source: (*Ackermann Steering Geometry - Wikipedia*, Szakács, 2010)

If we delve on it, "Ackerman is the difference in turn radius between the front tires. On oval track cars it can be desirable to create a situation where the left front tire turns faster than the right front tire. The Ackerman effect can help the car turn better through the center of the turn. You can measure the amount of Ackerman you currently have by using a set of turn plates. Typically, Ackerman is measured by turning the right front 10 degrees to the left. If you have Ackerman, the left front will travel further than the right front. A typical amount would be three degrees in 10 degrees of steering. To simplify, moving the right front from zero through 10 degrees of steering will cause the left front to move say 13 degrees in this scenario. Ackerman is created by your front end geometry. Tie rods that angle forward from the inner pivot point out to the spindle will have more Ackerman.

You can usually adjust the Ackerman by moving the left front tie rod end in a slotted spindle arm. Moving the tie rod end closer to the ball joint will create more Ackerman. Some cars use an offset slug design to make the adjustment. Offset wheelbases have an effect as well.

Just like with rear stagger, too much Ackerman will make the car loose on turn exit or will cause premature tire wear. Too much Ackerman can over heat the left front so that it will not perform on the long run. Just as with rear stagger the right amount of Ackerman will help you through the middle of the turn. Too much and you will not be good on the long run. Through trial and error, you can fine tune the car with Ackerman. Too much can also slow the car down as your horsepower has to overcome the dragging of the left front through the turn. The dragging condition will also be very hard on the performance of the left front tire.

On small tracks Ackerman can be added in aggressive amounts to see if there is a gain to be had. On large tracks a finer adjustment should be utilized. Remember that Ackerman will have the most effect on the car at the apex of the turn. At the apex, the steering is turned to the maximum amount for that turn. While Ackerman has an effect whenever the wheels are turned the effect is going to be most dramatic at the apex. There are times when the car will cut to the center better on turn entry due to the effects of Ackerman. In this condition, chassis set ups or track layouts load the left front tire more helping the car get to the center. While the turn in benefit helps, it may cause a loose condition on exit due to the steering being overturned at that point in the corner. A balance must be found. You may find that you notice the Ackerman effect on higher banked tracks due to the loading of the left front whereas on flat tracks the left front has less weight on it causing more of a undesirable dragging condition" - *(ACKERMAN EFFECT, n.d.)*

5.1.2 Simulink simulation

Next, a 2D simulation of the vehicle will be carried out with the Simulink tool during its movement and in which it will be possible to observe the differences between the path followed by the center of gravity and the rear axle of the vehicle.

The simulation will also help define the maximum turning angle that the front wheels should make, as well as the minimum circumference radius that the dolly will be able to make.

To carry out the simulation, an existing Simulink program "Kinematic Steering Model - Rolling without slipping", by (Marc Compere-2011) has been used and modified, adapting it to the characteristics of the dolly that is treated in this project. The parameters that we have

modified regarding the original study are the wheel base and the track width. The program has been simulated according to the block diagram shown in figure 52 and 53.

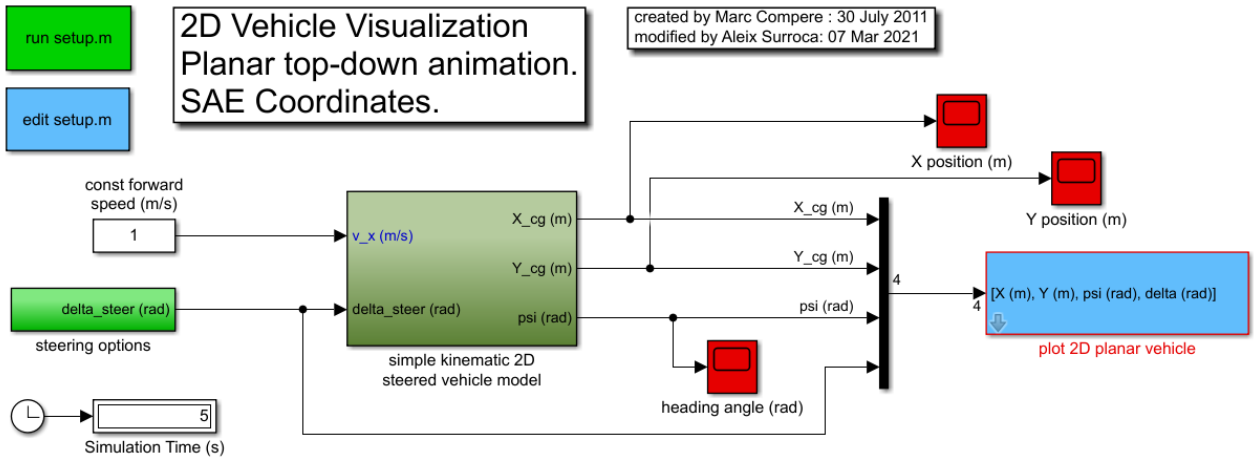

Figure 51. Simulink simulation block diagram 1. *(Source: Kinematic Steering Model – Marc Compere)*

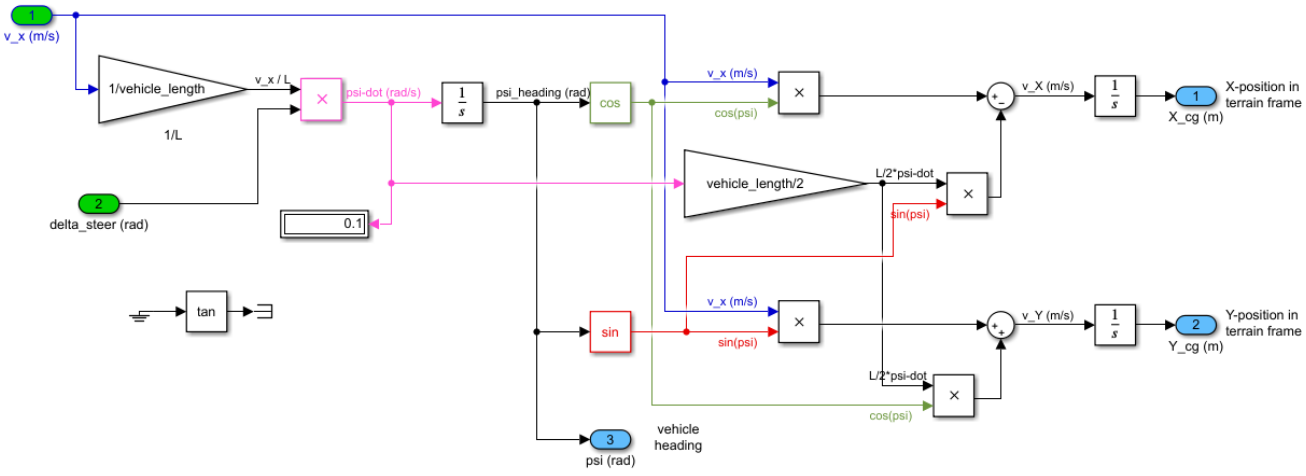

Simple kinematic vehicle model of wheelbase length L and width W.
Non-holonomic constraints on front and rear wheels allow rolling at low speed with no slipping:

$$v_X = [\, v_x \cdot \cos(\psi_{heading}) - (L/2)\cdot\omega_z \cdot \sin(\psi_{heading}) \,]$$
$$v_Y = [\, v_x \cdot \sin(\psi_{heading}) + (L/2)\cdot\omega_z \cdot \cos(\psi_{heading}) \,]$$

where:
v_x - body-fixed vehicle velocity
v_X - terrain frame X velocity
v_Y - terrain frame Y velocity
ψ-dot - same as ω_z
ψ-dot - $(v_x/L) \cdot \delta_{steer}$

Figure 52. Simulink simulation block diagram 2. *(Source: Kinematic Steering Model – Marc Compere)*

If we execute the modified program for a simulation time of 30 seconds, the results obtained are shown in figures 54 and 55.

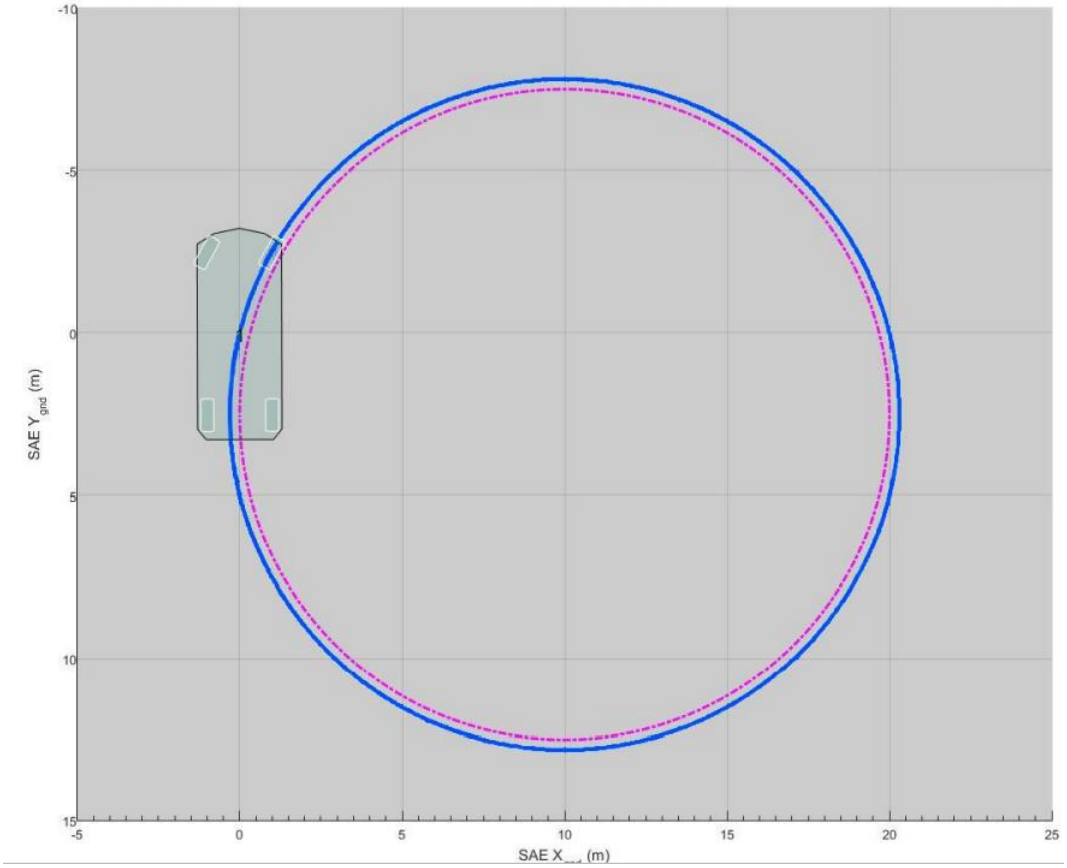

Figure 53. Simulink simulation: radius of turn. *(Source: own elaboration)*

In the image 54 above, it can be seen that according to the physical parameters of the dolly (wheelbase and track width) configured in the program to carry out the simulation, the dolly will be able to make a complete turn by tracing a minimum circumference of 10 m radius. Since the main function of the dolly is to maintain a fixed direction in a straight line and the turns it makes will only be to correct small deviations, it is important that the minimum turning radius is high, to ensure smooth turns and avoid the loss of stability that could occur by taking an excessive turn.

After performing the simulation, it is considered that the minimum turning radius of 10 m is within the desired range in accordance with the requirements and objectives discussed.

On the other hand, in figure 55 below, the different trajectories that follow different points of the dolly are shown. With the blue color, we can appreciate the trajectory that the center of gravity of the dolly follows, which is characterized by a discontinuous path. On the other hand, highlighted in purple, you can see the trajectory that the center of the rear axle of the dolly follows, which is completely continuous, unlike the previous one.

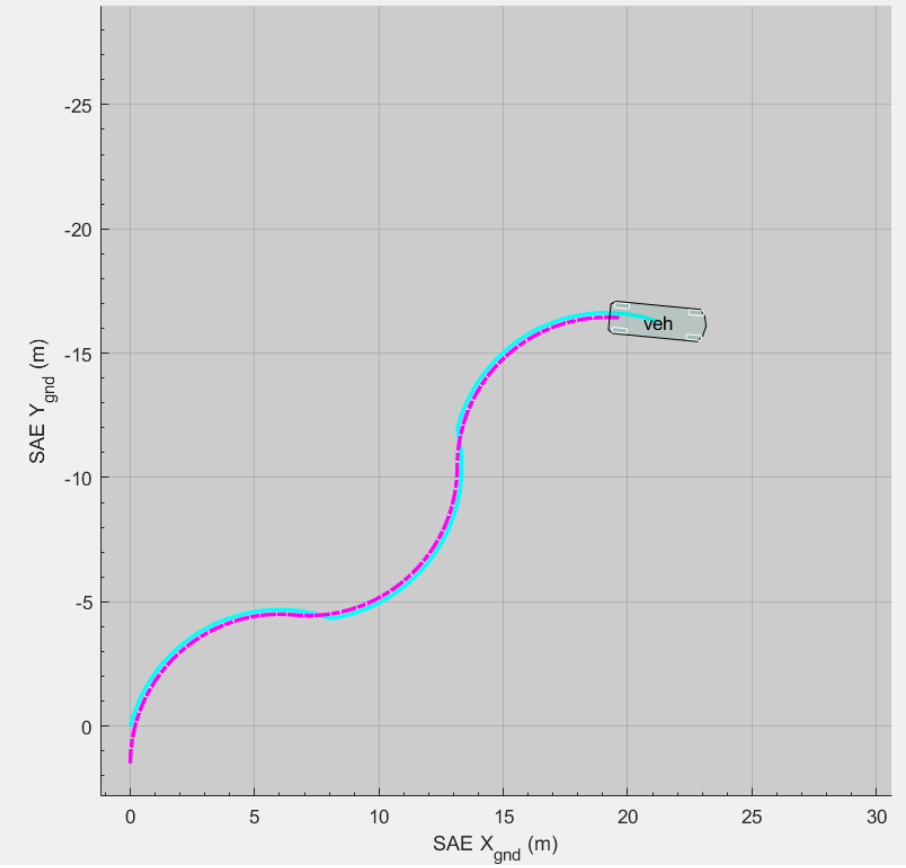

Figure 54. Simulink simulation: trajectories of the CG and the center of the rear *axle*. (*Source*: own elaboration)

5.2 Study of the existing mechanical steering systems

After having reviewed the main factors that must be considered for the design of the steering system, we will now focus on studying the types of existing steering systems to analyze them and choose the most convenient for the operation of the dolly.

As the existing information regarding the steering systems used in dollies is practically nil, we will focus on the steering systems used in cars to acquire knowledge about the operation of each of the models and then select the most suitable system.

Although it is true that throughout history many different types of steering systems have been used, depending largely on the technology and budget available, but also of the requirements of each application. In this project only the two methods most used today worldwide since they are considered the most effective and economical, will be studied. These are the crank steering system, and the rack and pinion system.

It should be noted that the proposed steering systems have not considered the possibility of adopting a suspension system, since initially it is not considered necessary. This is because the plane is intended to be taken off on an asphalt runway under normal conditions. In any case, the adoption of a suspension system for the dolly will be left to the section on possible improvements or future modifications.

5.2.1 Crank and connecting rods steering system

The crank and connecting rod steering system, although it is not currently used in the manufacture of automobiles due to its high number of moving parts and the volume that they require during their operation, is widely used in the design and manufacture of RC cars and even in go-karts. This is due to its simplicity, both in assembly and in the production of its parts. At the scale of an RC car, in which the speeds are lower and above all the efforts suffered by the vehicle as well, the parts that make up the steering system suffer much less, with which the crank and connecting rod system adapts perfectly. At the real scale of a car, things change, the friction between the parts are such that makes the system non-effective.

The proposed system is as follows: First, the servo motor that will be chosen later will transmit a rotational movement to a crank to which it will be fixed. In turn, the crank, located in the geometric center of the steering axle, will transmit the movement caused by the servomotor to two connecting rods (3) (one for each wheel) that will transmit the movement to the steering levers (4) which are attached to the wheel (1) and it will modify the path of the vehicle.

In the figure 56 below, you can see each of the components that take part in the process described, although in the case of the project the steering wheel is replaced by a servomotor.

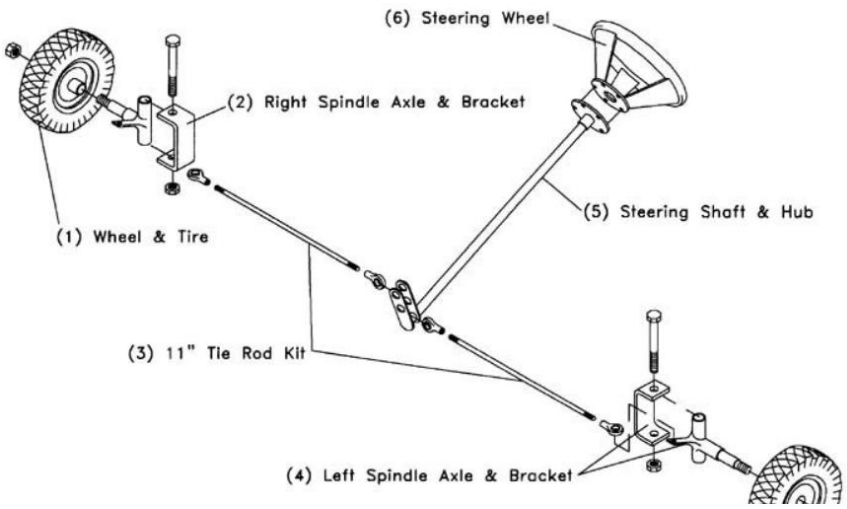

Figure 55. Crank and connecting rods steering system *(Source:* (Bruno Borges, (2018) Pinterest | Build your own car)

Advantages:

- The simplicity of the system is the main advantage of using this method.
- Few parts and easy production in the whole system
- Minimum mass. The system is light compared to other designs
- The manufacturing cost is very low
- Easy to manufacture and assemble

Disadvantages:

- Many moving parts that cause greater friction than in other alternatives
- Poor precision due to gaps that arise in the joints between connecting rods.
- System bulky in its operation.
- Impossibility of reducing or increasing the speed and torque transmitted by the servo. The gear ratio is fixed.

5.2.2 Rack and pinion steering system

The rack and pinion steering system is the most widely used in cars, vans and small trucks worldwide. Its principle of operation in these vehicles is the following: "rack and pinion steering uses a gear-set to convert the circular motion of the steering wheel into the linear motion required to turn the wheels. It also provides a gear reduction, so turning the wheels is easier.

It works by enclosing the rack and pinion gear-set in a metal tube, with each end of the rack sticking out from the tube and connected to an axial rod. The pinion gear is attached to the steering shaft so that when the steering wheel is turned, the gear spins, moving the rack. The axial rod at each end of the rack connects to the tie rod end, which is attached to the spindle." - *(Rack and Pinion System with Power Steering | MOOG, n.d.)*

In figure 57 below, a real steering system of a car is shown.

Figure 56. Rack and pinion steering system of a real car *(Source:* (Matt Robisnon, CarTrhottle (2018) | What Actually Is Rack And Pinion Steering?) *)*

The specific case that is dealt with in this project differs from the previously mentioned system used mainly in automobiles. The proposed system for the dolly (shown in figure 58) consists of designing and building a pinion (3) of suitable dimensions that will be coupled to the servomotor (2). In turn, the pinion will be meshed with a rack (4) which can only move horizontally along a guide. The rack will be connected at its ends with two small connecting rod (4) (one for each wheel) that will transmit the movement to the steering levers and these in turn will transmit it on the wheels, thus turning the dolly.

The system proposed in essence is very similar to that used in cars, the main difference on the one hand is the use of a servomotor instead of a manual steering wheel and on the other hand, that in a real car the parts are subjected to a greater effort and must be better coupled, as well as greased and protected from dust and dirt.

In addition, in cars it is common today that they go on the market with a power steering system that makes it easier for the user to turn the steering wheel, especially in heavy

vehicles or when the vehicle is stationary, by means of a servomotor (electric power steering) or by means of a hydraulic pump (hydraulic power steering).

In figure 58 below you can see a simplified design of the rack and pinion system used in automobiles, as mentioned, the steering wheel should be replaced by the servomotor to be adaptable to the dolly.

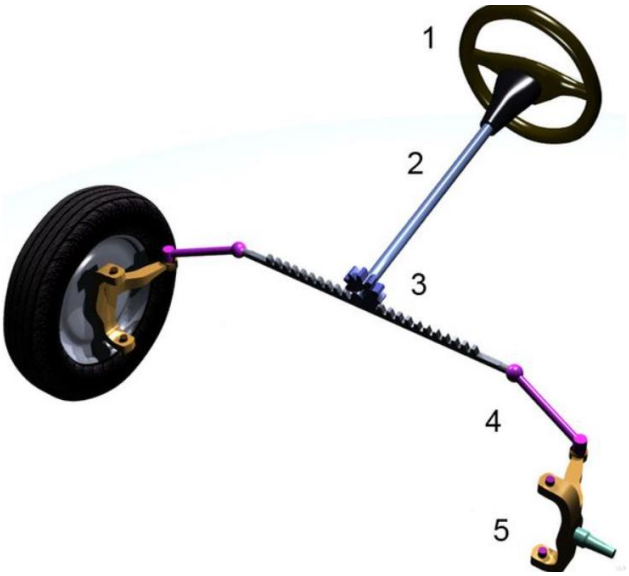

Figure 57. Rack and pinion steering system. *Source:* (Matt Robisnon, CarTrhottle (2018) | What Actually Is Rack And Pinion Steering?)

Advantages:

- The system in general is almost as simple as that of the connecting rod and crank, except for the design and calculation of the transmission ratio between the rack and pinion.
- As the rack moves linearly in a single dimension towards one end or the other, the space required for its application is much less.
- It is a more precise system since it works by gear, the appearance of wobbly is more difficult.
- The mass of the system as a whole is similar to the previous one.
- The greatest advantage that it provides in the case of the dolly is to be able to adjust the transmission ratio and define the rotation of the wheels according to the rotation of the servo, while in the crank crank system this capacity is limited
- Another advantage is that it's possible to print in 3D both, the rack and the pinion.

Disadvantages:

- The main disadvantage regarding to the previous model is that its elaboration is more laborious and more calculations are involved, both for the transmission ratio and to define the parameters of the rack and pinion.
- Another of its defects is that in the event of damaging any of the parts of the system, it will be more difficult to fix than in the previous system.
- The manufacturing and assembly time is high.
- It is also usually more expensive than the previous system.

5.2.3 Conclusions

After reviewing the two main possible systems and studying their advantages and disadvantages, it has been determined that the system chosen will be the rack and pinion system. The choice has been made on the basis that although the design and construction of the rack and pinion system is more difficult and laborious, with this we achieve a smoother steering without wobbly. This will increase the stability of the dolly during its operation and the precision of its turns. In addition, another determining factor for the choice is that with the rack and pinion system, the transmission ratio can be adjusted. This is very positive, since the angle of rotation of the inner and outer wheels can be defined for a certain angle of rotation of the servomotor.

5.3 Steering system calculation

Finally, as determined in the previous chapter, the system chosen was the sprocket and rack system. The operation of this system, adapted to the dolly is as follows:

The main drive, as in other cases, is a servo motor. The difference is that in this case, it is not attached to a crank but is coupled to a sprocket that engages directly on the rack. If we look at Figure 59, the rack (1) will move linearly in a longitudinal direction, to one side and to the other, moving the connecting rods (2) and (3), which will cause the turn of the steering levers and these will turn the wheels.

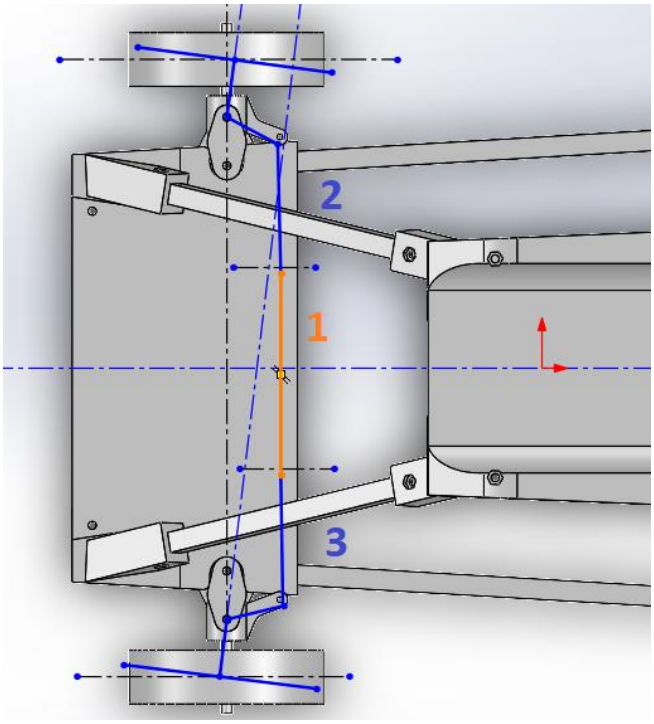

Figure 58. Sketch of the steering system. (Source: own elaboration)

5.3.1 Ackermann calculation

As seen before, according to Ackermann's relation, the inner and outer wheels adopt different angles from the horizontal during the turn. This is because they have a common instant center of rotation (Ackermann ratio) so that the wheels do not slide. This common center of rotation is achieved by aligning the steering lever arms to the center of the rear axle.

Naturally, if the two wheels have a common center of rotation but different radius, the radius of the outer wheel will be equal to that of the inner wheel plus the width of the car. The perimeter of rotation to be traversed by the outer wheel will also be larger in the same proportion, and therefore the angle of the inner wheel from to the horizontal will be smaller than that of the outer wheel, as it will have to travel less distance for the same time and for a common center of rotation.

The aim will be to control the angle of rotation of the inner wheel regarding to the horizontal axis in each case, since as just mentioned it will be the highest.

To establish a relationship between the angle of rotation of the inner wheel and the angle of rotation of the outer wheel, we will use the Ackermann ratio.

If we look at Figure 60, which shows the parameters that will be taken into account for the calculation, we can see the following:

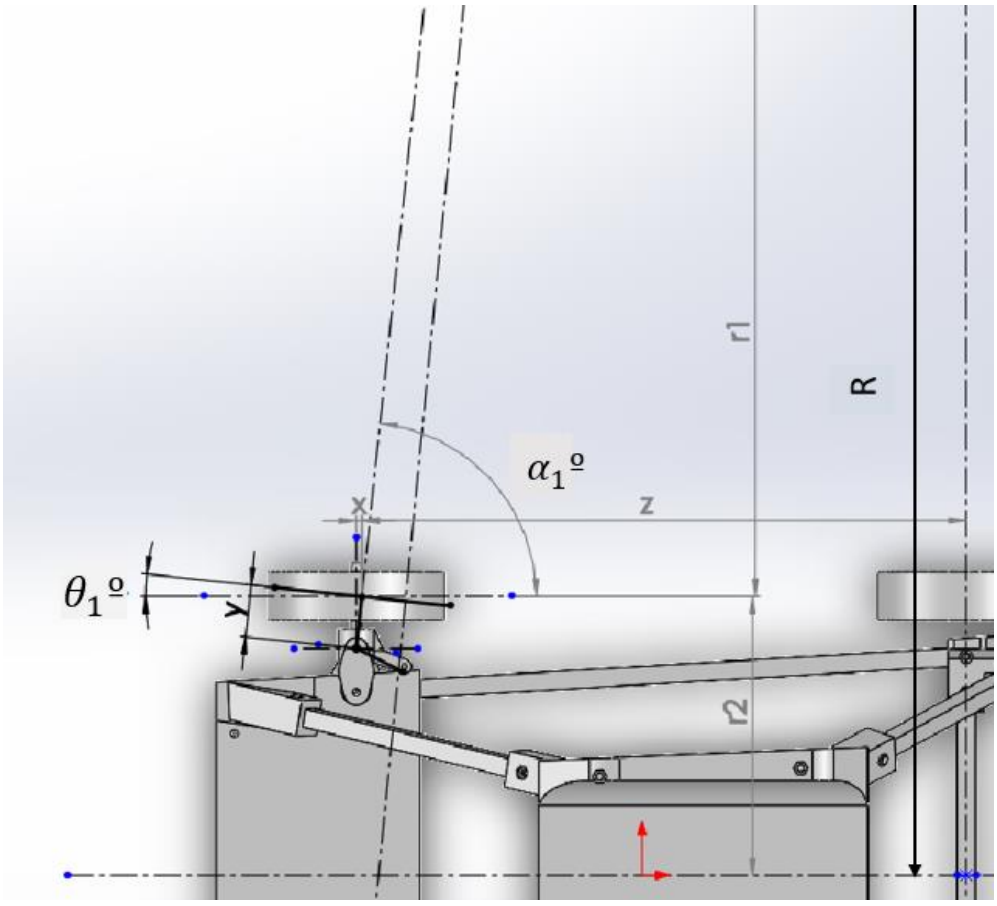

Figure 59. Ackermann calculation *(own elaboration)*

First, the distance “x” is defined as a function of the angle θ_1. The latter refers to the angle with respect to the horizontal that forms the inner wheel when turning. It is the variable that will be worked with. The distance “y” is the separation between the center of the wheel and the rotation axis of the steering system. It’s a fix term.

Using trigonometry relations as in equation 1:

$$\sin(\theta_1) = \frac{\mathrm{x}}{\mathrm{y}} \rightarrow \mathrm{x} = \mathrm{y} * \sin(\theta_1) \quad (\mathrm{eq1.})$$

We first set the length of the leg opposite to the angle "θ_1" as the variable "z.". “d” is the distance between the front and rear axles (wheelbase).

So id we observe the equation 2 and 3:

$$\mathrm{d} = \mathrm{z} + \mathrm{x} \quad (\mathrm{eq\ 2.})$$

$$\mathrm{z} = \mathrm{d} - \sin(\theta_1) * \mathrm{y} \qquad (\mathrm{eq\ 3.})$$

We define the length of the radius that the inner wheel will make with the variable “r1”. It will depend on the turning angle ” θ_1” of the ineer wheel.

The radius of Ackermann "R" that is the radius what the center of the front axle will draw, will be equal to the distance "r1" corresponding to the radius of the inner wheel regarding the instant rotation center, added to half the track width "r2”. So if we observe the equation 4:

$$\mathrm{R} = \mathrm{r1} + \mathrm{r2}\ [\mathrm{m}] \qquad (\mathrm{eq\ 4})$$

So using the trigonometric relations and combining the equations 2 and 3, we can express the following equation 5:

$$\tan(\theta_1) = \frac{z}{r1} = \frac{d - y * \sin(\theta_1)}{R - r2} \qquad (\mathrm{eq\ 5})$$

Finally expressing the Ackermann radius in function of the only variable “θ_1”. We obtain the equation 6. The other parameters of the formula were fixed during design.

$$R = \frac{d - y * \sin(\theta_1)}{\tan(\theta_1)} - r2 \qquad (eq\ 6)$$

Figure 61 below shows the relationship of angles and distances between the inner and outer wheels of the turn.

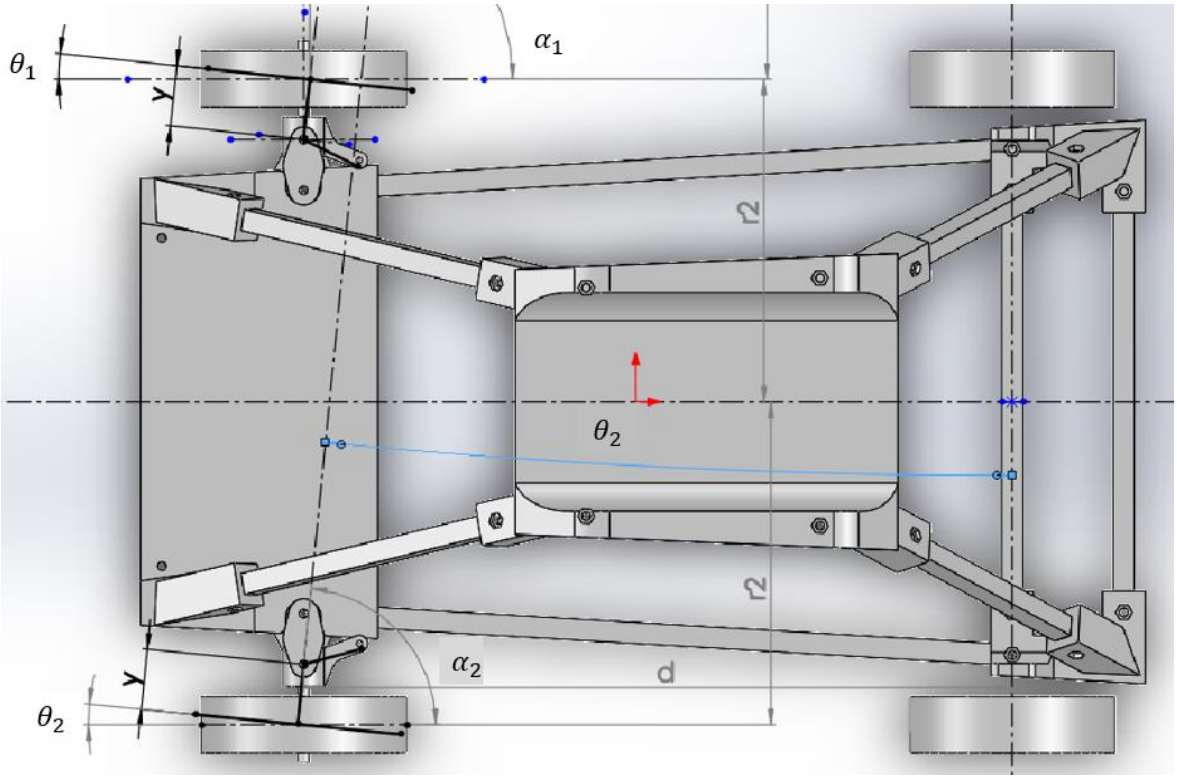

Figure 60. Ackermann relationship *(own elaboration)*

The main objective is to describe the Ackermann radius in function of the turn angle of the outer wheel. By trigonometry equation 7 is obtained.

$$tan\ \theta_2 = \frac{d + y * \sin(\theta_2)}{R + r2} \qquad (\text{eq } 7)$$

Finally, equation 8 determines the Ackermann radius in function of the angle of the outer wheel "θ_2" .

$$R = \frac{d + y * \sin(\theta_2)}{\tan(\theta_2)} + r2 \qquad (\text{eq } 8)$$

5.4 Calculation of the gear assembly

Now that the type of steering system to be used for the dolly has been chosen and the Ackermann parameters have been determined, the next step will be to calculate the parameters of the gears that will take part in the steering system.

As mentioned above, the system chosen for the steering has two elements such as the rack and pinion that will be meshed with each other. For the mesh between the two to be compatible, the mechanical parameters of both must be defined. Another factor to define will be the transmission ratio between the pinion and the rack, which will relate the angle of rotation of the wheels to the position of the servomotor.

In the case of the dolly that is studied in this project, it must make very open turns so that the model is stable. To do this, the maximum rotation that the wheels can make will be mechanically limited. The first step in calculating the gear system will be to define the minimum turning radius necessary to make a turn on itself. This will correspond to the radius that the inner wheel will trace when turning and therefore refers to the term (r1) seen in the previous chapter. The minimum radius defined according to the specifications and requirements of the Dolly is 5m.

If we start from r1 = 5m and substitute in equation 4, determined in the previous chapter, we can determine the maximum angle that the inner wheel will adopt to achieve a minimum turning radius of 5m. Substituting in equation 4, it has been determined that to obtain a minimum Ackermann radius of 5m, the angle (θ_1) corresponding to the maximum angle of the inner wheel cannot exceed 10º.

Once the parameters of the minimum Ackermann radius and the maximum angle of rotation of the wheels have been determined, table 9 has been created, which has all the calculation formulas of the parameters involved in the system, so that changing the starting values, highlighted in the yellow boxes, the table recalculates the results of the parameters according to the defined starting values. This has allowed multiple tests and simulations to be carried out to correctly size the steering system. The table created is made up of multiple columns, first the element to be treated for each case is detailed, followed by its symbol and its units. The formula used for the calculation and to which the results box of that row will be subject is detailed below. Finally, the value of the treated parameter is calculated, distinguishing whether it refers to the pinion or the rack. As mentioned, the yellow boxes are intended for manual data entry, from which the rest of the parameters will be automatically calculated.

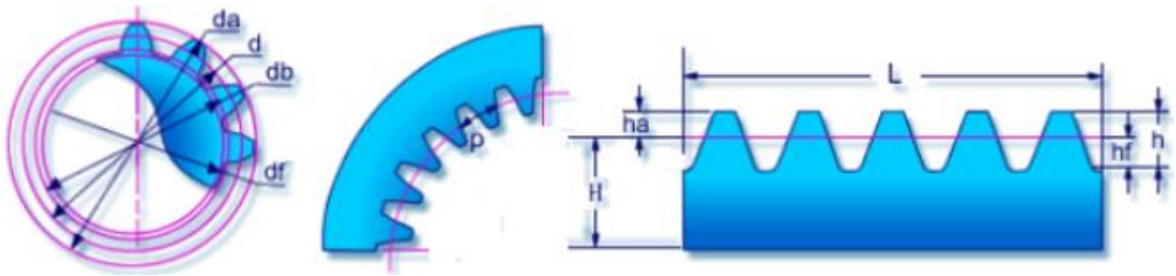

Figure 62. Rack and pinion parameters. *(Source:* (*Rack and Pinion System with Power Steering | MOOG*, n.d.)

Item	Symbol	Units	Formula	Components (data in yellow)	
				Pinion	Rack
Displacement distance of the rack for 10º turning at the inner wheels	dsmàx	mm	-	-	10,03
Displacement distance of the rack for each lap of the pinion	ds	cm/lap	*(d · 4) / 10*	-	4,012
Nº of tooth per centimeter of the rack	n	tooth/cm	*n = z / ds*	-	2,99
Module	m	-	*m = Dp / z*	1,125	
Pressure angle	α	º	-	20	-
Number of tooth	z	-	-	12	-
Rack height	H	mm	-	-	
Primitive pitch	P	mm	*P = m · π*	3,5343	-
Primitive diameter	Dp	mm	*Dp = m · z*	13,5	-
Exterior diameter	de	mm	*de = Dp + 2m*	15,75	-
Interior diameter	di	mm	*di= Dp - 2,5m*	10,6875	-
Diameter of the base	db	mm	*db=Dp·cosα*	5,509	-
Distance between the centers	c	mm			
Tooth height	h	mm	*h = 2,25 · m*		*2,53125*
Addendum	ha	mm	*ha = m*		1,125
Deddendum	hf	mm	*hf = 1,25 · m*		1,40625
Rack lenght	L	mm	*L=Np · P*		10,7
Nº laps servo	Nvs	-		0,25	
Number of pitch	Np	-	Np = z · Nvs	3	

Table 9. Gear assembly parameters calculation

For the calculation of the transmission ratio between the pinion and the rack and the calculation of the design parameters of these two, table 9 has been created.

Since in most calculations only formulas have been applied, the parameters of the yellow boxes will be commented, which are manual input data from which the other calculations are made. The first of the manual input data is the maximum linear displacement of the rack corresponding to the 10 ° of rotation of the inner wheel. This parameter has been determined experimentally by making sketches with the 3D CAD program SolidWorks, so that the required space was the minimum possible. From a design point of view, we are interested in keeping this value as low as possible since the ideal reduction system will be one in which for a high angle of rotation of the servo the wheels rotate very little, and therefore, the rack shifts. very little too.

On the other hand, since most servo motors only have a 180º range of rotation, the 90º degree of the servo will coincide with the straight position of the wheels. Therefore, the servo will only be able to rotate 90º to one side and to the other. From here comes the parameter that refers to the number of turns of the servo (0.25 corresponding to 90º).

The parameter corresponding to the pressure angle has been chosen according to the standard of 20º.

Regarding the modulus, it has also been extracted from the tables of standardized modules shown in figure 62 and it has been empirically verified that the modulus of 1.125 is the one that results in the most optimal design parameters for the case.

Modulo m	paso	Modulo m	Paso	Modulo m	paso
0.5	1.571	2	6.284	6	18.850
0.55	1.727	2.25	7.069	6.5	20.420
0.6	1.885	2.5	7.854	7	21.991
0.7	2.199	2.75	8.639	8	25.133
0.8	2.513	3	9.425	9	28.274
0.9	2.827	3.25	10.210	10	31.416
1	3.142	3.5	10.996	11	34.557
1.125	3.534	3.75	11.781	12	37.699
1.25	3.927	4	12.556	14	43.982
1.375	4.320	4.5	14.137	16	50.265
1.5	4.712	5	15.708	18	56.549
1.75	5.498	5.5	17.279	20	62.832

Figure 61. Table of standardized gear modules and pitch (UNE 3121). *(Source: (Cálculo de Engranajes: Ideas Esenciales En Tus Transmisiones Mecánicas – Blog CLR*, n.d.))

Finally, the number of teeth has also been chosen by empirically checking the results that most favor the development of the dolly, as well as the diameter of the gears that could not be excessive due to lack of space, but at the same time had to be enough to meet the system requirements.

5.5 Selection of standardized components

Now that the chassis and the steering system to be used has been defined, it is possible to proceed with the sizing, study and consequent choice of the different standardized mechanical and electrical components that will make up the steering system.

The components that will be selected in this chapter correspond to those that, due to lack of means, knowledge, time, or because it is more profitable, will not be designed and elaborated, but elements existing in the market will be selected for the fulfillment of different functions.

The selection of the components at this point of the work is important, since there is sufficient data on the general design of the dolly and the chassis structure to which they will be attached, to select them with adequate design criteria. On the other hand, the fact that the different standardized or existing components on the market are selected below, which are already defined and in many cases will have to be chosen from a limited range of products, will allow the design of future parts to be adapted to suit the requirements of these components to be selected below.

The elements that will be selected in this chapter are:

5.5.1 Wheels selection

The wheels are a fundamental component in the operation of the dolly. Previously, the characteristics that the wheels must have to ensure the stability of the system have been detailed, so the current task consists of looking for existing models on the market that meet the defined requirements.

The selected wheels are shown in figure 65 and its properties are detailed in table 11:

Figure 62. Selected wheels. *(Source: HKNA | Aliexpress (2019))*

The reason these wheels have been selected is mainly due to the shortage of other models compatible with the project requirements. Even so, the chosen model is considered optimal since the diameter and width of the wheel coincide with those defined, the price is acceptable, and the material and finish of the product are quite good. The only disadvantage of these wheels is that their weight is a bit high, it can make difficult to move the steering system if the servo is not powerful enough.

As there are no specific wheels on the market for dollies like the one designed in this project, electric scooter tubeless wheels have been used.

In table 11 its main properties are shown.

Brand	HKNA
Shop	Aliexpress
Tire Diameter	145mm
Tire Width	40mm
Tire Material	Rubber
Weight	0,4 kg
Inner diameter	8 mm
Price	13,52 €
Units	4
Origin	China

Table 10. Wheel Characteristics

The purchase link is the following:

https://es.aliexpress.com/item/4001130428893.html?aff_fcid=4206ca37e16d4be7ba55a6746f25667c-1615462555438-08590-_dXTaSdi&aff_fsk=_dXTaSdi&aff_platform=portals-tool&sk=_dXTaSdi&aff_trace_key=4206ca37e16d4be7ba55a6746f25667c-1615462555438-08590-_dXTaSdi&terminal_id=3db1b801fe4b41888dd9567c2e8ed09e&tmLog=new_Detail

5.5.2 Connecting rods Selection

The connecting rods are a fundamental element in the steering system mechanism, since they are responsible for transmitting the movement of the rack to the steering lever, and the latter to the wheels.

For their selection, the criteria applied is as follows: the cranks chosen must have a length between 95 and 100 mm, since it is the distance between the rack housing and the steering lever housing. In order to adjust the steering correctly and avoid possible wheel deviations, another requirement will be that the length of the connecting rod is adjustable by means of a threaded axle. Finally, the connecting rod must be light so that the servo must make the least possible force to turn the wheels.

The selected connecting rods are shown in figure 64:

Figure 63. Selected connecting rods. *(Source:(AXSPEED Varilla de Tracción Para Servo, 2 Uds., Longitud Ajustable Para 1/10 RC Crawler Axial SCX10 Traxxas TRX4 D90 TF2 CC01|Partes y Accesorios| - AliExpress*, n.d.*))*

As there are no specific connecting rods on the market for a vehicle such as the treaty, connecting rods used in the directions of RC cars have been compared, specifically the ones at 1/10 scale.

Finally, these have been the selected connecting rods since they meet all the requirements to correctly perform their function. First of all, they comply with the possibility of adjusting their length between 95 and 100mm, which has been the most difficult feature to find in other models. They are also light and of good quality.

Its main features are shown in the table 11 below:

Brand	AxSpeed
Shop	Aliexpress
Length	Adjustable between 95 - 100 mm
Diameter	8mm
Material	Aluminum
Hole diameter	3mm
Price	7,55 €
Units	2

Table 11. Characteristics of the Selected Connecting rods

The purchase link is:

https://es.aliexpress.com/item/4000214668493.html?spm=a2g0s.9042311.0.0.650963c0fJvg5A

5.5.3 Servomotor Selection

The servo motor can be considered an electro-mechanical component since it will be the element that will provide the necessary rotation torque to physically move the wheels, but at the same time it will be powered by an electrical power source and controlled by a microcontroller that will give it the orders of position in degrees. For its selection it will be necessary to take into account its mechanical parameters, as well as its electrical parameters.

There are many types of servo available on the market, but we will focus again on those used in RC cars, as they are the most suitable for dolly application. "Most of the hobby Servo motors operates from 4.8V to 6.5V, the higher the voltage higher the torque we can achieve, but most commonly they are operated at +5V. Almost all hobby servo motors can rotate only from 0° to 180° due to their gear arrangement"- *(MG90S Micro Servo Motor Datasheet, Wiring Diagram & Features, n.d.)*

For the use of the dolly, the MG90-S servomotor will be used, since the Lightening Research Group of the ESEIAAT has provided this component for its application on the dolly. Although the servo has been assigned, its main characteristics have been analyzed in order to ensure that it is valid for the project.

After reviewing its datasheet, attached in the annex, the necessary information about its characteristics has been obtained. It is shown in the table 12 below.

Operating voltage	4.8V to 6V (Typically 5V)
Stall Torque:	1.8 kg/cm (4.8V)
Max. Stall Torque	2.2 kg/cm (6V)
Operating Speed	0.1s/60º (6V)
Gear Material	Metal
Rotation	0º - 180º
Weight	13.4 g
Price	5,43€

Table 12. Servo Tower Pro MG90S Features

The only limitation that could exist in this case, based on the fact that its supply voltage is in the stipulated range of 4.8V - 6.5V, is the torque of the motor. If it were too small, it might not be able to move the steering system, and if it were too high, the system would be oversized.

In the case of the MG90S servo, the max torque of the motor is 2.2kg / cm. It "means that the motor can pull a weight of 2.2kg when it is suspended at a distance of 1cm. So if you suspend the load at 0.5cm then the motor can pull a load of 4.4kg."- *(MG90S Micro Servo Motor Datasheet, Wiring Diagram & Features, n.d.)*

After selecting the servo which will be used for the project, we will focus on the requirements for its use. The servomotor has three wires coming out that we will have to connect to the microcontroller. The servo and its wiring are shown in figure 65:

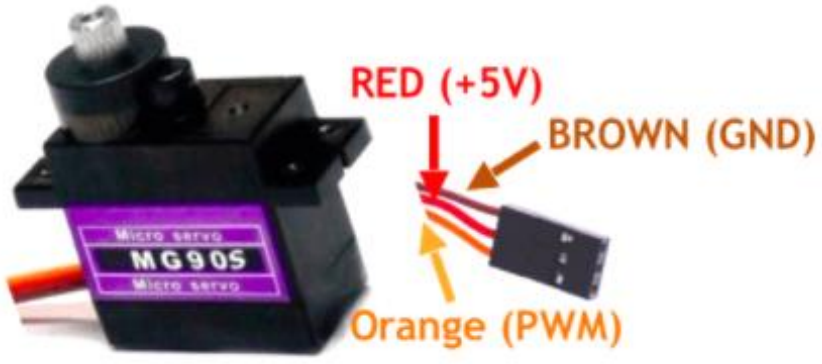

Figure 64. Servo MG90S Wiring *(Source: (MG90S Servo, Metal Gear with One Bearing*, n.d.*))*

The table 13 below has been created in order to describe the function of each wire which come out of the servomotor:

Wire Color	Description
Red	This wire powers the motor with +5V
Brown	This is the ground wire which is connected to the ground of the system
Orange	This wire provides the PWM signal in order to drive the motor.

Table 13. Servo wiring definition

As it's shown in Table 13, "to make this motor rotate, we have to power the motor with +5V using the Red and Brown wire and send PWM signals to the Orange wire. Hence we need something that could generate PWM signals to make this motor work, this something could be anything like a 555 Timer or other Microcontroller platforms like Arduino, PIC, ARM or even a microprocessor like Raspberry Pie.

In order to understand how to control the direction of the motor, let's took a see on figure 68 obtained from its datasheet since it shows the PWM needed on the orange wire of the servo:

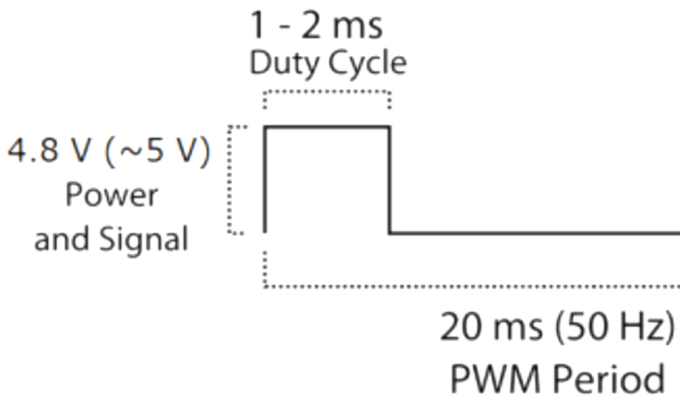

Figure 65. PWM signal of the MG90S *(Source: MG90S Servo, Metal Gear with One Bearing, n.d.)*

From the figure 66 we can affirm that the PWM needed to control the servo should have a frequency of 50Hz, then the PWM period should be 20ms. "Out of which the On-Time can vary from 1ms to 2ms. So when the on-time is 1ms the motor will be in 0° and when 1.5ms the motor will be 90°, similarly when it is 2ms it will be 180°. So, by varying the on-time from 1ms to 2ms the motor can be controlled from 0° to 180°"- *(MG90S Micro Servo Motor Datasheet, Wiring Diagram & Features, n.d.)*

The rest of the parts that make up the system that are not standardized and therefore have not been purchased anywhere, will be manufactured by 3D printing in a similar way to the chassis joints detailed above. The drawings of each of the pieces are attached in the annexes and the program files for the manufacture of the pieces will be delivered together with the project.

The manufacturing process of the parts using 3D printing will be detailed later.

5.6 Final Design of the Steering System

This chapter will show the final 3D design of the Steering System. All the components have been designed based on the studies, analyzes and calculations carried out, as well as the conclusions obtained. Detailed drawings as well as program files and datasheet of normalized components are attached to the project. Selected standard parts have been detailed before. Figures 67 and 68 show the top and front views, respectively, of the steering system. The numbered parts are described in table 14.

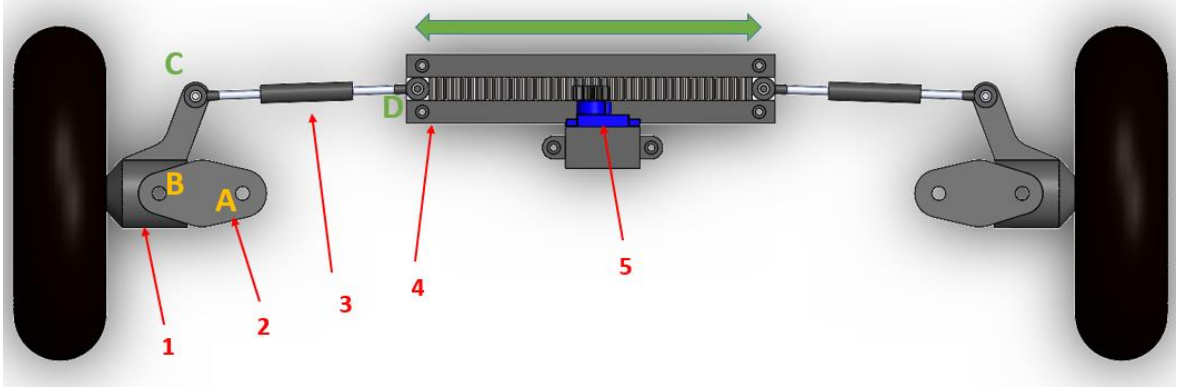

Figure 66. Top view of the steering system *(Source: own elaboration)*

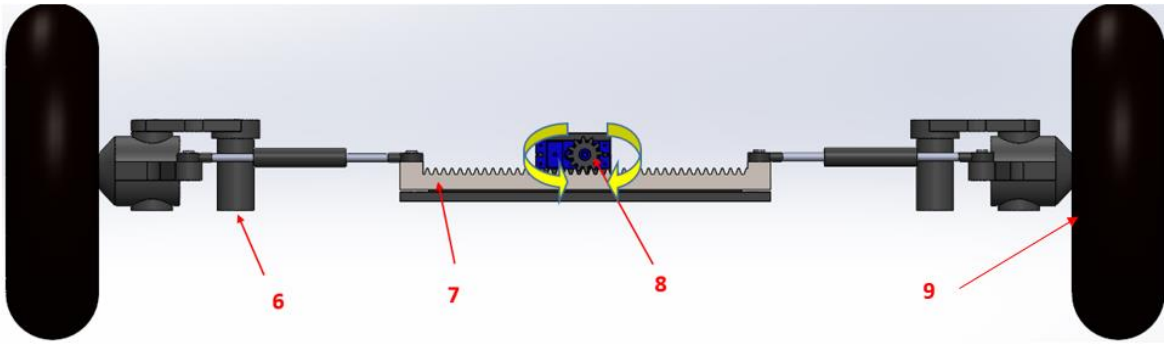

Figure 67. Front view of the steering system *(Source: own elaboration)*

NUMBER	PART
1	Steering Lever
2	Support of the steering lever
3	Connecting Rods
4	Servo Support + Rack Guide
5	Servo
6	Space bar
7	Rack
8	Pinion
9	Wheel

Table 14. Parts of the steering system

Next, the operation of the steering system will be described taking into account all the parts that constitute it. As the standardized elements have not yet been chosen, the components of the steering system may later undergo minor modifications in order to adapt them to standardized elements such as the servomotor, bearings or hardware. Even so, the operation of the system and the parts involved are defined below:

The operation of the mechanical system begins when the servomotor (5) receives an order from the heading control system in which the position in degrees to which it must be located is specified. This will rotate its shaft, also rotating the pinion (8) that is attached to it. As the pinion has all movements restricted except rotation, and is engaged with a rack (7), this will move linearly to one side or the other depending on the direction of rotation of the pinion. The rack will move linearly thanks to the fact that it is fitted in a linear guide (4), which in turn acts as a support for the servomotor. The displacement of the rack will be transmitted to the connecting rods (3), since they are joined at point “D”. At the other end, the connecting rod is attached to the steering lever (1) at point "C". The steering lever is directly connected to the wheels (9), so its angle of rotation will correspond to the angle of rotation of the wheels. The steering lever will be able to rotate since it will be attached at its center of rotation "B" to the support (2), which in turn is attached to the chassis at point "A", by means of a spacer (6).

6 Design of the heading system

Now that most of the components and systems that together will allow the operation of the dolly have been defined, it is time to design the heading control system.

As previously mentioned, the heading control system will be the system in charge of controlling the steering system, ensuring the dolly's heading in a previously set direction and correcting possible deviations due to the slope of the runway or other factors.

In this chapter we will first introduce the heading control system, then we will detail the parts that compose it, as well as selected components and software used. Next, the block diagrams representing the heading control part of the program will be shown and finally the electrical connections between components will be defined.

6.1 Introduction to the heading system

In the field of technology in general, heading control systems are being used more and more to control unmanned vehicles or to make driving easier for the pilot over long distances. However, these types of systems are used in practically all types of vehicles, whether land, sea or air vehicles, and at all scales of size.

The development of this type of system began after World War II, during the Cold War. Their use was initially limited to military purposes such as commanding missiles or unmanned

military vehicles in which application, the missile or the vehicle has to follow a setted direction to meet the oponent.

Although its initial purposes were not ethical, the development of the technology later allowed the application of this knowledge to a multitude of very diverse uses, such as: course control in ships, airplanes or cars, control of UAV's or even automated forklifts such as those used in the warehouses of large logistics companies.

In the specific case of the project, since the dolly does not have a steering wheel or a remote control, as neither of these meet the requirements of the project, the heading control system will be in charge of governing the previously designed steering system. After setting a target direction, the heading system will be able to send a PWM signal in the form of electrical pulses to the steering system servomotor, to regulate its position, move the dolly wheels and thus correct possible deviations to maintain a fixed direction.

To read the direction, both to establish the target direction in the first measurement and to know the instantaneous direction and to be able to correct deviations, various types of sensors can be used, whether electronic compasses, accelerometers or even GPS modules. The reading obtained by these sensors, which will be selected later, will be sent to a microprocessor or a microcontroller, which will process the information received as specified in its programming code and send a position signal to the servomotor. A simplified schematic of the functions of the heading control system is shown in the figure below:

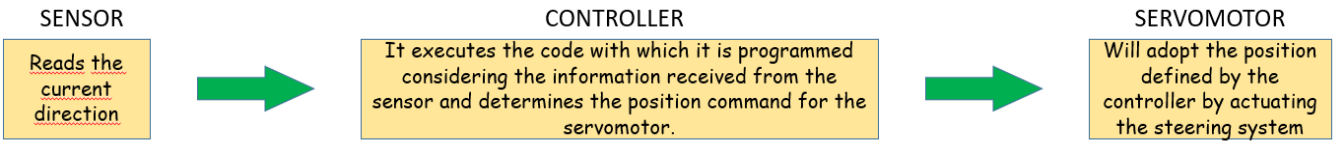

Figure 68. Simplified schematic of the heading system. *(Source: own elaboration)*

6.2 Selection of the controller

The first element to be defined, on which the other elements of the steering system will depend, is the controller. The controller can be considered as the brain of the heading system and will be in charge of managing all the information received from the sensors in order to determine an output for the actuators.

The control of the system can be delegated to many types of controllers, although the most commonly used are the following three: PLC, Arduino and Raspberry.

6.2.1 PLC

The PLC, which stands for Programmable Logic Controller "is a ruggedized computer used for industrial automation. These controllers can automate a specific process, machine function, or even an entire production line. The PLC receives information from connected sensors or input devices, processes the data, and triggers outputs based on pre-programmed parameters.

Depending on the inputs and outputs, a PLC can monitor and record run-time data such as machine productivity or operating temperature, automatically start and stop processes, generate alarms if a machine malfunctions, and more. Programmable Logic Controllers are a flexible and robust control solution, adaptable to almost any application.

A PLC program is usually written on a computer and then is downloaded to the controller. Most PLC programming software offers programming in Ladder Logic, or "C". Ladder Logic is the traditional programming language. It mimics circuit diagrams with "rungs" of logic read left to right. Each rung represents a specific action controlled by the PLC, starting with an input or series of inputs (contacts) that result in an output (coil). Because of its visual nature, Ladder Logic can be easier to implement than many other programming languages."C" programming is a more recent innovation. Some PLC manufacturers supply control programming software." - *(What Is PLC ? Programmable Logic Controller - Unitronics, n.d.)*

The main features and capacities of the PLC are the following ones:

- The CPU of the PLC's stores and processes program data, but input and output modules connect the PLC with the rest of the machine that the PLC controls.
- The input and output modules provide information to the CPU and trigger specific results. I/O can be analog or digital.
- The PLC offer a range of ports and communication protocols allowing the communication with other kind of systems.
- Usually a HMI is required for the user in order to interact with the PLC.

After analyzing the different characteristics of PLCs, as well as their method of operation, programming language, and communication protocols with other systems, the following conclusions have been reached:

- The number of applications and robustness of a PLC is not surpassed by any other type of controller today, which is why it is the type of controller used in virtually all industries for their assembly lines and automation processes.
- It is the controller that has more programming libraries available, mainly applied to the industrial field. It is also the one with more types of accessories, modules and compatible extensions.
- Its price is quite high compared to the other two controllers presented. Its price can be between 200€ and 10,000€, or even more, depending on the type and number of modules to which it is attached.
- It is intended to be used mainly in the industrial field, to control machines in automation processes. For this reason, its total volume together with the modules is usually high, as well as the necessary power supply.

6.2.2 Raspberry Pi

Unlike the other two control elements studied in this chapter, the Raspberry Pi is not a controller but a microprocessor. Although the Raspberry is not a controller itself, it can be used as such.

To understand what exactly is a Raspberry Pi, we will show the description offered by the manufacturers themselves on their official website: “The Raspberry Pi is a low cost, credit-card sized computer that plugs into a computer monitor or TV, and uses a standard keyboard and mouse. It is a capable little device that enables people of all ages to explore computing, and to learn how to program in languages like Scratch and Python. It’s capable of doing everything you’d expect a desktop computer to do, from browsing the internet and playing high-definition video, to making spreadsheets, word-processing, and playing games. What’s more, the Raspberry Pi has the ability to interact with the outside world, and has been used in a wide array of digital maker projects, from music machines and parent detectors to weather stations and tweeting birdhouses with infra-red cameras.” - *(What Is a Raspberry Pi?, n.d.)*

As you could read in the previous excerpt from the manufacturer's website, the Raspberry Pi is a low-cost microprocessor, capable of performing a wide range of different applications, practically the same applications that a computer can perform. It can run an Operating System provided by the Raspberry Pi Foundation, they also provides a Debian based Linux Distribution called the Raspberry Pi OS. “Another important thing about Raspberry Pi is, as it is a Linux based Computer, you can develop software using several Programming Languages like C, C++, Python, Java, HTML, etc. Despite its original intentions, which is to promote programming (like Python and Scratch Programming Languages) in schools, the original Raspberry Pi SBC became extremely popular among DIY builders, hobbyists and enthusiasts for developing several applications like Robotics, Weather Stations, Camera based security systems etc.” - *(What Is a Raspberry Pi?, n.d.)*

After delving into the applications of a Raspberry Pi, we can conclude the following:

- The Raspberry unlike the other two elements studied is a microprocessor and not acontroller, so its use is more similar to the use of a computer than that of a logic programmer.
- Even so, it is capable of performing the basic functions of a logic controller such as reading inputs and executing outputs, but it can also perform many more operations such as storing data, comparing it with internet databases, sending results by mail etc.
- Despite it was designed for an educational use, is also good for performing multiple tasks, driving complicated robots, playing videos, connect to internet, interface cameras, etc.
- The main programming languages in Raspberry Pi are Python, Scratch, Ruby, C, C++
- The price of the microprocessor board Raspbeyy Pi is around 35€.

6.2.3 Arduino

Arduino is an open source electronics creation platform, which is based on free hardware and software. The free hardware devices are "devices whose specifications and diagrams are publicly available, so that anyone can replicate them. This means that Arduino provides the basis for any other person or company to create their own boards, which may be different from each other but equally functional from the same base."- *Traduced from: (Qué Es Arduino, Cómo Funciona y Qué Puedes Hacer Con Uno, n.d.)*

Arduino is essentially a Microcontroller development board also created with an educational purpose with the target of creating and easy tool for a fast prototyping. "Arduino boards are able to read inputs - light on a sensor, a finger on a button, or a Twitter message - and turn it into an output - activating a motor, turning on an LED, publishing something online. You can tell your board what to do by sending a set of instructions to the microcontroller on the board. To do so you use the Arduino programming language (based on Wiring), and the Arduino Software (IDE), based on Processing." - *(Arduino - Introduction, n.d.)*

To develop a project with Arduino, first of all you have to download its software (Arduino IDE), which is provided on its official website. Then the user will write the application code based on C++ language, following the programming software guidelines. Then the program will be compiled, action in which the program will convert the code written in C++ to binary code. Finally connecting the Arduino board to a USB port and uploading the code to the microcontroller the program will be ready to execute.

After reviewing the main features of Arduino, the following conclusions can be reached.

- The Microcontroller that the Arduino board includes, contains the CPU, ROM and RAM, and the other hardware is for power supply, programming and wiring.
- The cost of the original Arduino UNO is around 20€ but there are a lot of imitations which can be found for around 5€.
- By using shields, which plug into the pin headers of the Arduino, it's possible to add additional feature or functionality like Wi-Fi, motor driver, Ethernet connection, touchscreens, etc.
- Arduino needs less current than the Raspberry or the PLC.
- It's the simplest way to control the heading system such the ease of its programming languages, the amount of libraries that are available, and also the amount of drivers, sensors, and actuators that are available specifically for its use on Arduino.

Although both the PLC and the Raspberry Pi offer better and extended qualities in a general scope of application, it has been finally decided that the Arduino microcontroller will be used to govern the heading control system and other automated systems that will incorporate the dolly. This is because in the case of the PLC, its application in the dolly is not feasible since they are too bulky, expensive and heavy to meet the requirements of the dolly. On the other hand, the Raspberry could have been considered for use in the project because it meets the requirements, even so, its programming language and its concrete application for the project would be more difficult and laborious than that of a microcontroller such as Arduino. As in the case that two options meet all the requirements, the simpler and cheaper one will always be selected, in this case Arduino has been selected.

6.3 Selection of the Arduino board

The Arduino company currently provides a variety of different boards for different applications. They differ from each other in factors such as size, as for example the Arduino Nano was designed to be as small as possible, but above all they differ in that many come standard with specific shields such as Wi-Fi or Ethernet installed, while in the most basic versions these modules can be added separately.

For use in the dolly, an Arduino UNO board has been selected, since it is the most basic and economical board, but it more than meets the requirements of the project. Another reason why this board has been selected is that the author of the project had never worked before with the Arduino platform, and as stated on the company's official website: "Arduino UNO is the best board to get started with electronics and coding. If this is your first experience tinkering with the platform, the UNO is the most robust board you can start playing with. The UNO is the most used and documented board of the whole Arduino family." - *(Arduino Uno Rev3 | Arduino Official Store, n.d.)*

In figure 70, the last version of Arduino UNO, which is the Arduino UNO Rev3, is shown:

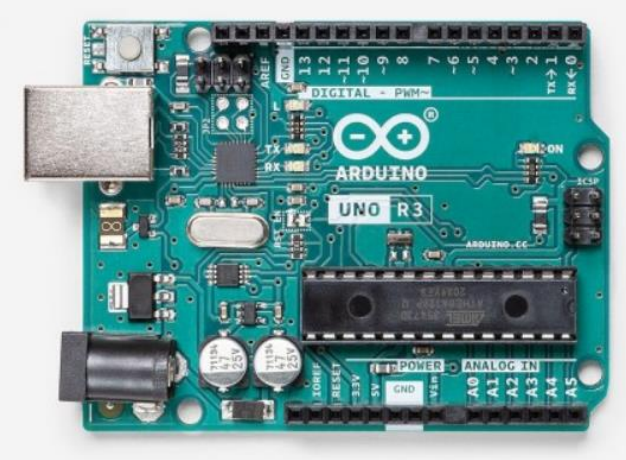

Figure 69. Arduino UNO Rev 3. *(Source: (Arduino Uno Rev3 | Arduino Official Store*, n.d.) *)*

The complete datasheet and schematics of the Arduino UNO board are attached in the annex, but in figure 71 its main features are shown.

Microcontroller	ATmega328P
Operating Voltage	5V
Input Voltage (recommended)	7-12V
Input Voltage (limit)	6-20V
Digital I/O Pins	14 (of which 6 provide PWM output)
PWM Digital I/O Pins	6
Analog Input Pins	6
DC Current per I/O Pin	20 mA
DC Current for 3.3V Pin	50 mA
Flash Memory	32 KB (ATmega328P) of which 0.5 KB used by bootloader
SRAM	2 KB (ATmega328P)
EEPROM	1 KB (ATmega328P)
Clock Speed	16 MHz
LED_BUILTIN	13
Length	68.6 mm
Width	53.4 mm
Weight	25 g

Figure 70. Arduino UNO rev 3 features. *(Source: (Arduino Uno Rev3 | Arduino Official Store*, n.d.*))*

As you can see, the board has 12 pins for digital inputs or outputs, on which a PWM (Pulse Width Modulation) signal is provided in 6 of them. The PWM is a technique in which the duty cycle of a periodic signal (e.g., sinusoidal or square) is modified to transmit information over a communications channel or to control the amount of power sent to a load.

On the other hand, it also has 6 pins dedicated to analog inputs or outputs. While digital signals are discontinuous and can only take as value 0 and 1, analog signals are continuous in time and can take infinite values. This type of signals are commonly used for physical measurements such as temperature, position, level, etc.

Although its operating voltage is 5V, a voltage between 7 and 12V must be supplied to the board. It is usually provided through a USB cable. External power supplies can also be used.

The Arduino UNO features an ATmega328P microprocessor with a 32KB Flash Memory, a 1KB EEPROM and a 2KB SRAM.

The clock speed provided is 16 MHz.

It can be purchased at the official store for only 20€ in the following link: https://store.arduino.cc/arduino-uno-rev3

6.3.1 Arduino IDE

After having described the characteristics of the hardware included in the Arduino UNO board, we will now describe the working environment with which the Arduino works and with which the code to control the system will be written.

As previously mentioned, the IDE (Integrated Development Environment) consists of the text editor, which can be written in c, c++ and java, a set of default libraries and the programming and compilation tools needed to work. It is available in versions for the main operating systems. The installation of the development environment is done directly and free of charge from the company's official website.

Once the development environment has been downloaded and installed, the next step is to select the communication port with the Arduino board from those available on the computer, then select the board model to work with. In this case Arduino UNO.

As for the programming language of the source code, it is based on Processing/Wiring, which in turn is based on the C programming language. In this language the structures of the initialization and task execution operations are formed by the setup( ) and loop( ).

- The setup( ) function will be executed only when starting the Arduino and is usually used for device, pin and data initialization tasks.
- The loop( ) function is executed indefinitely after the previous function is finished and will contain most of the code.

6.4 Selection of the sensors

Now that the microcontroller to be used has been determined, we can start working on the code that will be used to control the system, but first, we must define the type of sensors that will be used to measure the direction of the dolly at each moment.

The selection of the sensor that will provide the direction measurement at each instant is fundamental since this direction measurement will be taken in one way or another depending on the type of sensor. Therefore, it will condition the program code and its structure.

As previously mentioned, different possibilities have been considered for the selection of the sensors focused on the steering system. Mainly the following:

- GPS
- Accelerometer
- Magnetometer
- Gyroscope

Each of them will be described below in order to choose the most suitable one.

6.4.1 GPS module

As it is popularly known, GPS or Global Positioning System is a satellite navigation system that uses about 24 satellites. GPS works anywhere in the world, 24 hours a day, free of charge.

The satellites that make up the navigation system orbit the Earth and provide a signal that allows GPS devices to decode and calculate the user's location accurately. "Basically, the GPS receiver measures the distance to each satellite by the time it takes to receive a transmitted signal. With distance measurements from a few more satellites, the receiver can determine the user's position and display it. To calculate its 2-D position (latitude and longitude) and track movement, a GPS receiver must receive the signal from at least 3 satellites. With 4 or more satellites in view, the receiver can determine its position in 3-D (latitude, longitude and altitude). Typically, a GPS receiver tracks 8 or more satellites, but that depends on the time of day and where you are on Earth."- Traduced from *((How to Interface GPS Module (NEO-6m) with Arduino - Arduino Project Hub, n.d.)*

When the connection to the relevant satellites has been successfully established and the user's position has been determined, the GPS system can provide the following data:

- Speed
- Bearing
- Track
- Trip dist
- Distance to destination

In order to work with a GPS module in the Arduino IDE platform, two libraries are provided that must be used:

- SoftwareSerial library
- TinyGPS library

As Arduino is a free software and hardware company, there are many GPS modules available on the market. One of them is the NEO-6M GPS which can track a maximum of 22 satellites through 50 different channels with the highest level of accuracy available at the moment, i.e. -161 dB tracking, consuming only 45mA.

Figure 72 below shows the main characteristics of the module. These have been extracted from the data sheet supplied by the manufacturer.

Parameter	Specification			
Receiver type	50 Channels GPS L1 frequency, C/A Code SBAS: WAAS, EGNOS, MSAS			
Time-To-First-Fix[1]		NEO-6G/Q/T	NEO-6M/V	NEO-6P
	Cold Start[2]	26 s	27 s	32 s
	Warm Start[2]	26 s	27 s	32 s
	Hot Start[2]	1 s	1 s	1 s
	Aided Starts[3]	1 s	<3 s	<3 s
Sensitivity[4]		NEO-6G/Q/T	NEO-6M/V	NEO-6P
	Tracking & Navigation	-162 dBm	-161 dBm	-160 dBm
	Reacquisition[5]	-160 dBm	-160 dBm	-160 dBm
	Cold Start (without aiding)	-148 dBm	-147 dBm	-146 dBm
	Hot Start	-157 dBm	-156 dBm	-155 dBm
Maximum Navigation update rate		NEO-6G/Q/M/T	NEO-6P/V	
		5Hz	1 Hz	
Horizontal position accuracy[6]	GPS	2.5 m		
	SBAS	2.0 m		
	SBAS + PPP[7]	< 1 m (2D, R50)[8]		
	SBAS + PPP[7]	< 2 m (3D, R50)[8]		

Figure 71. NEO-6M GPS Module Datasheet. *(Source: NEO-6 u-Blox 6 GPS Modules Data Sheet NEO-6-Data Sheet This Document Applies to the Following Products: Name Type Number ROM/FLASH Version PCN Reference, 2011)*

As shown in the figure above, even though it is the most sensitive GPS module for Arduino on the market, the sensitivity offered by the NEO-6M GPS is lower than that required for the heading control system. The sensitivity offered by its most advanced version, the NEO-6G/Q/T is 2.5m with the GPS signal, while it can reach about one meter using the SBAS (Satellite Based Augmentation Signal) technique, which is a signal correction system to improve the accuracy of the signal. Although it is a very useful device in many other types of applications, in the case of this project it does not meet the requirements due to lack of precision.

6.4.2 Accelerometer

Accelerometers are devices currently used in all kinds of devices, with purposes that can range from determining orientation in mobile devices, detecting free fall, measuring steps, stabilization systems for video cameras, vibration sensors, etc.

For the accelerometer proposal, a three-axis accelerometer will be considered, since it will be able to detect acceleration in the X, Y and Z axes.

This type of devices are usually very accurate as they have a high sensitivity, although this can lead to erroneous measurements that should be filtered out.

There are several types of accelerometers on the market, and although they all have the same purpose, their operation varies depending on the application or the conditions in which they are going to work. The existing types of accelerometers are:

- Mechanical
- Capacitive
- Piezo electric
- Piezo resistive
- Thermal

Accelerometers are widely used in cell phones to determine in which orientation the device is placed, and thus regulate the position of the screen depending on whether it is placed vertically or horizontally. The mobile accelerometer consists of a moving part that moves according to the applied acceleration, and a fixed part that interprets the voltage resulting from this movement to determine the speed at which it moves and its orientation. In modern mobiles, three-axis accelerometers are used to measure motion in the X, Y and Z axes. Thus composing a three-dimensional space.

"Accelerometers can be based on other operating principles, such as the microchip-packaged mems accelerometers. Mems accelerometers are designed for easy integration with Arduino or other microcontrollers these days, with common ones being the ADXL sensor series (popular ones being ADXL345, ADXL335). With its miniaturized sensors, Mems accelerometers are applicable for IoT usages, low-power, industrial and automotive applications, healthcare, etc. Accelerometers are most commonly used to detect position, velocity, vibration, and to determine orientation." - *(Accelerometer vs Gyroscope Sensor, and IMU, How to Pick One? - Latest Open Tech from Seeed Studio, n.d.)*

6.4.3 Magnetometer

The magnetometer is another type of sensor whose operation is based on measuring and quantifying the magnetic forces acting on it. It is often used as a magnetic compass to locate the Earth's magnetic North Pole. The magnetometer can also measure the magnetic field surrounding, for example, a robot.

It is also often used for heading control of simple vehicles such as the one discussed in this chapter, taking north as angle 0º and measuring the instantaneous angle with respect to magnetic north at each moment. If it is placed inside or very close to a metallic structure whether it is a chassis or electrical piping, or any large motor, all of these will have significant and noticeable effects on its measurements.

6.4.4 Gyroscope

The Gyroscope is a device which is used in order to measure rotational changes, and it's based on the principle of preserving angular momentum.

Gyroscopes are usually used as an integral part of navigational systems we commonly see nowadays:

- Aircrafts
- Space stations
- Stability in vehicles; motorcycles, ships
- Inertial guidance systems

- Consumer electronics through MEMS gyroscopes (Most mid-range to higher-end Andriod phones)

The gyroscope is used to measure the instantaneous angular momentum around each axis, i.e. the rate of rotation. note that angular momentum is not directly compatible with Euler angles, but it works similarly for small angles. The signal is of very high quality in the short term because there is not much noise, but as the angular position has to be integrated into the gyro it will accumulate error causing inaccuracies in the long term, i.e. during prolonged use. This makes it widely used in cell phones to complement the information provided by the accelerometer, especially to detect rotation with high accuracy. For example, when an App asks the User to tilt the mobile in a certain position or another, it is the gyroscope that is calibrated to come into use.

6.4.5 Conclusions

Of the modules mentioned above, all except the GPS meet the requirements to be used for the purpose detailed in the project. In an advanced system, all of them specially the GPS could even be used by applying redundancy relationships where the measurements of each of the sensors will be compared to improve the accuracy of the system.

Even so, if for the choice of the sensor to be selected in the project if simplicity is highlighted as the determining element among the different options that meet the requirements, the simplest programming code would be to use the accelerometer to measure the rotations around the X and Y axes. Use the magnetometer for the Z axis.

After analyzing the different components and their functions, it can be concluded that the best solution would be to use the three sensors (accelerometer, magnetometer and gyroscope) obtaining the data from the gyroscope and using a fusion algorithm between accelerometer and magnetometer to correct the drift of the gyroscope.

Even so, for the project in question the take-off time will be between 4 and 7 seconds approximately from the moment the dolly is placed in position. So the accumulated error will not exceed the allowable limits of the project. So the solution adopted is to use a single sensor that in turn incorporates accelerometer + magnetometer, so you can compare the measurements between the two and adjust the accuracy of the result.

6.4.6 Selection of the sensor board

The sensor model chosen is an LSM303DLHC of which the data sheet is attached in the annexes.

As described in its data sheet, the LSM303DLHC device is a system that includes a 3D digital linear acceleration sensor and a 3D digital magnetic sensor. “LSM303DLHC has linear acceleration full-scales of ±2g / ±4g / ±8g / ±16g and a magnetic field full scale of ±1.3 / ±1.9 / ±2.5 / ±4.0 / ±4.7 / ±5.6 / ±8.1 gauss. All full-scales available are fully selectable by the user. LSM303DLHC includes an I2C serial bus interface that supports standard and fast mode 100 kHz and 400kHz.The system can be configured to generate interrupt signals by inertial wakeup/free-fall events as well as by the position of the device itself. Thresholds and timing of interrupt generators are programmable by the end user on the fly. Magnetic and

accelerometer parts can be enabled or put into power-down mode separately. The LSM303DLHC is available in a plastic land grid array package (LGA) and is guaranteed to operate over an extended temperature range from -40 °C to +85 °C*" - (This Is Information on a Product in Full Production. LSM303DLHC Ultra-Compact High-Performance ECompass Module: 3D Accelerometer and 3D Magnetometer Datasheet-Production Data Features, 2013)*

As also specified in its data sheet, the applications for which it is designed are as follows:

- Compensated compass
- Map rotation
- Position detection
- Free-fall detection
- Pedometer
- Intelligent power-saving for handled devices
- Display orientation
- Gaming and virtual reality input devices
- Vibration monitoring and compensation

Figure 73 below, also taken from the LSM303DLHC sensor data sheet, shows the direction of the accelerations detectable by the built-in accelerometer, as well as the direction of the magnetic fields detectable by the magnetometer. Both incorporated in the chip.

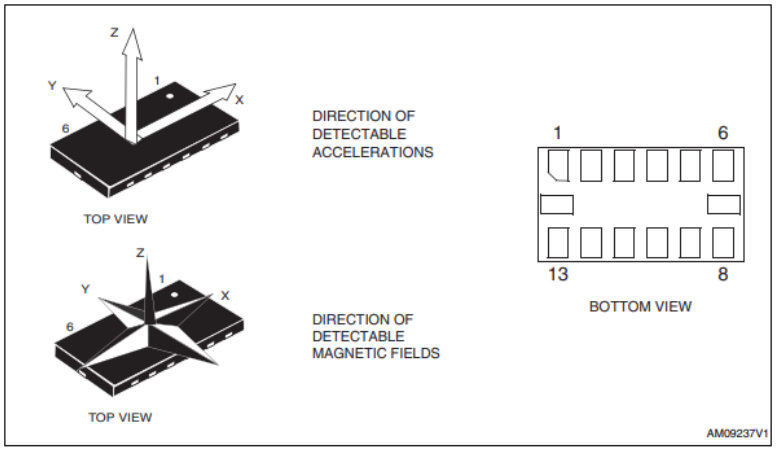

Figure 72. Direction of the accelerations and magnetic fields. *(Source: (This Is Information on a Product in Full Production. LSM303DLHC Ultra-Compact High-Performance ECompass Module: 3D Accelerometer and 3D Magnetometer Datasheet-Production Data Features, 2013)*

Table 15, also extracted from the component datasheet provided by the manufacturer, shows the description of the different pins incorporated in the LSM303DLHC.

Pin#	Name	Function
1	Vdd_IO	Power supply for I/O pins
2	SCL	Signal interface I^2C serial clock (SCL)
3	SDA	Signal interface I^2C serial data (SDA)
4	INT2	Inertial Interrupt 2
5	INT1	Inertial Interrupt 1
6	C1	Reserved capacitor connection (C1)
7	GND	0 V supply
8	Reserved	Leave unconnected
9	DRDY	Data ready
10	Reserved	Connect to GND
11	Reserved	Connect to GND
12	SETP	S/R capacitor connection (C2)
13	SETC	S/R capacitor connection (C2)
14	Vdd	Power supply

Table 15. Pin Description of the LSM303DLHC. *(Source: (This Is Information on a Product in Full Production. LSM303DLHC Ultra-Compact High-Performance ECompass Module: 3D Accelerometer and 3D Magnetometer Datasheet-Production Data Features, 2013))*

6.5 Main Features of the Heading Control System

Now that the main elements that will take part in the heading control system have been selected and detailed, the next step will be to define each of the operations that will be carried out in this process.

The complete program code necessary to control the Arduino will be shown in the annexes, but this chapter will discuss its detailed operation as well as its main features and components.

First of all, before going on to the detailed description of the whole process, some factors that must be taken into account to understand the operation of the system will be discussed.

6.5.1 PID Controller

A question to understand before going to the detailed explanation of the heading control system is the operation of the *Proportional Integral Derivative Controller*.

The calculation of the position to which the servo should be placed will be made from the error experienced in the measurement with respect to the target value, the latter being the first measurement value determined at the beginning of the process. The PID algorithm will be used to perform this calculation. This algorithm has an input signal that comes from sensors and an output that acts on the system in order to keep it operating within certain thresholds. The signal provided by the sensors (input) subtracted from the set point signal will provide the error signal. The main function of the controller will be to keep this error

signal at 0, which will mean that the sensors are measuring the target signal and therefore the system is stable and working correctly. To achieve this goal, the three components of the PID will act as follows:

- P: this parameter Kp is multiplied by the error signal. In this example, if you want to rotate the wheels in the opposite direction to that in which you are taking the error measurement value, you could multiply the error reading by -1. If only this parameter is available in the algorithm, you have a P system.

- I: this parameter seeks to minimize the stationary error, that is, it corrects the offsets of the output. The integral parameter can be defined as the cumulative sum of the error over time of each measurement. The factor Ki is multiplied by the accumulated error and in uniformly sampled discrete systems, it is multiplied by the sampling period.

- D: this parameter takes into account the speed of changes in the error signal, if there are rapid changes in the input, rapid changes will be made in the output. The Kd factor is multiplied by the slope of the error signal.

By playing with the above parameters we can have a P system if it only incorporates proportional part, a PI system if it incorporates Kp and Ki, and a PID system if it incorporates all three parameters. The process used to determine the value of the previously calculated parameters is called tuning process and in this project is done by the Ziegler-Nichols method..

The tuning process of the controller by this method starts with a proportional system in which values are attributed to the variable Kp until the system becomes unstable. The value of Kp is then taken as 60% of the value that causes the instability. The period of oscillation of the unstable output (Pcr) is then measured and Ki and Kd are calculated as in equation 8 and 9:

$$Ki = 2 * \frac{Kp}{Pcr} \quad (eq\ 10)$$

$$Kd = Kp * \frac{Pcr}{8} \quad (eq\ 11)$$

In general, the output angle that is written to the servo, calculated by the PID is represented by equation 10:

$$Output = Kp * e + Ki * \int e\ dt + Kd * \frac{de}{dt} \quad (eq\ 12)$$

In the case of the project, the position angle command for the servo will be 90º minus or plus the measured error, depending on whether the error is positive or negative. This is because the servo will act between 0º and 180º, with 90º being the center position with the wheels straight, and the magnetometer will provide a measurement angle between 0º and 360º.

6.5.2 Libraries Used

In this section we will describe the different libraries to be included in the programming code. The libraries used in programming software "are pieces of code made by third parties that we use in our sketch. This makes programming much easier and allows abstraction making our program easier to make and understand." - *Traduced from: (Librerías Arduino | Aprendiendo Arduino, n.d.)*

The libraries to be used for the Heading Control System and to be included in our programming code using the nomenclature "#include< library name>, are the following:

- <Adafruit_LSM303DLH_Mag.h>: This library provided by Adafruit, the manufacturer of the LSM303DLHC sensor, is specially dedicated to the use of the magnetometer. With the use of this library, we will only have to use its characteristic function "mag.getEvent()" to include a new sensor measurement, followed by the function "(atan2(event.magnetic.y, event.magnetic.x) * 180) / Pi" in order to calculate the instantaneous angle between the vectors of the Y and X axes, and then normalize the calculated angle from radians to degrees, between -180º and 180º. Without the use of the library that directly provides the angle of measurement, it would be necessary to perform a large number of physical calculations related to the magnetic fields captured by the sensor, to subsequently determine the desired angle.

- <Wire.h> : To use the LSM303DLHC board, the Arduino Wire.h library is also required, as it allows it to communicate with devices via I2C (Inter-Integrated Circuit or 2-wire) bus. It uses two lines: SDA (data) and SCL (clock). It connects the GNDs. "The I2C bus is extremely useful for connecting multiple devices, as they can all share the same two wires (plus ground of course). This is because the devices are "addressable". Each device must have a unique address in the range of 8 to 119. Address 0 is reserved as a "broadcast" address, addresses 1 to 7 are reserved for other purposes." – *Traduced from ((Wire - ArduWiki, n.d.,)*.
  At Arduino UNO, the pin connected to the SDA of the chip is the analogical pin A4, and the pin connected to the SCL of the chip is the also analogical pin A5.

- <Servo.h>: As its name indicates, this library will be used to command the servo motor. For its use, first, we must define the name of the variable that we will use to name the servo by means of the function "Servo(servo variable name)". Then we set the output signal to be sent to the servo on one of the digital pins available on the board using the function "servo.attach(digital pin) variable name". Finally, to send a position command to the servo so that it is usually positioned at an angle between 0º and 180º, we will use the function "servo.write(position angle)".

- <PID_v1.h>: For the case of PID, although it can also be applied "by hand", there is also a library that will facilitate the code and also improve the accuracy of the results. In this library the function "PID control (&input, &output&, &setpoint , kp , ki, kd, DIRECT)" is used to declare the variables that will be used in the computation. First of all, the angle measurement signal at each instant will be introduced as input, the "output" variable will be the one in which the PID will assign us the value resulting from the calculation, which will be the angle of position to be sent as a command to the servomotor. The setpoint variable will be declared with the first measurement taken of the direction angle that we want to maintain, the PID will use this variable

as a goal and will try to make the input equal to the setpoint. Finally the parameters kp, ki and kd will be introduced. Other functions included in this library are the function "control.SetMode(AUTOMATIC)", which initializes the operation of the PID, the function "control.SetOutputLimits(-90, 180, which defines the threshold of output values that the PID can adopt. Finally, the function "control.Compute()" allows the calculation of the PID.

6.6 Detailed operation of the heading control system

After having reviewed the different factors that will be involved in the heading control system, as well as: the microcontroller board, the programming software, the sensors, the PID controller and the libraries used, all the ingredients are available to explain in detail the operation of the heading control system.

As mentioned above, the programming code is attached in its entirety in the annexes, but for the detailed explanation of the system operation we will rely on the block diagram shown in Figure 75. Although it is possible that the final program may vary from the one shown in the figure, due to the incorporation of the propulsion system that will be discussed in the next chapter, this is the proposed scheme for the heading control system.

The system starts running when we connect the Arduino UNO board to the power supply. Then, a 4 s timer will be executed, to give the user time to place the dolly in the desired position since this direction will be later set as the heading to be maintained. When the 4 seconds of the timer have elapsed, the working loop of the system will start.

First of all, it will be obtained as input from the sensors: on the one hand by means of the LCM303DLHC the orientation angle will be obtained taking the North magnetic pole of the earth as reference of 0º and the value will be assigned to the variable "heading". On the other hand, by means of the clock incorporated in the Arduino, the time of the instant in which the angle measurement is taken will be measured and assigned to the variable "currentT", to be used later by the PID.

Once the previous measurements have been taken, it will be evaluated if it is the first loop of the process, if so, the position and time values (respectively) obtained from the sensors will be assigned to the variables "Goal" and "previousT". In the case of the "Goal" variable, it will be set as the orientation angle to be maintained and the "previousT" variable will be used to store the time of the previous measurement and will be used later to calculate the time elapsed between one measurement and another. Once these two variables have been assigned in the first loop of the process, this block will not be executed again.

The process starts again by taking the orientation and time measurements from the sensors and assigning them again to the variables "heading" and "currentT". In this case, as it is not the first loop, the process continues to move forward. Then, the variable "Error" is assigned the value corresponding to the difference between the angle

value corresponding to the difference between the measured angle and the target angle is assigned to the variable "Error". And the variable "elapsedT" is assigned the difference between the current time and the time of the previous measurement, obtaining the elapsed time between the two measurements.

The fact that the values of the measured angle can range from 0º to 359º and that it is possible that the variable "Error" is calculated by making the difference between an angle in the first quadrant and the other in the fourth quadrant could bring problems for the system. For example: in case the target angle measurement is 355º and the measurement of the

current angle is 5º, the difference between both would be equal to 10º. However, the variable "Error" would calculate the difference between the target angle and the actual angle (355º - 5º = 350º) and would give us an error value of 350º, which is totally wrong. To solve this, the following two blocks have been incorporated. The specific function of these 2 blocks is to ensure that the measurement of the angle between the two vectors is performed on the side where the angle is smaller as shown in green in Figure 74. If the absolute value associated with the variable "Error" is greater than ± 180º it means that the angle between the wrong quadrants is being measured as shown in red in Figure 74. To solve it, ±360º will be applied to these angles.

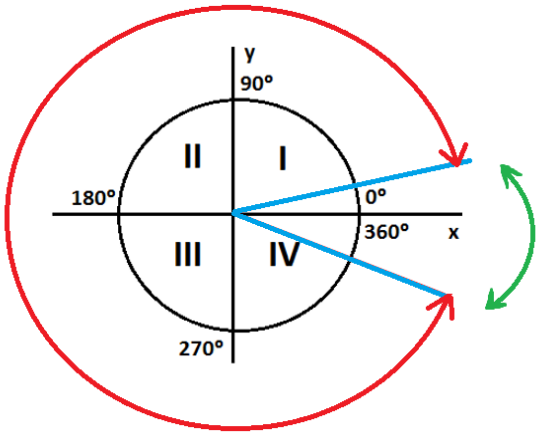

Figure 73. Angle Between Vectors. *(Source: own elaboration)*

Once the measured angle has been corrected, all the data are available to start the calculation of the PI controller (only the proportional and integral parts have been considered for the system design). For its representation in the block diagram, we have opted for the application of the PI controller in manual format, instead of using the library intended for this purpose. In this way, the operations performed by the controller can be seen. The PID first calculates the integral of the error and assigns it to the variable "errorT". Then, it calculates the PID output, applying in this case only the constants Kp and Ki to the error and the integral of the error, respectively. It should be noted that the negative sign is included in the equation because the servo will have to move in the opposite direction to the one it would be if direct transmission were used, since the rack will rotate in the opposite direction to the servo and it will be the latter that will move the wheels. At the end of this block the system assigns the time value in which the angle measurement was taken in this loop to the "previousT" variable, in order to remember it for the next loop.

Finally, the last operation before starting a new loop is to send as a setpoint to the servo the value of the position angle at which it should be positioned. The angles of position in which the servo can be placed are between 0º and 180º, being the angle 90º, the position of the servo corresponding to have the wheels completely aligned. For this reason, 90º are added to the PI output value to give the order to the servo, since in case the PID output was 0 value, which would mean that there is no error between the target angle and the heading angle the servo should be placed in its 90º position (dolly aligned wheels) to maintain that direction.

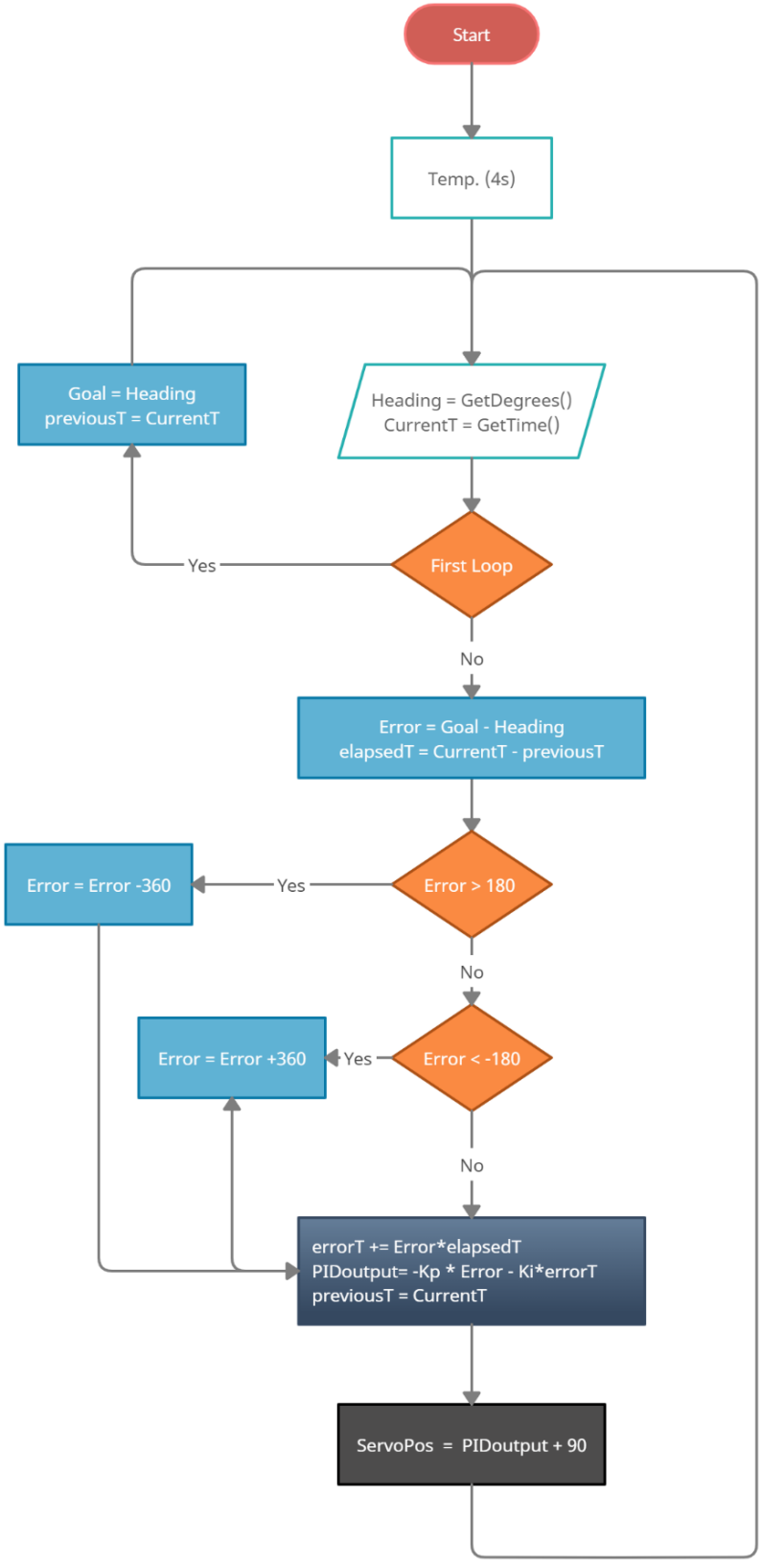

Figure 74. Block Diagram of the Heading Control System *(Source: own elaboration)*

6.6.1 Wiring

To complete the program code summarized together with the block diagram of the previous section, Figure 76 shows the wiring diagram that will allow the first tests to be made with the heading control system before joining it with the propulsion system, to ensure its correct operation and to make the pertinent modifications. It should be noted that the power supply of the system can be delegated to a USB source for testing and to a 9V battery for its application in the dolly.

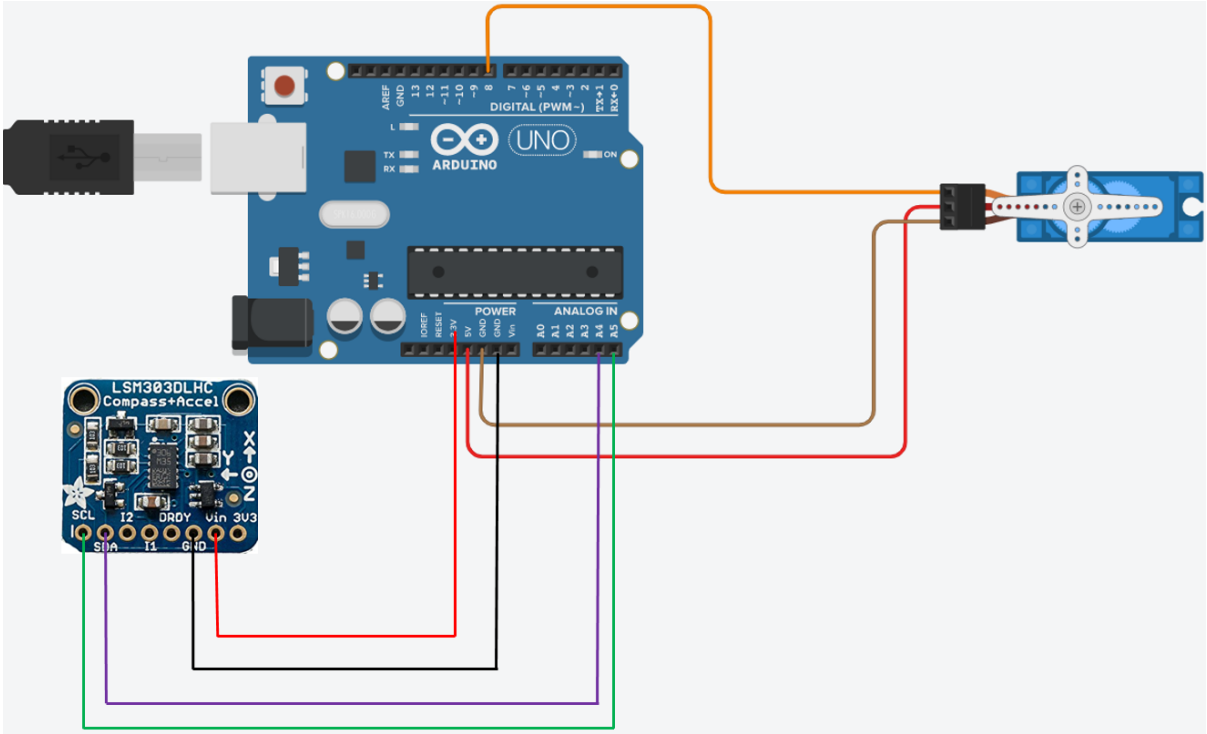

Figure 75. Wiring of the Heading Control System *(Source: own elaboration)*

7 Design of the propulsion system

This section will focus on the review of existing propulsion systems applicable to the dolly for comparison and selection of the most optimal system, as well as the subsequent selection of the elements that compose it, description of its detailed operation, programming and design.

As indicated by its name, the propulsion system discussed in this chapter will aim to provide additional propulsion to the dolly-UAV assembly. Although the aircraft has its own propulsion system studied previously, which will provide the main acceleration force during operation, the need to implement a propulsion system in the dolly will be studied to provide an additional acceleration force to reach the necessary speed to take off the aircraft in less time. This will also reduce the distance required for takeoff and thus reduce the possibility of instability of the dolly by having to travel fewer meters.

7.1 Propulsion system proposals

For the propulsion system, the two main alternatives that can be applied to the dolly have been studied. On the one hand, the implementation of a conventional propulsion system, consisting of an electric motor located on the rear axle of the vehicle or a propulsion system consisting of a ducted fan. In both cases, a control system will be required, which will be carried out by means of the Arduino UNO board previously selected. Therefore, this chapter will also detail all the selected electronic components, as well as their programming code and system wiring.

As mentioned above, two types of propulsion systems will be distinguished and the advantages and disadvantages of each one will be reviewed in order to choose the optimal one for the system. The two proposed methods are the following:

7.1.1 Propulsion system based on driving wheels

In the first of the two possible methods, it is proposed to join the two rear wheels by means of an axle and the subsequent incorporation of an electric motor coupled by means of a gear to the rear axle of the vehicle. The gear coupled to the rear axle, which would mesh directly with the pinion coupled to the motor, should be sized to achieve a transmission ratio suitable for the parameters of the dolly, taking into account the diameter of the chosen wheels and the torque provided by the selected motor. The control system should incorporate electronic components as well as an ESC to control the motor and a battery to power it. While with the heading control system a 9V battery was sufficient, in the propulsion system a battery with more capacity should be used, due to the high electrical consumption of the motor. The controller used will be the same as for the heading control system, so that all the code will be centralized in a single program and a single microcontroller board.

The advantages and disadvantages of this type of propulsion system will be defined below.

Advantages:

- The main advantage of using this system is that it is the most widely and globally used system in practically all land vehicles. This means that the amount of information in relation to its application is much greater.

- Another advantage derived from being also the most used system in RC cars, is that both the range of motors and controllers to choose from, as well as the number of examples of programming codes relating to the propulsion system using a motor coupled to an axis, are also higher than with the other system.

- For the same motor power, the acceleration of the dolly with this system will be higher, since the torque is applied directly to the wheels in contact with the ground.

- The price of the motor and the elements as a whole is usually cheaper than in the other proposed system.

Disadvantages:

- The incorporation of this type of system would entail the union by means of an axle of the two rear wheels of the dolly. Since the use of a differential like the one used in automobiles would complicate the design a lot, this would mean that the two rear wheels would rotate at the same time. Although in the working range of the dolly this will not be a fundamental problem, since the speeds reached will not be very high and the turns will not be very tight, the connection of the rear wheels by means of an axle could lead to a lack of stability as well as skidding in tight turns.

- The fact that the incorporation of a suspension system has not been considered means that the wheels of the dolly may lose contact with the ground at certain times. With a propulsion system based on the contact of the wheels with the ground this can cause that the system is not used to its full potential as well as instabilities in the case that the wheel of one of the sides is in contact with the ground and therefore accelerating the vehicle while the rear wheel of the other side is suspended in the air due to an irregularity of the terrain, without providing acceleration on that side. This would work against us considering that one of the objectives of the dolly is to maintain a fixed direction.

- On the other hand, the incorporation of a propulsion system based on a motor coupled to the rear axle, involves more parts than in the other system proposal. In addition to having to perform gear ratio calculations as well as gear design.

- Although the acceleration is higher with this system, this can lead to problems since the aircraft must be attached as little as possible to the dolly in order to be free to take off. If the acceleration is too high at start-up the UAV could fall over.

7.1.2 Propulsion system based on a ducted fan

In this other alternative it is proposed the use of a propulsion based on a ducted fan of similar specifications to those used in model airplanes or even in vehicles such as the overcraft. This ducted fan should be attached to the back of the dolly by means of a support and its operation, unlike those used in airplanes, would be based on thrust instead of suction. The control of the same would also be done by an ESC which in turn would be controlled by the Arduino UNO microcontroller board, unifying the programming code of the heading control system and the propulsion system. In this case it would also be necessary a battery preferably lithium, due to the high requirements of the motor, which in this case would be even higher than the other proposed system for propulsion.

Advantages:

- The most outstanding advantage is the simplicity of the system since in this case it would only be necessary to design a support to attach the ducted fan to the dolly and a rear axle could be dispensed with, as well as the design and construction of the gears. Therefore, not only does this system require fewer parts, but also its calculation and assembly are much simpler.

- The fact of dispensing with the rear axle allows the dolly wheels to rotate independently, improving the stability of the whole, especially in turns.

- Another notable advantage is that since the propulsion system is not based on the contact of the wheels with the ground, the suspension system becomes dispensable on tracks in "normal" conditions (without many bumps). This is because the ducted fan will be providing propulsion at all times equally and unlike the previous case, if at a certain moment one wheel is touching the ground and the other is not, the stability of the whole will not be affected so seriously. Since if the ducted fan is located in the middle of the two wheels, the deviation produced in the above mentioned case will be minimal.

- In this case, although the acceleration at the moment of start-up is lower, this can be done in a smooth and progressive way, so that the UAV, which must be little held by the dolly to facilitate its take-off, will be more stable at the beginning and there is less chance of it falling.

Disadvantages:

- One of the main disadvantages is that there are few ground vehicles at a general level that use this type of propulsion system, with the result that information on this is also more reduced and it will be necessary to resort in many cases to searching for information on this system applied in airplanes.

- Another disadvantage is that for two engines with the same power, the propulsion system based on driving wheels will provide more acceleration than the system based on a ducted fan.
- The range of products available for selection to meet the requirements is smaller than in the previous case.

- The price is usually higher than in the case of the drive wheel system.

7.2 Simulation of the propulsion system

After comparing the advantages and disadvantages of each of the two propulsion methods, the use of the ducted fan as a propulsion element clearly stands out as the most advantageous method for use in the dolly. Even so, a simulation will be carried out using the "Algodoo" physical phenomena simulation software, in which we will first study whether the incorporation of an additional propulsion system is really necessary, and if so, which of the two proposals is more favorable at a practical level. In order to carry out the simulations as close to reality as possible, a dolly and UAV model have been designed that are very similar to the original in terms of shape, size and weight. In addition, thanks to the eCalc simulation performed at the beginning of the paper, it was possible to conclude that the static thrust was 2kg, equivalent to 20 N. Therefore, as an approximation and considering a certain safety factor, the aircraft will be assigned this thrust force on its propeller.

The purpose of the different simulations is to compare the performance of each of the proposals. First of all, it will be verified that the system manages to reach the necessary speed to take off the aircraft, which according to the eCalc software is around 9.2 m/s. On the other hand, the stability and speed with which this speed is reached will be evaluated, as well as the distance traveled to achieve it. Finally, the maximum acceleration of the set will also be evaluated, since if it is too high the plane could fall off the dolly before takeoff.

7.2.1 Simulation without an additional propulsion

First, a simulation of the first case will be performed, in which it is considered that no additional propulsion system is included, so that the model of the first simulation will be driven only by the propeller that incorporates the UAV. To simulate the thrust force performed by the propeller, a force vector of 20 N has been applied to the tail of the aircraft. This value corresponding to the thrust force of the aircraft has been determined in the report shown above provided by the eCalc software, but in addition, it has been empirically verified in the program that with the given conditions, if a force value higher than 25 N is applied, the aircraft falls off the dolly due to the acceleration, while if a force value lower than 15 N is applied, the assembly never reaches the take-off speed. Figure 77 shows the design made for the simulation:

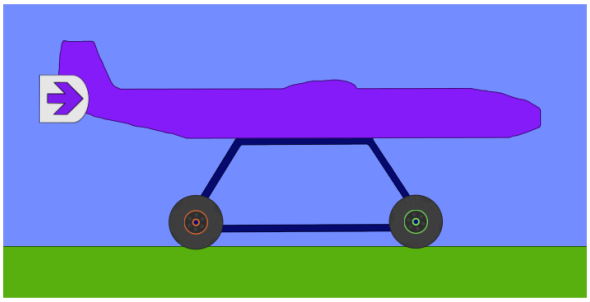

Figure 76. Algodoo Simulation of the dolly without additional propulsion.
(Source: own elaboration)

Figure 78 below shows the speed-time graph provided by the same program.

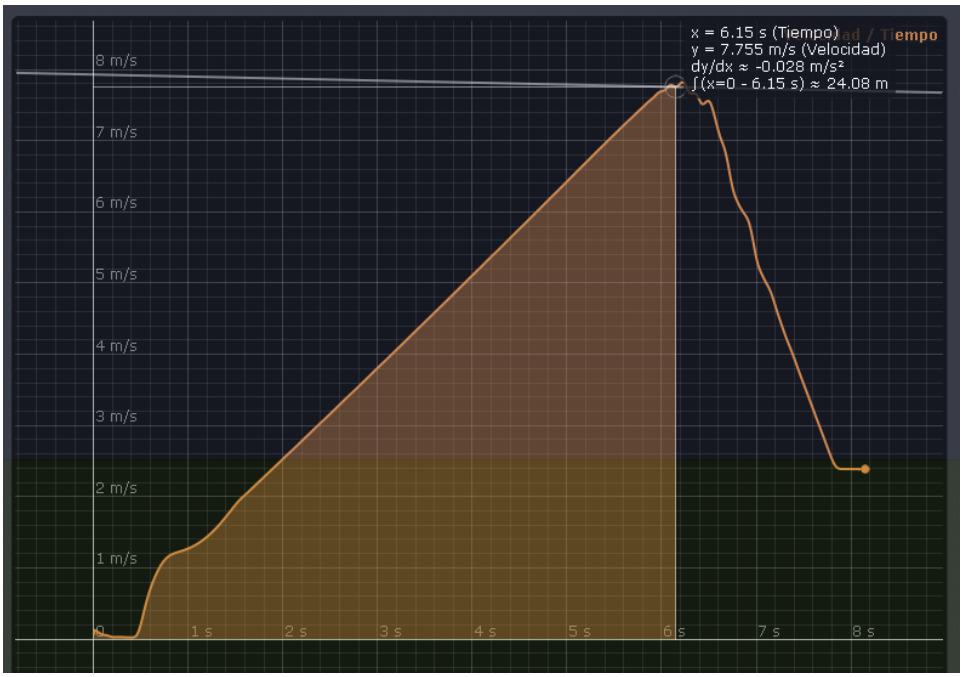

Figure 77. Simulation graph of system without additional propulsion. *(Source: own elaboration)*

As can be seen in this first simulation graph of the system without additional propulsion, the dolly-UAV assembly is quite stable. As shown in the graph the peak is reached at 6.15 s from acceleration and culminates with a maximum velocity of 7.76 m/s. From that moment on, the speed plummets because the aircraft separates from the dolly and the dolly does not incorporate a propulsion system.

7.2.2 Simulation with a ducted fan incorporated in the dolly

In this second case, we consider the application of a ducted fan as additional propulsion. The previous parameters in terms of material, weight, shape, wheel diameter and propulsion of the aircraft remain the same, only differing from the previous simulation in the addition of a new propulsion system.

As the propulsion system incorporated in the aircraft is practically sufficient for take-off, the additional system will serve only as a booster to provide additional acceleration, and for this reason it has been sized to provide a thrust force of 15N. This value has been experimentally proven to be the most optimal by performing four simulations. It has been seen that for lower values, the impact of the additional propulsion system was minimal, while for higher values, the acceleration at the initial moment was such that the aircraft fell off the dolly.

Figure 79 shows the new design used for the simulation.

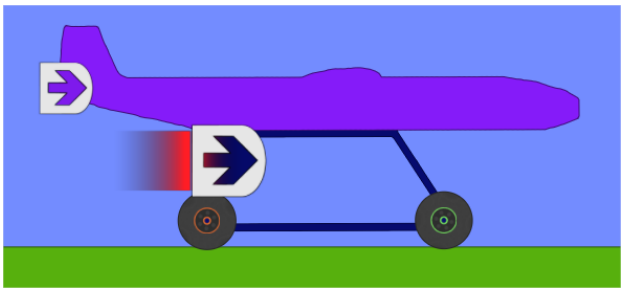

Figure 78. Algodoo simulation of the dolly with a ducted fan as additional propulsion. *(source: own elaboration)*

As shown in Figure 80, the value of thrust force that must be applied to the dolly for takeoff to occur under ideal conditions has been tested. First of all, it should be noted that for an additional thrust force of 5N, the behavior with respect to the system without additional thrust varies very little, since it is also not able to reach the speed necessary for the aircraft to take off. On the other hand, the simulation with an additional thrust force of 20 N has turned out to be quite critical, since the initial acceleration makes the airplane on the verge of falling off the dolly. In order to ensure a correct take-off, the additional acceleration with a thrust force of 15 N has been proposed.

The graph shows that for an additional thrust force of 15N, the airplane would lose contact with the dolly after almost 3 seconds from the start and would reach a velocity of 9.2 m/s.

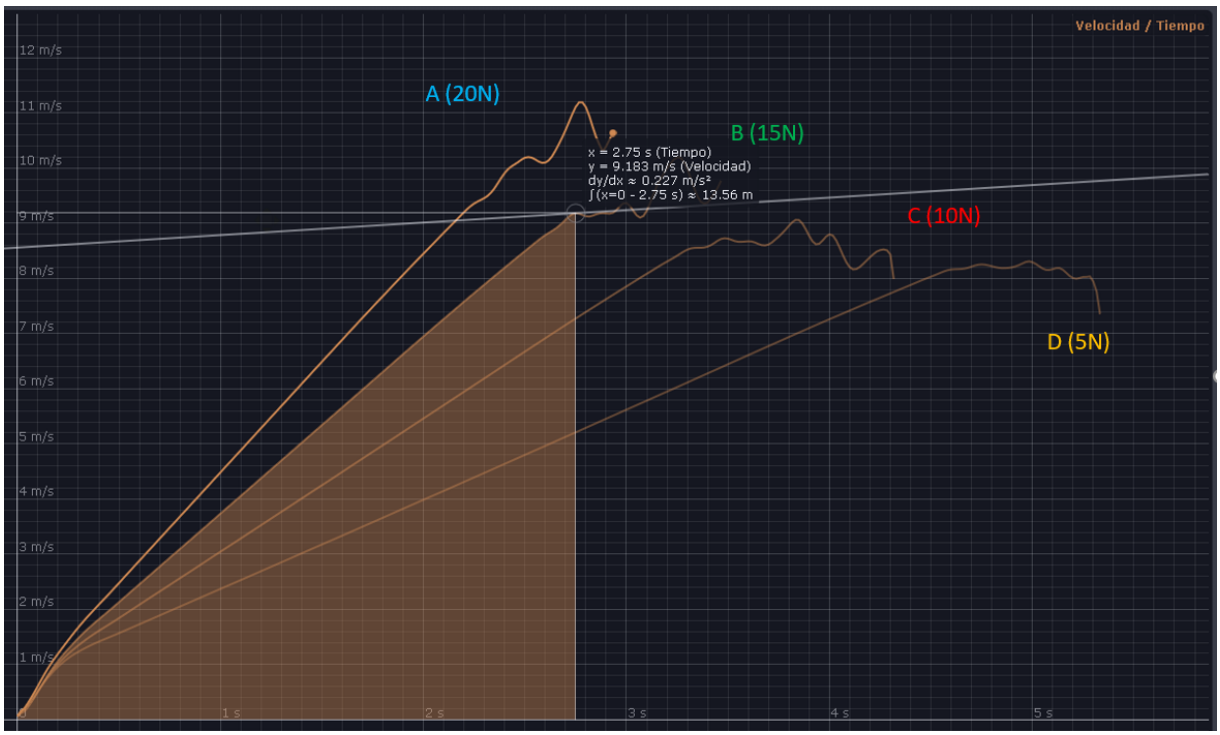

Figure 79. Simulation graph of system with a ducted fan as an additional propulsion. *(Source: own elaboration)*

7.2.3 Simulation with tractive wheels incorporated in the dolly

In this last proposal, it is proposed to replace the ducted fan by a conventional traction system driven by a motor. In this case, the simulation graph corresponding to a motor of 150 rpm and 150 Nm is shown directly in Figure 81.

It can be seen that, as predicted, although the initial and maximum acceleration is higher using a system of this type, the maximum speed is higher using the ducted fan propulsion system. In the case of this simulation, if the engine properties such as rpm or torque are increased, the initial acceleration becomes such that the aircraft drops, while the final speed is still lower than with the other system.

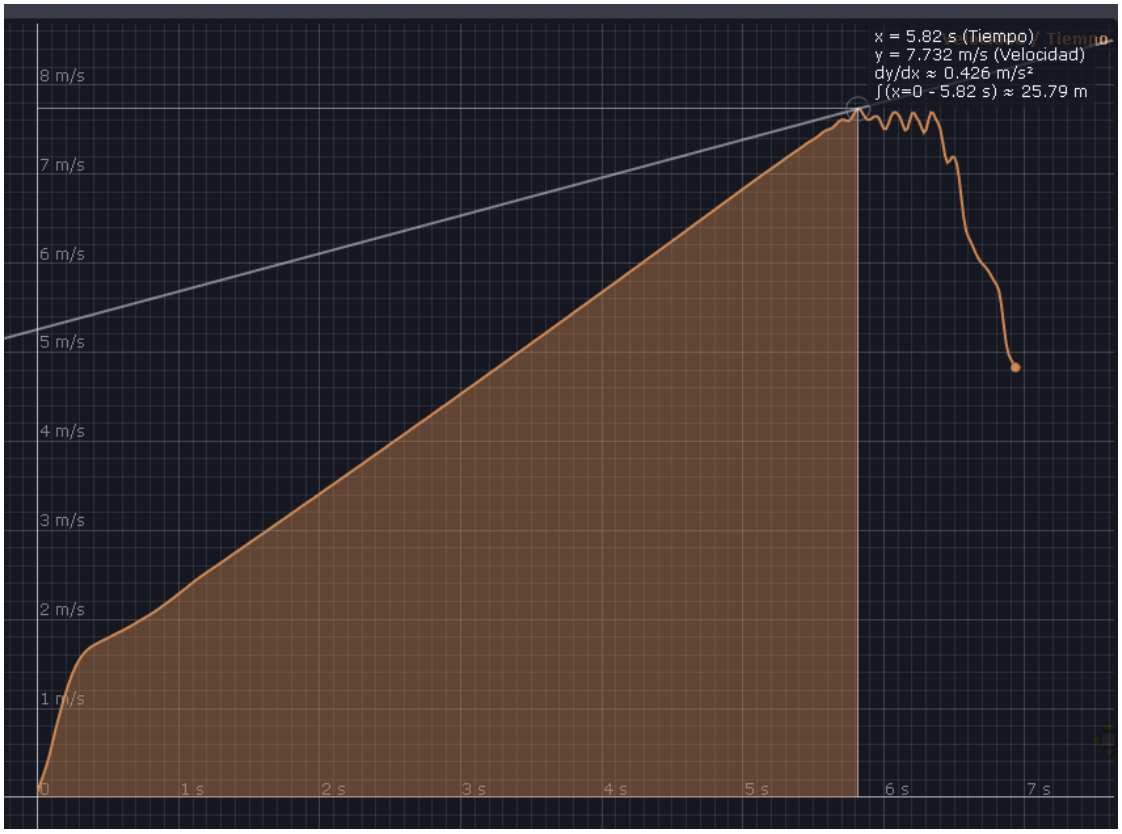

Figure 80. Simulation graph of system with tractive wheels as an additional propulsion. *(Source: own elaboration)*

As mentioned above, after reviewing the functionalities of each of the systems, the first to be discarded was the propulsion system with driving wheels, since its final speed does not compensate for the high acceleration it provides at the beginning. Using this system would require regulating the delivery of torque and power when accelerating, so that it would be done more smoothly. Yet this would require additional work. On the other hand, as evaluated in the previous sections, it was the most unfavorable system.

Due to the need for an additional propulsion system, which could also be seen in the simulation in which the dolly had no propulsion at all, the ducted fan propulsion system was selected for application in the dolly.

7.3 Ducted fan selection

After having studied and compared the different propulsion systems, the ducted fan has been chosen as the optimal system to provide the additional thrust force needed to reach the take-off speed in an optimal time. This chapter will review both the specific model chosen and the electronic components needed to control it, as well as the mechanical support that will attach it to the dolly.

First of all, it should be pointed out that a ducted fan differs from a turbine mainly in that "the turbofan or fanjet is a type of air breathing jet engine that is widely used in aircraft propulsion. The word "turbofan" is an acronym of "turbine" and "fan": the turbo portion refers to a gas turbine engine which achieves mechanical energy from combustion, and the fan, a ducted fan that uses the mechanical energy from the gas turbine to accelerate air rearwards."- *(Turbofan - Wikipedia, n.d.).* As in our case the propulsion only incorporates the second part of the acronym, it will be called ducted fan.

As for the ducted fan model to be used, again the Lighting Research Group of ESEIAAT provided the model shown in Figure 82 for application in the dolly. Its technical characteristics will be reviewed below to ensure that it meets the requirements to be used.

The proposed model is a common model used in aeromodelling. As the ducted fan has a brushless motor (BLDC), it will be necessary to use an ESC to control its operation with the Arduino UNO microcontroller board. On the other hand, a battery will also be necessary as a power source due to the high power consumption of the motor.

Figure 81. Selected ducted fan. *(Source: (Avión RC Motor, 64 Ducts 4500KV Motor Sin Escobillas + Propeller Power Kit Para Hasta 1200g RC Modelo Avione: Amazon.Es: Juguetes y Juegos*, n.d.*))*

Table 16 below shows the main characteristics of the chosen ducted fan, taken directly from its data sheet:

Brand	QXmotor
Store	Amazon
Motor Model	4500 KV-QF2611
Motor Type	BLDC (brushless)
Motor Material	Aluminum
Configuration	9N6P
Max Continuous Current	27A
Max Continious power	280 W
Max Efficiency	>70%
Propeller Material	Plastic (n.e.)
Recommended ESC	30 A
Dimensions	65mm x 65mm x 70 mm
Weight	60 g
Number of Blades	5
Indicative Load	1200g
Price	23,87 €

Table 16. Duct fan features

From the above table of characteristics, it can be noted that the ducted fan is suitable for loads up to 1.2 kg, which approximately coincides with the thrust force applied in the simulation with Algodoo. With this data we can take for granted the choice of model for the additional propulsion of the dolly.

It is also noted that it has a 4500KV motor, which means that if we supply 10V to the motor, it would be able to rotate at a maximum of 45000 rpm. Since the KV rating of a BLDC defines the rpm per volt of the motor running without load. As for the other data, It should be noted that the motor can withstand a maximum peak current of 27A, that it can reach a maximum power of 280W and that its maximum efficiency is over 70%. In addition, it is also important to highlight the manufacturer's recommendation regarding the amperage for the ESC (Electronic Speed Controller) that should be used preferably its 30A.

The type of motor that incorporates the ducted fan is a BLDC (Brushless DC) motor. Unlike conventional motors that use a gas collector and brushes in its operation, this type of motors is based on the principle of alternating by electronic control, the polarity of its coils in order to rotate the magnetic field and in turn the rotor of the motor, at the desired speed. This type of motors usually has permanent magnets in the rotor, while the stator is wound. So the polarity of the rotor is fixed, but by controlling the polarity in the three stator coils can attract and repel the poles of the rotor magnet and thus regulate its speed. To carry out the process, sensors called "Hall effect sensors" are used by a controller (ESC) to monitor the exact position of the rotor." – *Traduced from: (¿Qué Es Un Motor BLDC Con Sensor y Cómo Funcionan Mejor?, n.d.)*

Figure 83 shows the basic motor operation scheme.

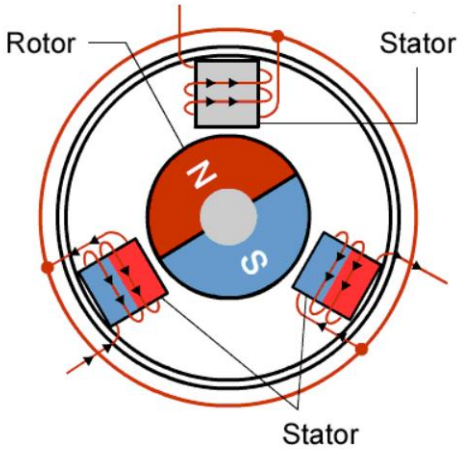

Figure 82. BLDC basic operation *(Source:* (*What Are Brushless DC Motors* | *Renesas*, n.d.) *)*

As for the wiring of the brushless motor chosen, the red, yellow and black wires correspond to the three phases of the motor and their connection to the ESC is indifferent.

7.4 Selection of the ESC

To control the speed of the BLDC motor that incorporates the ducted fan, it will be necessary to use an ESC (Electronic Speed Controller), which is the electronic device that will allow us to exchange the polarities of the motor windings.

The ESC uses the same control signal as the servos in Arduino, as shown in Figure 84, is controlled by 50Hz pulses with a PWM signal, which in the case of this project will be sent as a setpoint from the microcontroller board. In the same way as if it were a servo, the higher the Pulse Width, the higher the revolutions per minute, which in the servo would be a greater angle of rotation. In this way, you can easily control the speed of the motor through the programming code uploaded to the Arduino UNO microcontroller board.

As mentioned above, Figure 84 below shows the control process by which the setpoint is sent to the motor:

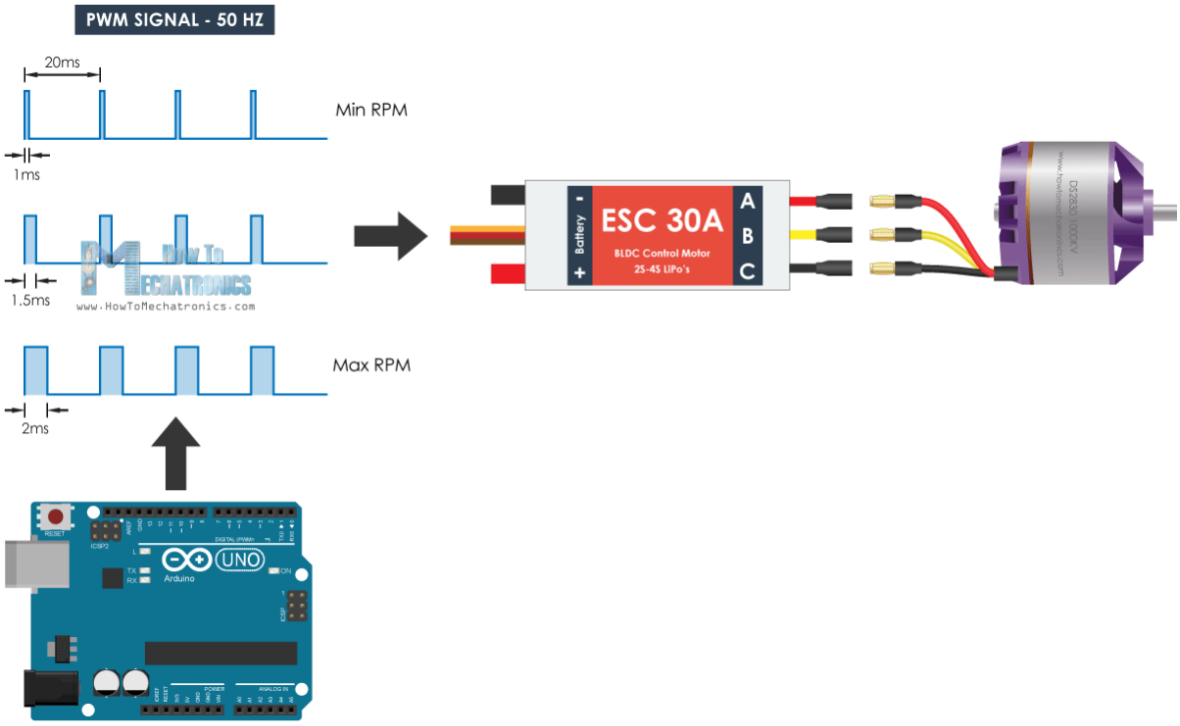

Figure 83. BLDC controll using Arduino UNO. *(Source: https://howtomechatronics.com/tutorials/arduino/arduino-brushless-motor-control-tutorial-esc-bldc/)*

In the case of the ESC, it has also been provided by the Lightning Research Group of ESEIAAT. In this case, it is an Aeolinan ESC, model XP-30A-I, which meets the technical and quality requirements to control the BLDC used in the dolly.

Its main characteristics are shown below, extracted from its data sheet, attached in its entirety in the annexes.

Model	Continuous Current	Burst current (10S)	Li-XX	Size(mm) L*W*H	Weiht (g)	BEC (Linear)	Program Function
XP-30A-I	30A	40A	2-4	50×28×12	34	2A	YES

Table 17. Aeolian XP-30A-I datasheet.

In its data sheet it can be seen that the ESC has the amperage recommended by the BLDC manufacturer. The data sheet also assures its compatibility with lithium batteries between 2S, 3S or 4S.

7.5 Selection of the battery

After choosing the previous elements, it is time to choose the battery that will serve as a power source for all the elements of the system. Among all the existing battery types in the market as well as lithium, gel, AGM or acid batteries, we will opt for a Lipo battery, because although they are usually more expensive, they are also more compact, have a longer life and are prepared to assume high charge and discharge cycles, as well as high depth of discharge. Within the lithium batteries, we will pay special attention to those used in RC vehicles.

In the case of the battery, it has also been supplied by the Lightning Research Group. As in this case the specific requirements are lower and virtually any lithium battery with a voltage between 11V and 15 V, a capacity between 1000 mAh and 5000 mAh and a weight between 50 and 350 gr, would serve us. As for the battery life, the real requirement is minimal since its application in the dolly does not imply a long time of use. The wear of the battery will occur in peaks of high intensity and short time, since the turbine motor, which will be the main consumption to supply, will consume about 280W but in separate intervals of about 10s in a row, which is the maximum time that is estimated to last the takeoff.

Figure 85 shows an image of the battery to be used.

Figure 84. Selected battery. *(Source:* (*Tattu Batería LiPo 2300mAh 14.8V 45C 4S Para Multicopteros FPV Racing Helicópteros Barcos y Modelos RC Diversos: Amazon.Es: Electrónica*, n.d.) *)*

The battery provided by the LRG is of the "Tattu" brand and its main characteristics are shown below:

Battery Capacity	2300 mAh
Battery Voltage	11,1 V
Discharge Rate	45C
Max Burst Discharge	90C
Cell Configuration	3S1P
Connector Type	XT60
Balancer Connector	JST-XHR
Weight	222 g

Table 18. Main features of the selected battery.

Next, we will discuss the main characteristics of the battery shown in the table above:

As for the capacity of the 2300mAh battery, we can say that the battery is capable of delivering 2300 mA for one hour. As for the voltage, its datasheet indicates that the battery can provide 11.1V and has a 3S1P configuration, which means that it is built from three 3.7V cells arranged in series.

As for the discharge rate of the battery, it measures the discharge rate of the battery, i.e., it measures the maximum current that the battery can safely deliver. The discharge rate will be determined by the capacity of the battery. In this case we observe that the battery has a continuous discharge rate of 45C and a max burst discharge of 90C. The second measures the maximum discharge rate or rate at which the battery can be discharged in a short period of time, usually about 10 seconds.

To evaluate the maximum current of the battery, the battery capacity must be multiplied by the discharge rate:

$$2300\ mAh * 45C = 103500mA\ = 103\ A$$
$$2300\ mAh * 90C = 207000mA = 207\ A$$

And to find out how long this current could be applied before the battery would cut off the supply, the following operation must be performed:

$$\frac{60\ min}{45C} = 1{,}33min \rightarrow 1min.18\ s$$

As can be seen from the above calculations, for the maximum continuous discharge rate of 45C, the battery could supply a peak current of 103A for one minute and eighteen seconds. And it could supply a peak current of 207A for approximately 10 seconds.

Following the above example, we can calculate an approximation of how long the battery will last with the chosen ducted fan operating conditions. As seen above, the ESC selected for the BLDC motor control has a nominal amperage of 30A. If we repeat the calculations made starting from a continuous current supply and equal to 30A (which in practice will not be the case but we consider the worst conditions), we obtain the following:

$$2300\ mAh * C\ = 30.000\ mA \rightarrow 13{,}04C$$

$$\frac{60\ \text{min.}}{13{,}04\text{C}} = 5\ min.$$

As it has been observed, in case of using the ducted fan motor at a continuous amperage of 30A, which is the maximum current that the ESC can supply under normal conditions, the motor could be used for 5 min. continuously. As the BLDC motor used can only supply a maximum amperage of 27A, the battery life will be longer than calculated. Even so, we will consider that this battery is valid since the take-off time of the aircraft is about 10s, so in case the battery life would be 5min. it would be enough.

7.6 Detailed operation of the propulsion system control

This section will detail the program code used to control the propulsion system by means of the Arduino microcontroller board and using an ESC to control the motor. This program code will not be the definitive one, since it would be necessary to join it to the code used for the heading control system and thus unify all the programming code in a single program file. Although this will be discussed in the next chapter, here we will focus on the code needed to control the propulsion system.

It should be noted that since the user will have his hands full commanding the airplane with its respective controller, the propulsion system and the whole control system of the dolly in general must be completely autonomous and not depend on the user's manipulation. For this reason, the program starts with a 5-second timer from the moment power is supplied to the microcontroller board. As seen in the heading control system, a four-second timer was applied before the first measurement of the steering angle, which would be the direction to be maintained. In this case, a five-second timer is applied to give the user time to set the dolly in the desired orientation, the heading control system to set the direction to hold and one second later the BLDC motor starts to run.

Each of the processes followed in the program code and detailed in the block diagram shown in Figure 86 will be detailed below.

First of all, when starting the program, and before the delay of 5 seconds, the variable "stop" will be declared and assigned a value of "0". This variable will be used to stop the system when the takeoff has finished. On the other hand, the variable "Throttle" will be declared and assigned a value of 1000. This variable will be used to control the motor speed. As mentioned above, the Arduino will control the ducted fan through the ESC in the same way as if it were a servo, therefore, the range of the BLDC speed setpoint will be between 1000 microseconds and 2000 microseconds. Being 2000 microseconds the maximum speed and 1000 microseconds with the motor off. Then a delay of 5 seconds will be applied to give the user time to place the dolly and hold the aircraft control.

Next, the time elapsed from the start of the program until now will be measured and assigned to the "Time" variable. Then, the motor will be initialized by sending a 1000 microsecond setpoint to the ESC.

After checking that the "stop" variable, which regulates the end of the process, is not activated, the system will enter a loop in which the motor speed will be progressively increased in steps of 25 microseconds every 25 milliseconds up to 30% of its maximum speed. Both the percentage of maximum speed and the acceleration process will be finalized empirically when the first tests are performed.

When the desired speed has been reached, the program will enter a new loop in which the time elapsed since motor activation will be checked. When this time is greater than 7 seconds, which is the approximate time required for take-off, the motor will be sent the command to stop, the value "1" will be assigned to the variable "stop" and the system will stop.

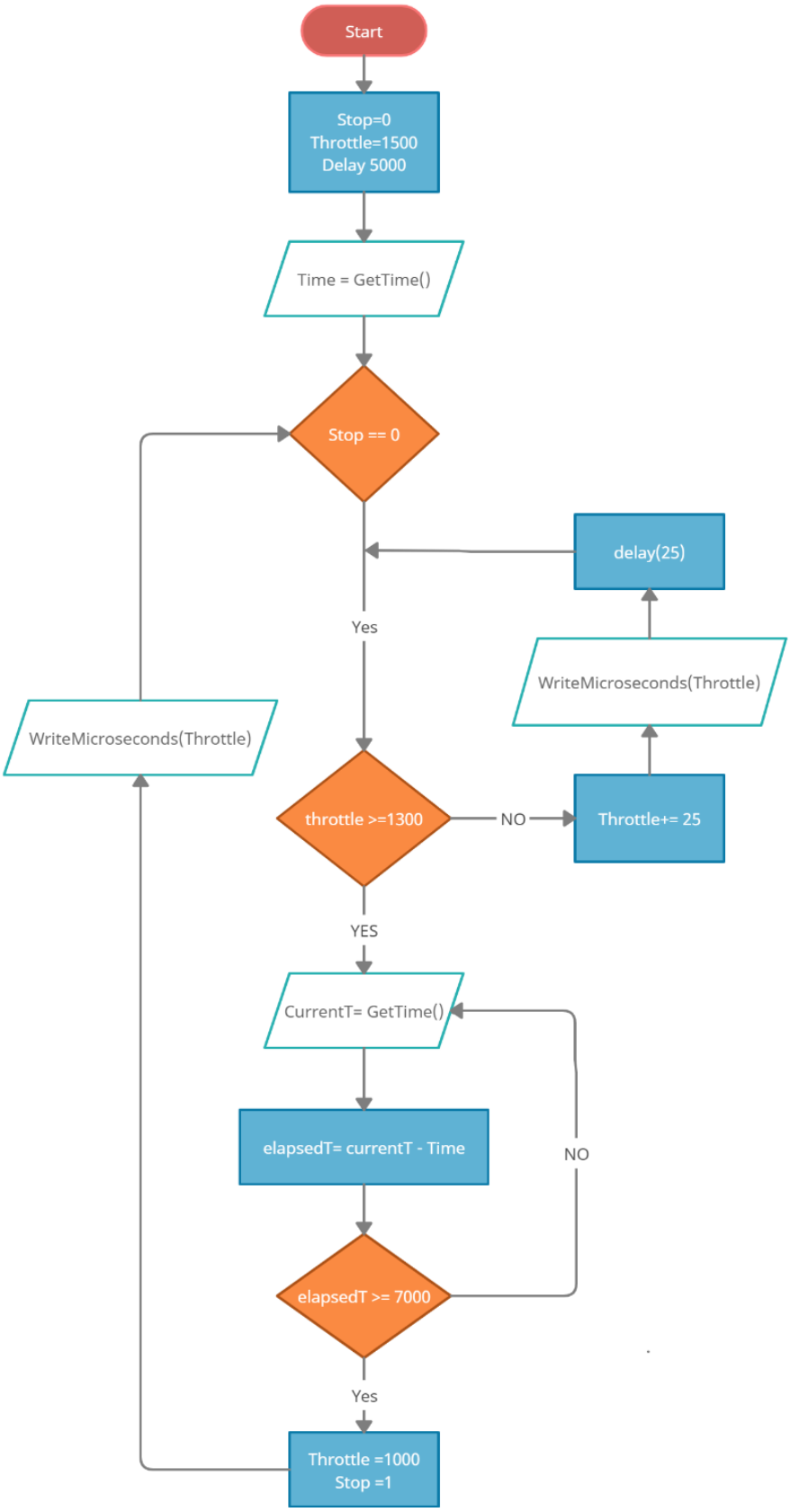

Figure 85. Block diagram of the propulsion system *(Source: own elaboration)*

7.7 Wiring of the propulsion system

After having detailed each of the elements that will take part in the propulsion system and having explained each of the processes that the programming code follows by means of a block diagram, we will proceed to explain the wiring of the system. First of all, it should be noted that this will not be the final wiring diagram for the dolly since it is not yet connected to the heading control system shown above. Therefore, the final schematic, including the two dolly control systems, will be detailed in the next chapter.

Figure 87 shows the connection diagram of the propulsion system.

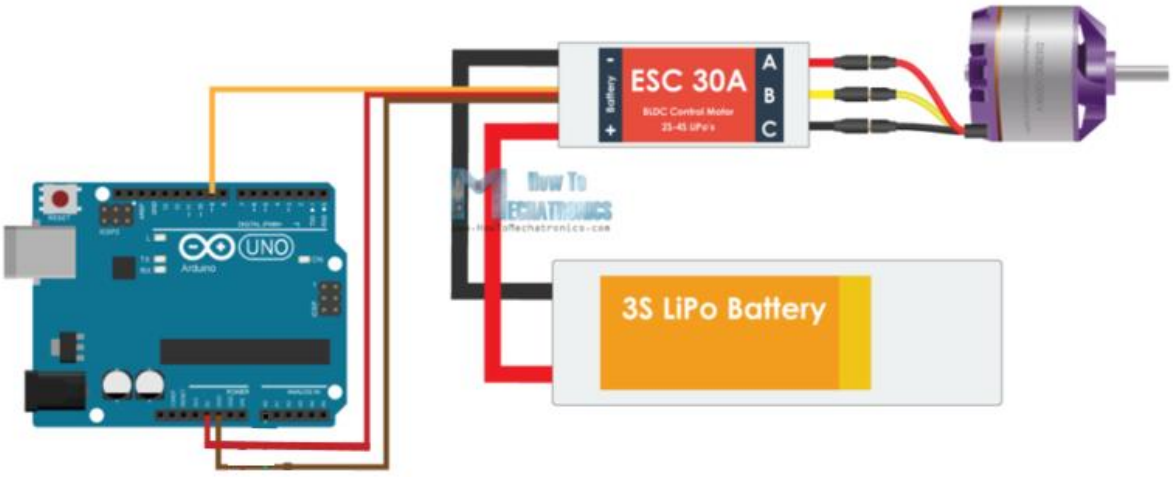

Figure 86. Wiring of the propulsion system. *(Source: (Arduino Brushless Motor Control Tutorial | ESC | BLDC - HowToMechatronics*, n.d.*))*

As shown in the schematic above, a total of 8 wires will come out of the ESC. The two thicker ones, red and black, will be connected to the Lipo battery. On the other hand, the three equal wires red, yellow and black will be connected directly to the three phases of the BLDC motor. The connection between phases is indifferent, as previously mentioned. Finally, returning to the other end, the three wires of lesser section, yellow, brown and red, will be connected to the Arduino UNO microcontroller board. Of these three wires, the brown and red wires will serve to directly power the microcontroller board and indirectly power the servo motor and magnetometer chosen in the previous chapter. In this way, the entire system can be powered by the Lipo battery. Finally, the yellow wire will be connected to a PWM digital pin of the microcontroller board. It will be through this wire, that Arduino UNO will send signals with a frequency of 50Hz varying the pulse width depending on the desired speed. The ESC will use an advanced system of sensors and transistors to convert the signal received from the Arduino into electrical pulses in order to alternate the polarity in the brushless motor coils.

8 Final design of the dolly

After having detailed and specified the design process, calculations, construction and selection of each of the components and systems that will form the dolly, this chapter will show the final model, composed of all the systems detailed above.

8.1 UAV support design

After the design of each of the parts and systems of the dolly, the only thing that remains to be determined is the support on which the aircraft will be placed for the take-off maneuver.

For this purpose, going back to the review of existing dollies that was made at the beginning of the document, two possible ways of holding the airplane are observed. First, the UAV can be attached in front of the wings, so that when the aircraft engine is accelerated, the wings impinge directly on the dolly, pushing and accelerating it. The other option for transporting the aircraft during acceleration is to hold it directly by its base, so that the friction with the dolly transmits the acceleration to the dolly. In reality, both options can be valid since they have been proven to work during the revision of existing models. Even so, both methods have advantages and disadvantages that will be reviewed below.

8.1.1 UAV supporting by the wings

As mentioned above, this first method of support consists mainly of adding a lever to the top of the dolly, which allows direct contact with the front of the UAV wings. In this way, the wings themselves push the dolly forward, accelerating it in the same way as the UAV.

The main advantage of using this system is that as the aircraft is held by the wings, butting directly against the dolly, no matter how high the acceleration of the whole, the aircraft will not fall or be left behind either of the two components, since there is a direct contact between the two and by the principle of action reaction described by Newton's second law, the acceleration in both will be the same. This means that with this system a maximum of power could be supplied to both the ducted fan of the dolly and the engine of the aircraft to reduce to the maximum the take-off distance and time, thus also reducing the possibility of problems during take-off.

On the other hand, the main disadvantage is that since the airplane is attached to the wings, when it reaches the "stall speed", speed from which it is self-supporting, the support or lever that joins the airplane to the dolly can hinder the freedom of the airplane to take off. This fact can cause an accident and as a consequence, the breakage of the UAV or even the dolly, since at the moment in which this problem can occur, the dolly-UAV assembly will be at a speed close to 40 km/h or even more.

The proposed solution to this problem will be considered in the chapter on possible improvements.

8.1.2 UAV supporting by the base

The second proposed method consists of supporting and holding the UAV by its lower base. In such a way that the friction between the UAV and the dolly surface is sufficient to prevent the aircraft from falling during acceleration. For this purpose, it is proposed to have a methacrylate base similar to the one used in the two lower bases, dedicated to support the electrical components as well as the BLDC motor, the servomotor, the pinion and the rack. In this case, the base will be placed on top of the dolly chassis and fastened by means of a bolt through to the upper joints. To ensure the orientation of the airplane and avoid lateral movement, a support will be included on each side, manufactured in PETG with the 3D printer, which will adapt to the shape of the airplane. Finally, to maximize friction, a rubber sheet will be included on the base of the dolly.

Compared to the previous proposal, the main advantage is that in this case the plane does not have any obstacle at the moment of take-off, so that when it exceeds the stall speed required for take-off, it simply separates from the dolly above, without having contact with any of its parts. On the other hand, its major disadvantage is that the acceleration of the assembly is limited to a smaller range since, not having a part that acts directly as a support, the aircraft runs the risk of flying off the front if its acceleration is much greater than that of the dolly. However, this problem is considerably diminished if we consider the insertion of the propulsion system intended to provide additional acceleration to the dolly and the placement of a rubber sheet on the methacrylate that will considerably increase the friction between both surfaces. All this added to the fact that the user also has the ability to reduce the acceleration peak of the airplane by means of his remote control, makes this the chosen solution, since the solution to the problem of the previous system affects to a greater extent the operation of the whole and is more difficult to solve.

8.2 Hardware

Before finalizing the modeling of the final version of the dolly, it will be necessary to include the screws needed to join the different parts together.

For the selection of the hardware, the web page: www.traceparts.com has been used to download the hardware models used, from a database of CAD files referring to standardized elements provided by the manufacturers themselves. These models are included in the project in the dolly CAD folder. On the other hand, the hardware and other selected elements will not be included in the drawings, since only the elements manufactured or modified by the author will be included.

A list of the hardware used is shown in Table 19 below:

Component	Rule	Dimension (mm)	Units
Joint	-	12 x 6 x 4	4
Bolt	DIN EN 24017	M6 x 30	23
		M6 x 50	7
		M8 x 60	4
	DIN 912	M3 x 10	4
		M3 x 12	6
		M5 x 12	4
Nut	DIN 934	M6	30
		M8	4
		M5	4
	DIN 433	M3	10
Washer	DIN 125	M3	10
		M5	4
		M6	30
		M8	4

Table 19. Selected hardware

8.3 Final 3D model

Finally, everything necessary to assemble all the parts that make up the final model is available. As mentioned above, the drawings of all non-standardized elements, as well as the bill of materials, assembly drawing and exploded view will be delivered together with the memory document. On the other hand, all the program files necessary to open the final assembly including all the components will also be provided.

Figures 88, 89, 90 and 91 show respectively the front view, top view, side view and isometric view of the final 3D model of the dolly

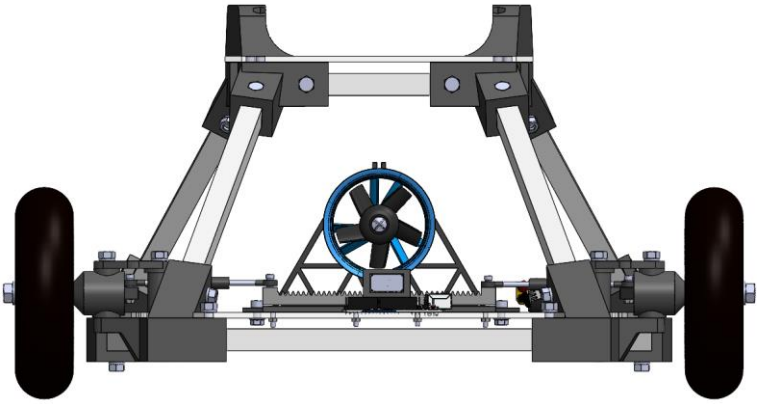

Figure 87. Dolly front view *(Source: own elaboration)*

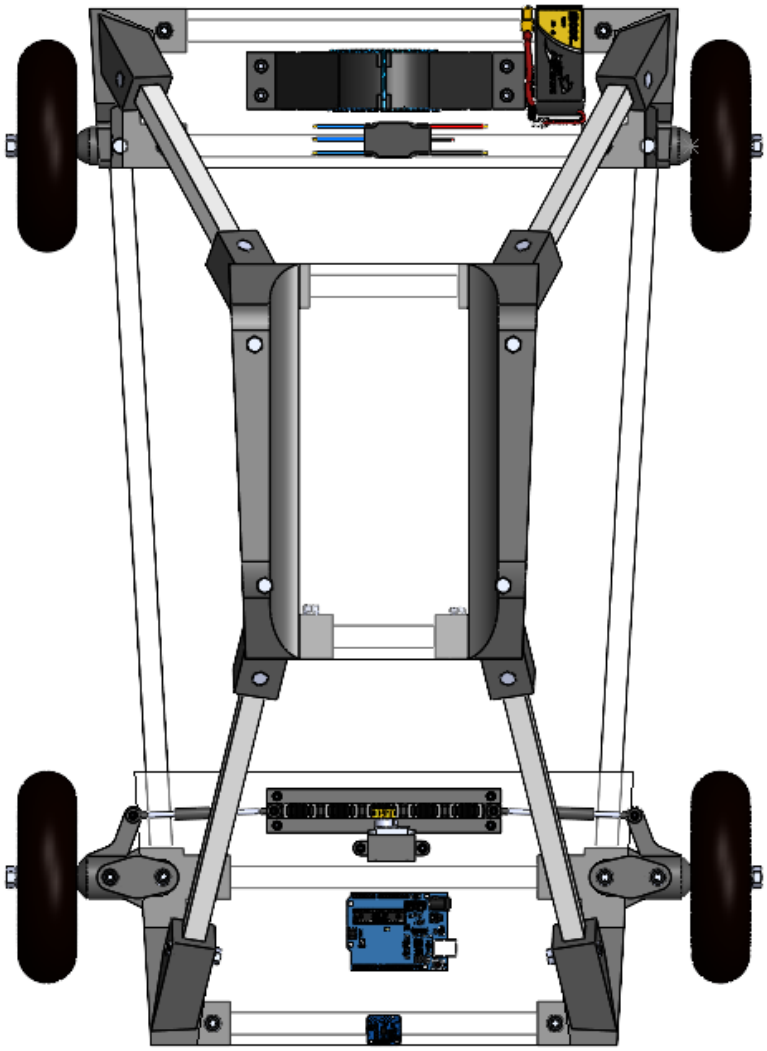

Figure 88. Dolly top view *(Source: own elaboration)*

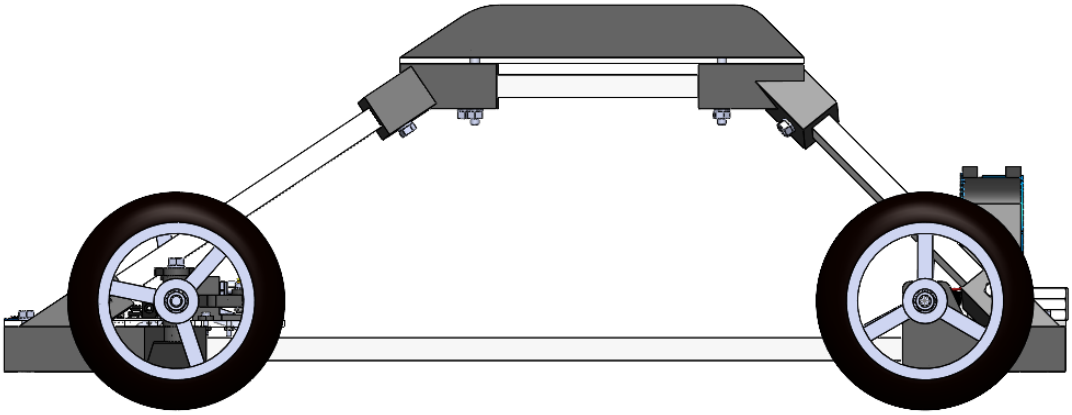

Figure 89. Dolly side view *(Source: own elaboration)*

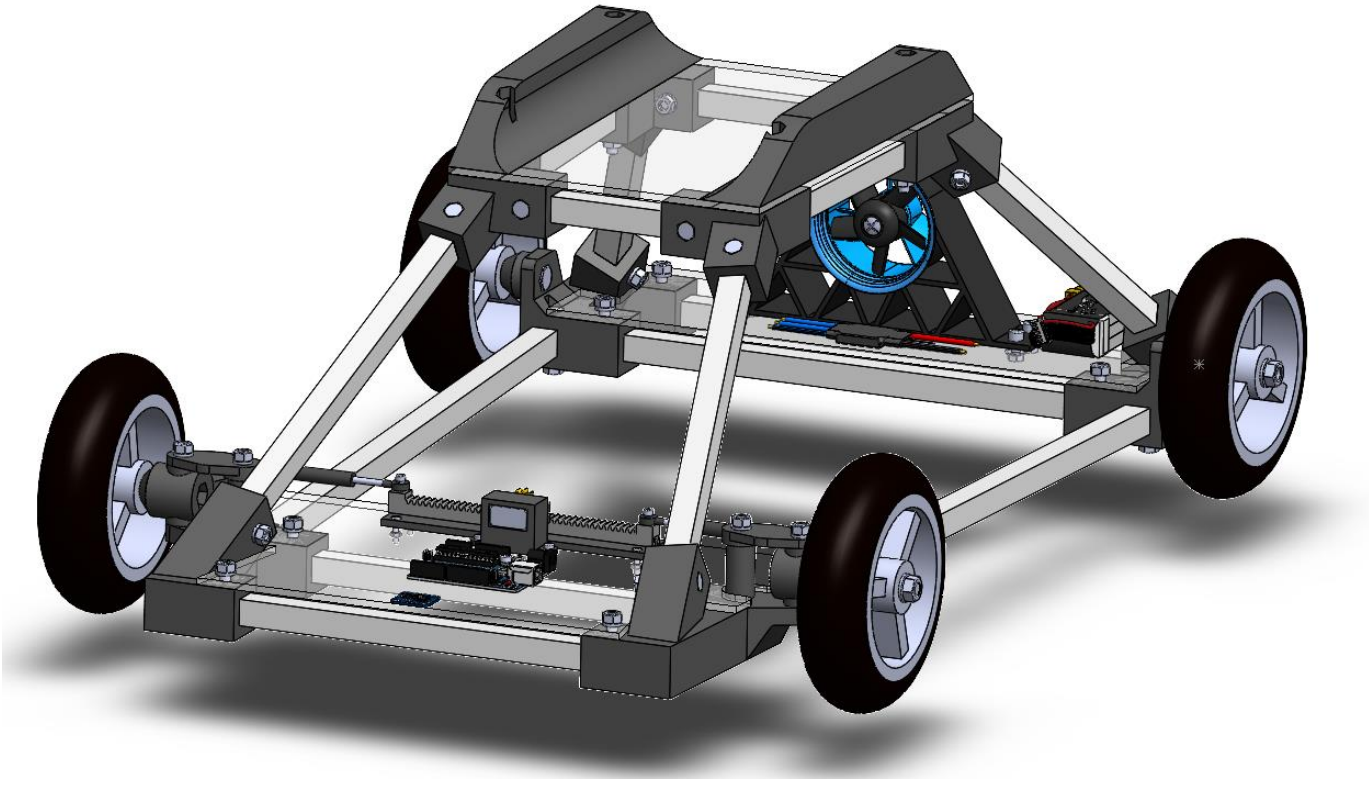

Figure 91. Dolly isometric view *(Source: own elaboration)*

As it has been seen, the previous figures show the final modeling of the dolly in SolidWorks, which includes each of the parts and systems that have been studied, designed or selected throughout this document. Including the chassis defined in chapter 4, the steering system

defined in chapter 5, the electronic components that make up the heading control system, defined in chapter 6, the propulsion system defined in chapter 7 and finally, the UAV fasteners and hardware defined in this same chapter 8. The fact of having modeled each of the parts that make up the dolly using the SolidWorks program, has allowed both studies of mass and center of gravity, as well as structural simulation studies using the finite element method. In addition, it has also allowed a quick realization of the drawings of the non-standardized elements, as well as the assembly drawing, bill of materials and exploded view. Another advantage of using this type of software is the possibility of incorporating all the elements designed and defined separately in a general assembly file, as shown in the previous figures.

Finally, Figure 92 shows the final dolly assembly incorporating the 3D modeling of the Bormatec Maja UAV that will be used in the scientific experiments conducted by the Lightning Research Group.

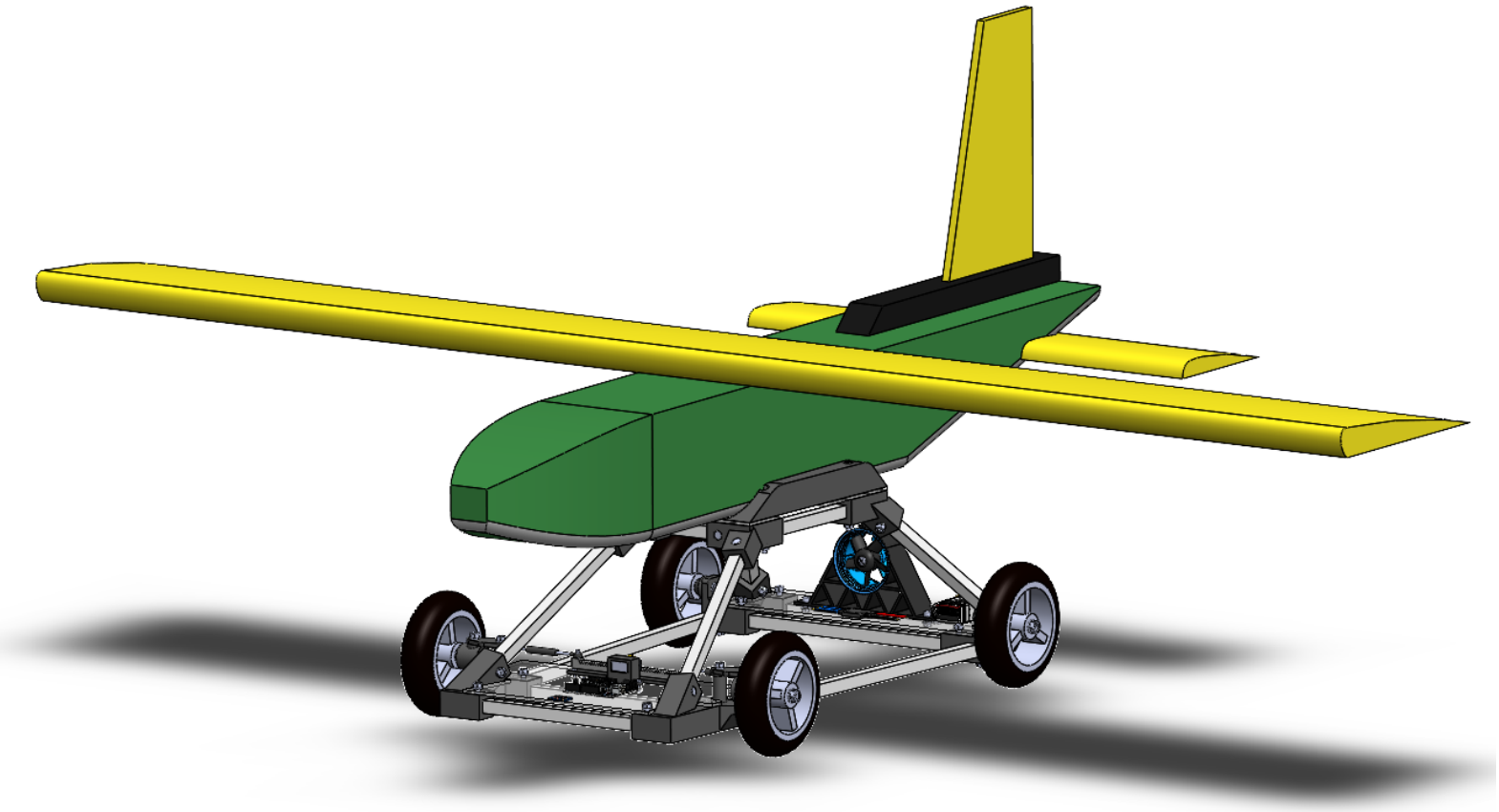

Figure 92. Dolly incorporating the UAV *(Source: own elaboration)*

8.4 Final Arduino programming code

Finally, the block diagram of the Arduino program code, resulting from joining the heading control system code with the propulsion system, will be shown. The complete programming code is attached in the annexes, but for a better understanding of each of the steps executed by the program, the block diagram shown in Figure 93 has been designed. Each of the blocks in the diagram will be described below.

First, when the program is started, the variable "stop" is assigned the value "0" and the variable "Throttle" the value "1000". In the case of the "stop" variable, it will be in charge of stopping the propulsion system when the aircraft takes off. The variable "Throttle" will be used to control the engine revolutions, being this variable between the values {1000 , 2000} with the engine stopped and the engine at maximum respectively.

In the next block, the first measurement of the orientation angle (in which North is taken as 0º) is performed and assigned to the variable "goal". Then a delay of 5 seconds is executed to give the user time to place the dolly in the desired position and grab the UAV controller. Then the ESC is initialized and the reference time is measured, which is assigned to the variable "Time" to be taken into account later.

The next block is already part of the main loop of the program, which means that from this point onwards the operations will be repeated until the system is shut down. In this case, we start measuring again the angle of orientation, which is assigned to the variable "heading". This will be the variable that will allow us to measure the difference with respect to the variable "goal" defined at the beginning. Next, the time instant in which the heading measurement was taken is measured, in order to take into account the time difference between measurements when calculating the PID.

Then the orientation and time errors are calculated with respect to the last measurements. As the system provides us with the instantaneous orientation angle of the dolly taking the magnetic North of the earth as 0º, if in the previous measurement an orientation measurement of 355º was taken and in the last measurement 2º is obtained, the program would calculate an error of 353º when the real error is 7º. To avoid this, a filter is introduced, which checks if the measured error is greater than 180º or less than -180º, which would mean that the difference between the angle on the wrong side of the 360º circumference is being measured. If this is the case, add or subtract 360º depending on whether it is positive or negative.

The next step is the calculation of the PID, using as input the time error, orientation error and the tuning parameters Kp and Ki. The PID output is added 90º, since the servo will be in its center position (with the wheels aligned) for a value of 90º.

Next, a block is included that will identify if the takeoff "stop" =0 has not yet been performed, if so, it will gradually increase the rotational speed of the motor up to a value of 1300 microseconds, which corresponds to 30% of the maximum. On the other hand, it will be checked that the time from the initialization of the BLDC engine does not exceed 10 seconds (approximate time needed to take off the aircraft). When the time exceeds ten seconds, the engine will be stopped by assigning a value of 1000 microseconds to the "throttle" variable and also assigning a value of 1 to the "stop" variable.

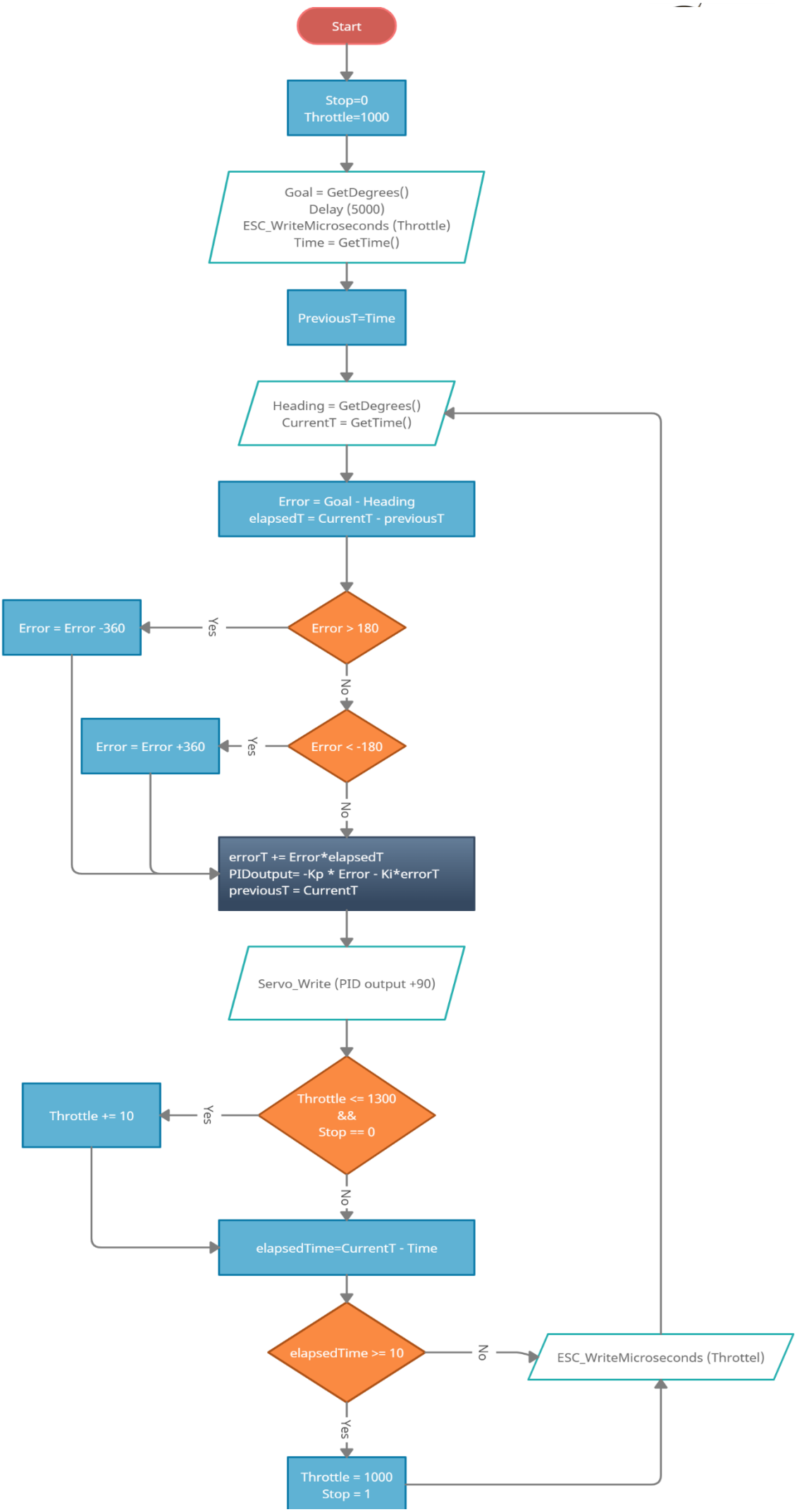
Start
Stop=0
Throttle=1000
Goal = GetDegrees()
Delay (5000)
ESC_WriteMicroseconds (Throttle)
Time = GetTime()
PreviousT=Time
Heading = GetDegrees()
CurrentT = GetTime()
Error = Goal - Heading
elapsedT = CurrentT - previousT
Error > 180
Yes
Error = Error -360
No
Error < -180
Yes
Error = Error +360
No
errorT += Error*elapsedT
PIDoutput= -Kp * Error - Ki*errorT
previousT = CurrentT
Servo_Write (PID output +90)
Throttle <= 1300
&&
Stop == 0
Yes
Throttle += 10
No
elapsedTime=CurrentT - Time
elapsedTime >= 10
No
ESC_WriteMicroseconds (Throttel)
Yes
Throttle = 1000
Stop = 1

9 Wiring of the final model

The final wiring diagram will be shown below, after implementing the two circuits corresponding to the heading control system and propulsion system.

As shown in Figure 93, the system is powered by the 3S Lipo battery previously selected. All the components are interconnected with the Arduino UNO microcontroller board that will be in charge of controlling the whole system.

First, the ESC is powered by the Lipo battery. The ESC has two main functions, on the one hand it receives the PWM signal from the microcontroller board and supplies the position commands to the motor by modifying the polarity in its coils, depending on the pulse width of the input signal. On the other hand, it transfers the 11.1V voltage from the battery to the Vin input pin of the microcontroller board, which can receive a voltage between 7 and 12v, which is then converted to the 5v with which it works.

Next, we have the connection block formed by the LSM303DLHC sensor and the microcontroller board, which will provide the position angle. The sensor will be powered on its Vin input pin from the 3.3V output pin of the Arduino board. On the other hand, the SCL and SDA pins of the sensor corresponding to the interface signal I^2 C of the serial clock and serial data respectively, are connected to pins A4 and A5 respectively, corresponding to the analog input/output pins of the Arduino.

Finally, the servo motor connection is shown. The control of which is the same as that of the ESC, by means of a PWM signal in which the position of the servomotor will depend on the pulse width of the signal sent by the Arduino UNO. When the pulse width is 1000 microseconds, the servo will be in its 0º position, while when the pulse width is 2000 microseconds the servomotor will be in its 2000 microseconds position.

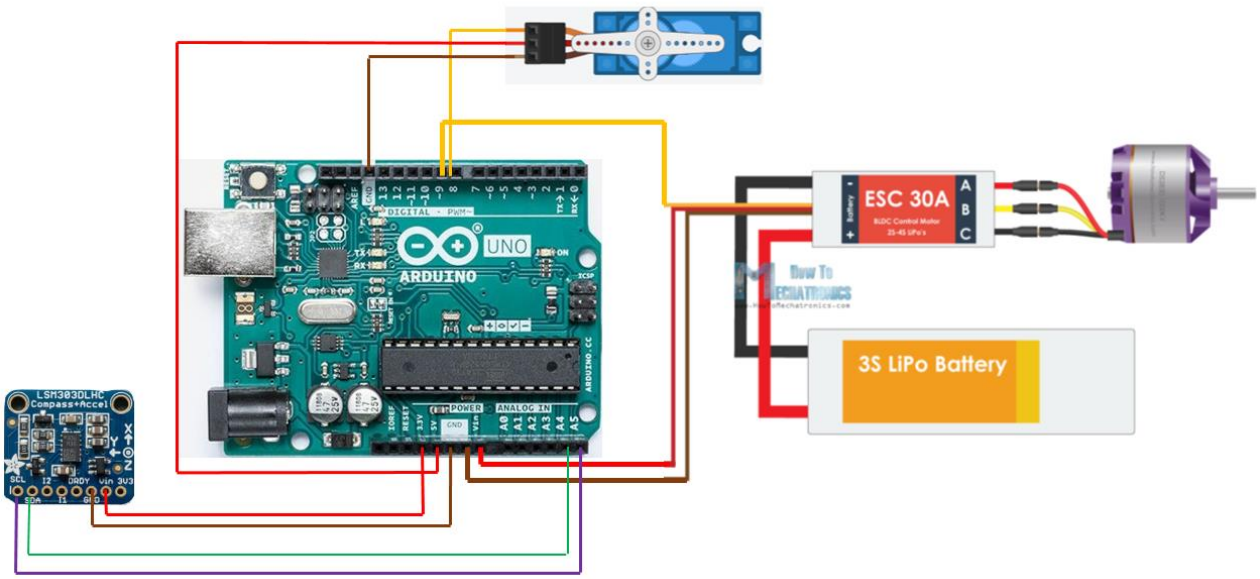

Figure 93. Wiring of the final model *(Source: own elaboration)*

10 Budget summary

For the realization of the budget of this project, the author of the project has been hired by the Lightning Research Group for the study, design and construction of a prototype to ensure the take-off of its UAV for scientific purposes. The take-off system must be based on a dolly vehicle incorporating an additional propulsion system and a heading control system. Both the budget and the overall project will be carried out by the author of the project. Even if all tasks are performed by the same person, different labor rates will be considered depending on the task to be performed. If the task is to be performed by an engineer, the labor price will be considered for that category. Likewise, if the task is to be performed by a technician, or only corresponds to hours of operation of a machine.

The entire estimate is attached to the project in a separate document. The quotation consists first of the cover page, which specifies the author's data as well as the title of the quotation, the code within the author's database and an approximate image of the final model.

The budget is then detailed by chapters. The first one refers to the cost of labor and consists of two sections. The first section a refers to the engineering hours dedicated to each of the parts of the study, design and programming process of the dolly as a whole. Therefore, the price of the hours contemplated in the first section is the same for all tasks. It should be noted that the hours contemplated in the budget do not coincide with the hours dedicated to the project, since the budget does not take into account the hours dedicated to learning the necessary knowledge to perform the different tasks. The second section refers to the hours dedicated to construction, assembly and wiring. Here the price of the hours will vary. In the first place appears the price/hour of the 3D printing of the joints due to the fact of having the machine occupied, then the price/hour of a technician who assembles the different parts of the dolly and performs the wiring and finally the price/hour of an engineer who performs the validation and commissioning.

The second chapter includes the price of the different materials used in the project, for which the technical data sheet is attached in the annexes. In this chapter the prices are completely real and coincide with the project. Next, the budget summary is shown, in which the amounts without taxes of the two previous chapters are added together. In addition, the payment conditions are shown. Then the total execution price of the estimate is shown, and finally, the terms of acceptance of the estimate. For the document to be valid, the customer must sign and stamp the last page included in the quotation.

Next, the summary of the quotation is shown where you can see the total price without tax of the quotation. Including labor and material.

BRAKEDOWN BY CHAPTER/ SUBCHAPTERS			IMPORT
CHAPTER	01	Design and construction	7.950,00€
CHAPTER	02	Material	307,15 €

Total budget:	**8.257,15 €**
(Taxes not included)	

Concept		Amount
TOTAL EXECUTION		8.257,15 €
	Accumulated:	8.257,15 €
21,00 % Taxes.		1.734,00 €
TOTAL EXECUTION (Euros):		**9.991,15 €**

The amount of the project execution is:

NINE THOUSAND NINE HUNDRED AND NINETY- ONE EUROS AND FIFTEEN CENTS

Form of Payment:

The Client agrees to pay the supplier the amount specified in the quotation, as agreed.

20% Upon acceptance of the budget.
40% Upon start design and delivery of material.
30% Upon validation of the prototype.
10% 60 days after validation.

**The detailed Budget is included on the annex*

11 Construction process

This section will describe the manufacturing process of the designed dolly prototype. After the 3D modeling of the different components that make up the dolly, as well as the selection of the standardized elements, the creation of the drawings (included in the annexes) and the selection of the hardware, the construction of the dolly can be carried out.

The construction process will be divided into the following parts: manufacture of the 3D printed parts, manufacture of the square aluminum tube that forms the chassis, the methacrylate bases that will form the base on which the different components will rest, assembly of components and wiring.

11.1 Printed 3D parts

First, the fabrication of the 3D printed parts will be discussed. For this purpose, as discussed above, the Flashforge Creator 3 3D printer, provided by LRG, will be used. The technical data sheet of the printer is attached in the annexes.

For the manufacture of the 3D parts, we will start from a file with extension (.stl) referring to each of the 3D modeled parts to be printed. This type of file refers to a mesh of points of a solid. This file will be loaded in the specific software of the printer to be used, in the case of the project, in the "Flashprint" software, shown in figure 94, specifically designed for Flashforge printers.

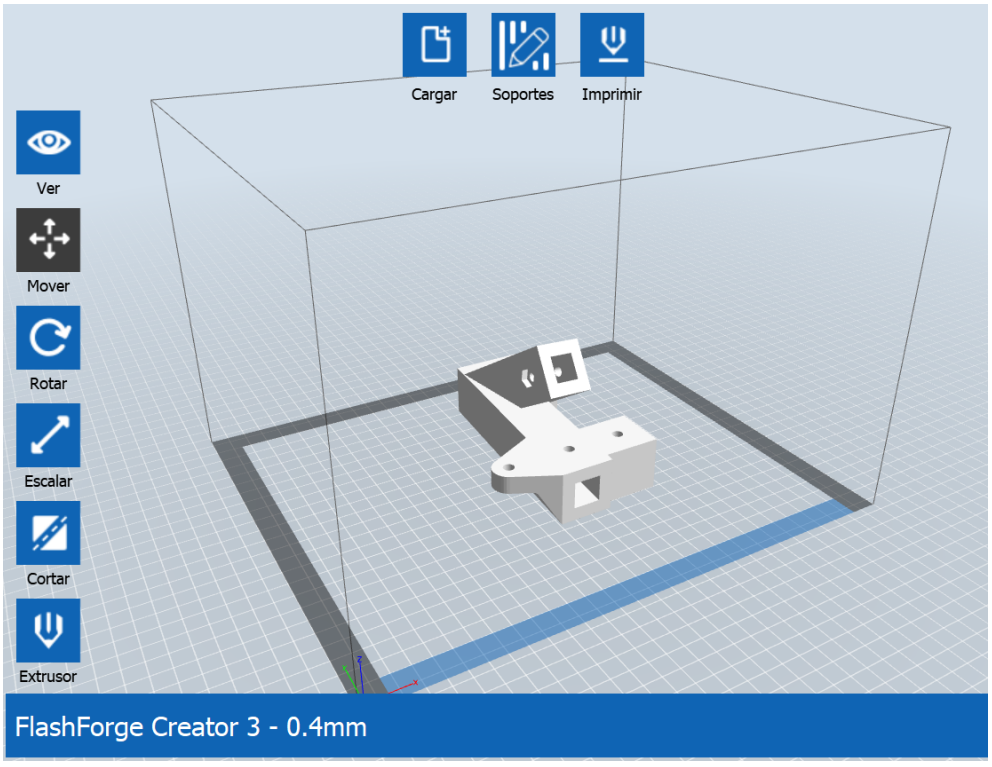

Figure 94. Flashprint interface. *(Source: own elaboration)*

The software will allow us, first of all, to make the pertinent adjustments in order to define all the parameters related to the printing to be performed. Such as the type and density of filler, extrusion and base temperature, type of supports, etc. Although all these parameters have already been defined for the case of the project, it should be noted that they may vary depending on the printer used and therefore, the ones mentioned in the document should not be taken as a reference. The second main function of the program will be to convert the mesh into a specific program file for each printer model, which includes the detailed movements to be performed by the printer. This will be the file that we will introduce in the printer to obtain our part. Having the specific file for the printing of the part and the filament ready in the printer, we will only have to press the print button to obtain the part.

The piece obtained as a result of printing usually contains small imperfections such as filaments from the supports or the base that must be removed. After having carefully cleaned and sanded the part (if necessary) it will be ready to be incorporated into the dolly. Figures 95 and 96 show the final result of one of the 3D printed joints after polishing.

Figure 95. 3D printed joint: example 1. *(Source: own elaboration)*

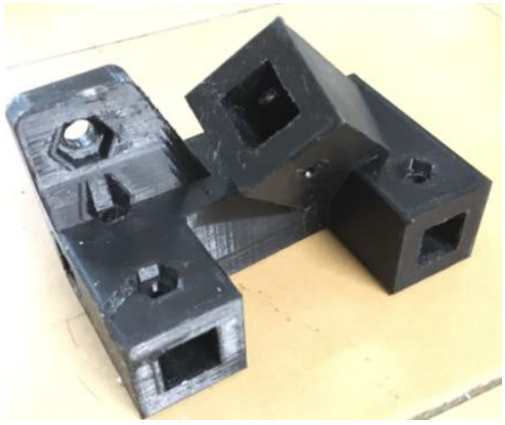

Figure 96. 3D printed joint: example 2. *(Source: own elaboration)*

In the case of the 3D printed parts, although the 2D drawings are attached, they will only be used to verify the internal tolerances in the slots where the aluminum bars are fitted. To ensure the fit between both parts, since the aluminum bars are delimited by the supplier, the tolerances will have a greater consideration in the 3D printed parts since they are manufactured in-house.

11.2 Aluminum bars

As for the aluminum bars that will form the structure of the chassis, as mentioned above, we will start with square 6063 T6 aluminum bars of 15mm x 15mm x 1.5mm.

In this case, they will only have to be cut to the desired size using a saw or grinder and then drill the holes with a drill. These two operations should be carried out on the basis of the drawings attached to the project, which detail the measurements and tolerances, as well as surface qualities for each of them.

In the case of tolerances and surface qualities, they will not be considered in the bars, since the external thickness will be delimited by the manufacturer and the user will only have to cut and drill them.

11.3 PMMA bases

Next, we will detail the fabrication of the bases that will support the electrical components, as well as the steering system in even the UAV itself. This can be done in two ways. The first and more effective way is to start from the CAD modeling of the bases to get a file (.dxf) or surface file, which can be introduced directly to a laser cutting machine that will ensure the perfect definition of the part. This method is better and more practical than the one detailed below, but also more expensive.

Another possible method is to start from the enclosed drawings detailing the measurements of the parts and with the help of a cardboard template as shown in Figure 97, cut the methacrylate sheet with a saw to obtain the desired shape.

Figure 97. PMMA bases fabrication. *(Source: own elaboration)*

In the case of the project, since it is a prototype, the second option has been chosen because it is more economical and the exact shape of the methacrylate bases is not essential for the correct functioning of the dolly.

11.4 Assembly

Next, the assembly of all the components will be carried out using the screws previously selected and detailed in the annexes.

To do this, we will start by joining the aluminum bars with the 3D printed joints, taking care not to damage the joints, and finally securing the system with the hardware. Then the other components will be added, as well as the wheels, the steering system, the propulsion system, the electrical components, etc. Finally the wiring of the control system including the microcontroller board, the battery, the ESC, the BLDC and the servomotor will be done.

Finally, the result obtained for the first tests with the prototype is shown in the following figures, which show the final model completely defined as described throughout the project. The only modifications that remain to be made to the model shown in the figures, after the first tests with the airplane, is to solder the wires to the terminals, since at the beginning they have only been considered in case modifications have to be made after analyzing the results of the first tests.

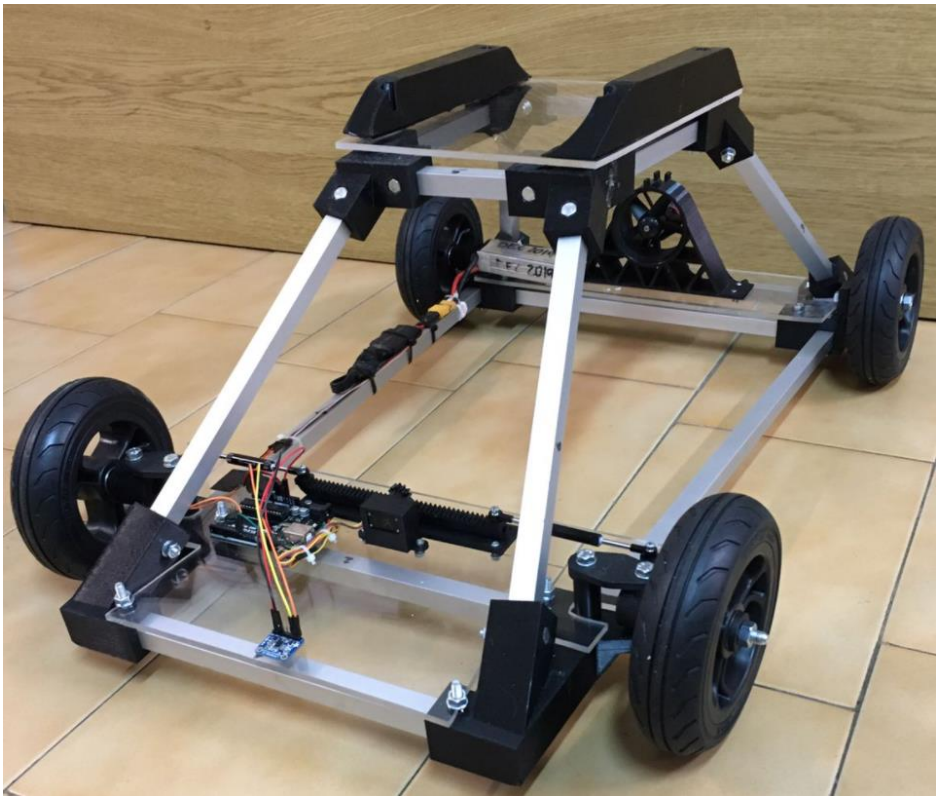

Figure 98. Dolly view 1. *(Source: own elaboration)*

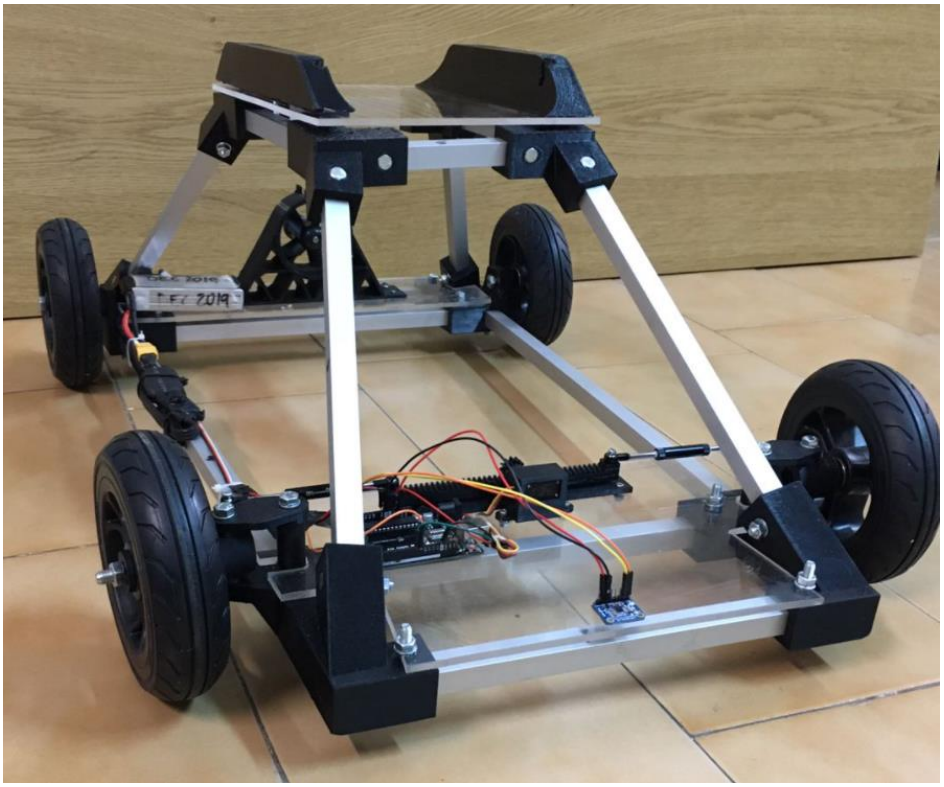

Figure 99. Dolly view 2. *(Source: own elaboration)*

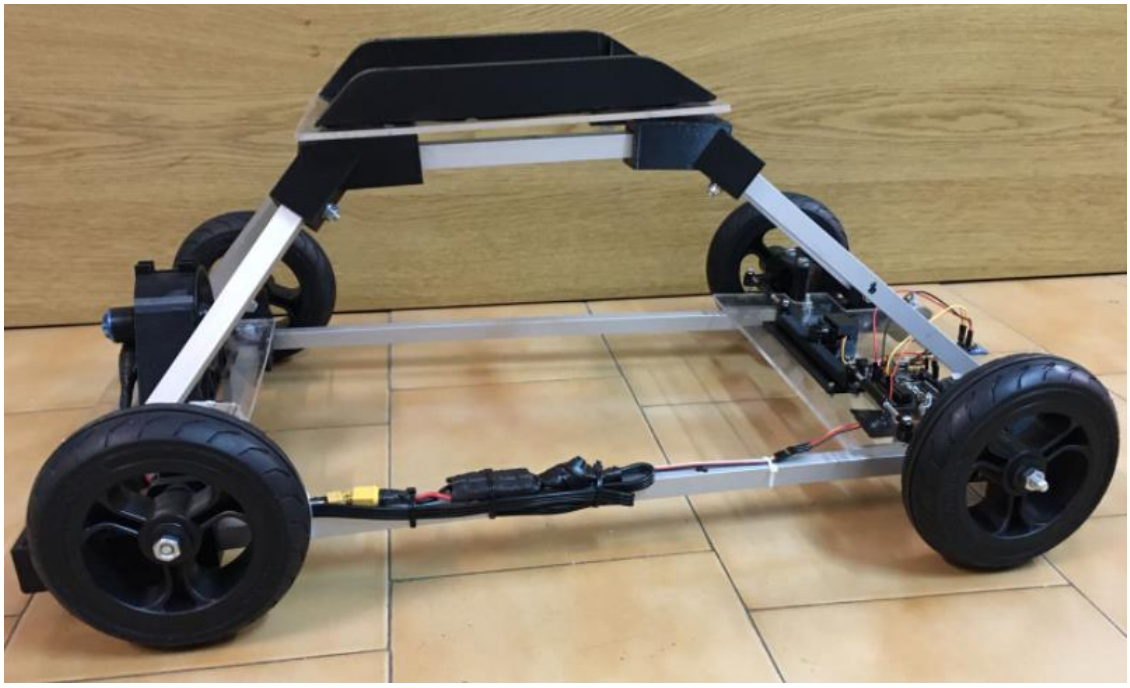

Figure 100. Dolly view 3. *(Source: own elaboration)*

Figure 101. Dolly view 4. *(Source: own elaboration)*

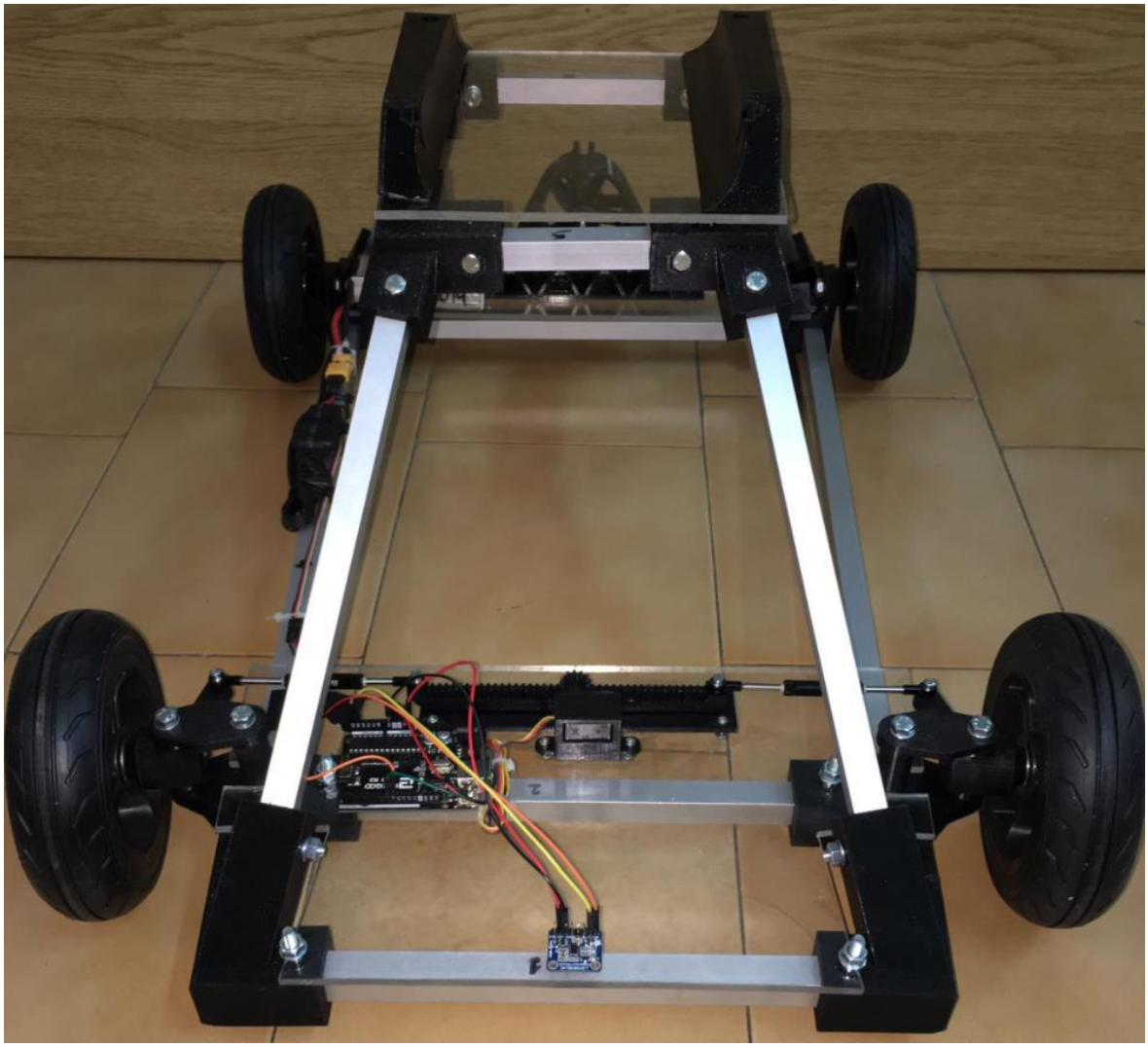

Figure 102. Dolly view 5. *(Source: own elaboration)*

From the previous figures showing the final design of the dolly in the absence of soldering the electrical terminals, it should be noted that all the elements included are those studied throughout the project. Even so, one aspect that should be emphasized is the position of both the battery and the BLDC motor and ESC, which have been placed as far as possible from the LSM303DLHC sensor so that the magnetic fields produced by these do not influence the accuracy of the dolly's orientation reading.

The electrical components such as the Arduino board and the orientation sensor have been attached with a special glue to the methacrylate base to prevent their movement during acceleration.

12 Analysis and assessment of environmental and social implications

As for the social and environmental implications, although the project has been carried out with the objective of solving an initial problem that does not directly involve either of the two, the environmental and social impact of the project has been considered at all times.

12.1 Environmental implications

As for the consideration of the environmental impact, it has been observed, for example, when choosing the materials, since their recyclability has been considered a determining factor in all cases. Finally, aluminum and PETG were selected as the materials that make up the chassis and the different parts included in the Dolly.

Regarding the aluminum, it is "lightweight, durable and infinitely recyclable, value-added aluminum products can lower energy costs and carbon emissions in dozens of applications. The Department of Energy's Oak Ridge National Laboratory found that an aluminum-intensive vehicle can achieve up to a 32 percent reduction in total life cycle energy consumption. From light-weighting to recycling, the aluminum industry is a solution to the world's energy needs." - *(The Aluminum Advantage | The Aluminum Association, n.d.)*

Regarding the PETG, it is a plastic made from 100% natural elements and 100% recyclable. It doesn't incorporate any toxic element and it's very strong and durable. These are the reasons which made PETG the most used printing filament in the medical ambit. Specially for human prosthesis.

As for the manufacturing process of the parts using the 3D printer, it can be said that on a small scale, as in the case of this project in which only one prototype is developed, it is much more efficient both economically and energetically than conventional production systems such as plastic injection, in which only the design and construction of a mold for one of the parts would involve much more energy expenditure than that required for all the parts using a 3D printer.

12.2 Social implications

As for the social implications, although the project is not specifically focused to this end, it has been contemplated the possibility of uploading to the internet all the program files needed for 3D printing of the different parts, as well as the program code used in the Arduino microcontroller board, so that anyone with a 3D printer and a microcontroller board could build an exact replica of the dolly model that has been designed throughout the project. Since many UAV models are sold on the market without landing gear, the provision of a dolly like the one designed would make it easier for the entire aeromodelling community to get their models off the ground. In addition to boosting craftsmanship and decentralizing production.

13 Conclusions

As conclusions of the project, it can be stated that the task has been more complicated than initially planned due to the large number of studies, selection of components and programs used, which have required a previous acquisition of knowledge before being able to put them into practice in the concrete application of the project. The lack of information about vehicles similar to the one proposed in the work, has also been a drawback in many phases of the project. On the other hand both the design and the construction of the dolly has also been longer than expected due to the lack of experience especially in Arduino programming and 3D printing of parts, which have been the two most laborious tasks for the author, who was completely unfamiliar with this field of knowledge and had no previous experience in similar projects. On the other hand, the lack of previous experience and the initial unfamiliarity with the procedures followed, has led to the learning of a lot of new knowledge that can be used in the future. This includes both programming and general handling of the Arduino platform with its Arduino UNO software, 3D printing of parts from modeling to the selection of printing parameters, as well as the corrections of each material due to thermal expansion and contraction. But it is not only technical knowledge acquired in this project but also much has been learned in relation to the drafting of engineering projects, as well as the correct structuring and presentation of all documents that make up the project in its entirety, such as memory, drawings, annexes, budget, etc..

As for the objectives set at the beginning of the document, practically all of them have been fulfilled throughout the project, since the construction of a dolly capable of taking off a fixed-wing UAV without landing gear while maintaining a fixed direction has been achieved, providing additional acceleration to the whole. All this while documenting the process of study, design or selection followed in each of the components and systems. Finally, the project has also been carried out considering the easy and fast reproduction of the project by anyone with a 3D printer and an Arduino microcontroller board using the program files included in the project. The only objective that could not be fulfilled mainly due to lack of time, was the incorporation of a braking system to stop the dolly once the plane has taken off. Although, as in the case of the Lightning Research Group, they have a runway, the braking system is not decisive, since the dolly has no possibility of impacting anything. Thus, the application of the braking system will be left for future development lines.

In summary, the project has served for the acquisition of a large amount of technical knowledge from different fields and has served as a simulation of a real engineering project of those that may be presented tomorrow. It is considered to have been a didactic and enriching activity since the way of acquiring knowledge has been different from that offered by the subjects of the degree.

14 Potential improvements

Finally, this last chapter will show those possible modifications of the final dolly model presented above, which, mainly due to lack of time or resources, could not be carried out.

14.1 Breaking system

Firstly, in order to meet the requirements of the project initially proposed, a braking system would be developed to stop the dolly once the UAV has taken off. Although, as mentioned above, due to lack of time and the fact that the LRG will use the dolly on a runway where there is no possibility of collision, the braking system has been omitted, in case of having more time, it would be considered as follows:

Since the wheels used in the dolly are actually designed for use on an electric scooter, advantage would be taken of their compatibility with the disc brakes carried by the scooters themselves, for incorporation into the dolly. As shown in Figure 103, these components can be easily purchased very cheaply, for a price starting at about 15 €.

Figure 103. Electric Scooter Disc Break *(Source:* (*Kit de Frenos de Disco Para Patinete Eléctrico, Almohadillas de Freno Para Hacer El Disco|Piezas y Accesorios de Scooter| - AliExpress*, n.d.))

For its application, the two rear wheels can be joined by an axle and work with a single brake disc or place a brake disc on each of the rear wheels. The brake caliper would be activated by a cable which would be driven by a servomotor. The programming code of the Arduino UNO should be adjusted so that after the set time (necessary for the takeoff of the plane), not only the BLDC motor would stop but also a servomotor would actuate the brake caliper by means of a cable and thus completely stop the dolly in a few meters.

Figure 104 shows a simplified sketch of the first of the proposals for a possible improvement and incorporation of the braking system. This proposal shows the connection of the rear wheels of the dolly by means of an axle and the arrangement of a single brake caliper that will act on both wheels equally. It will be operated by a servomotor, which will be programmed with Arduino so that at the desired moment it turns counterclockwise (as

shown in the figure), tightening the cable and applying the brake to stop the dolly in a few meters.

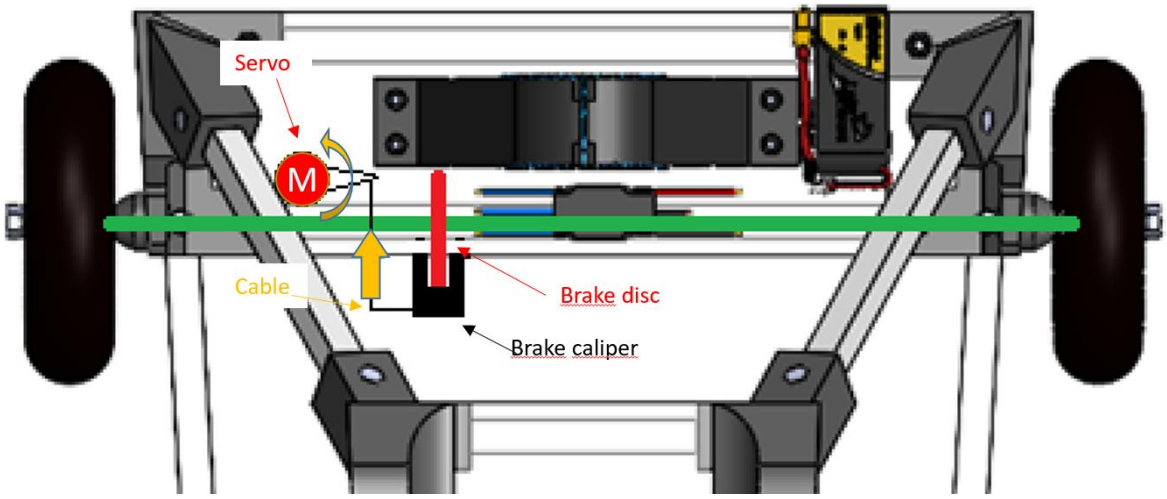

Figure 104. Breaking System *(Source: own elaboration)*

14.2 UAV automatic support

Another of the possible improvements proposed for the project is the adaptation of the supports that support the UAV.

In the selection process of the UAV support system, two possibilities were evaluated, the first one consisted of holding the aircraft with a lever, by the wings, during the acceleration process of the whole, but it was discarded due to the fact that at the moment when the aircraft had enough speed to take off, the fixed support that joined the wings of the aircraft with the dolly was a hindrance. The good part of this system, which was discarded compared to the one proposed and subsequently selected, is that since the UAV is attached to the wings, the rotational speed of the BLDC engine can be increased, thus providing greater acceleration to the whole and achieving a shorter takeoff time. With the system that was chosen, based on the friction between the upper base of the dolly and the lower base of the aircraft, the rotational speed assigned to the engine is only 30% of its capacity. Therefore, the possible improvement with the wing attachment system would be noticeable in terms of dolly acceleration. However, it was discarded because of the problem that arises when the aircraft reaches the necessary speed to take off.

In order to apply this system and benefit from its advantages in terms of dolly acceleration, it is necessary to solve the problem related to the obstacle that the supports represent for the airplane at the moment of take-off. The proposed solution involves the incorporation of a mobile lever instead of a fixed one, which is hinged in the center and, by means of the action of a servomotor to which it would be coupled, can rotate to clear the way for the UAV when it has the necessary speed to take off.

Figure 105 shows a sketch of the proposed solution considering the dolly model shown in Figure 5, corresponding to one of the existing dolly models.

Figure 105. UAV Automatic Support *(Source: own elaboration)*

15 References

CITADOS

¿Qué es un motor BLDC con sensor y cómo funcionan mejor? (n.d.). Retrieved June 6, 2021, from https://www.zikodrive.com/es/ufaqs/sensored-bldc-motor-brushless-motor-controlador-brushless-esc-can-i-use/

((*12) United States Patent*, 2017) . Alfredo Criado, Grzegorz M. Kawiecki, Jose L. Lemus Martin, Eduardo G. Ferreyra, Sergio Pereira Mayan. Retrieved July 16, 2021 from *https://patents.google.com/patent/US9708077*

(2)(The Car Tech). (n.d.-a). Retrieved March 3, 2021, from http://www.thecartech.com/subjects/auto_eng/Center_of_Gravity.htm

(3D printing filaments comparison). (n.d.-b). Retrieved June 19, 2021, from https://rigid.ink/pages/filament

3D printing - Wikipedia. (n.d.). Retrieved May 26, 2021, from https://en.wikipedia.org/wiki/3D_printing

Accelerometer vs Gyroscope sensor, and IMU, how to pick one? - Latest open tech from seeed studio. (n.d.). Retrieved June 2, 2021, from https://www.seeedstudio.com/blog/2019/12/24/what-is-accelerometer-gyroscope-and-how-to-pick-one/

Acero Inoxidable - AISI 304 - Catalogo en linea - Materiales en pequenas cantidades para el diseno - Goodfellow. (n.d.). Retrieved May 24, 2021, from http://www.goodfellow.com/S/Acero-Inoxidable-AISI-304.html

ACKERMAN EFFECT. (n.d.). Retrieved March 7, 2021, from www.longacreracing.com

Ackermann steering geometry - Wikipedia. (n.d.). Retrieved March 7, 2021, from https://en.wikipedia.org/wiki/Ackermann_steering_geometry

Arduino - Introduction. (n.d.). Retrieved May 20, 2021, from https://www.arduino.cc/en/guide/introduction

Arduino Brushless Motor Control Tutorial | ESC | BLDC - HowToMechatronics. (n.d.). Retrieved June 19, 2021, from https://howtomechatronics.com/tutorials/arduino/arduino-brushless-motor-control-tutorial-esc-bldc/

Arduino Uno Rev3 | Arduino Official Store. (n.d.). Retrieved June 2, 2021, from https://store.arduino.cc/arduino-uno-rev3

Avión RC Motor, 64 Ducts 4500KV Motor sin Escobillas + Propeller Power Kit para hasta 1200g RC Modelo Avione: Amazon.es: Juguetes y juegos. (n.d.). Retrieved June 19, 2021, from https://www.amazon.es/4500KV-Escobillas-Propeller-Modelo-Avione/dp/B07GBY81WF/ref=asc

AXSPEED varilla de tracción para Servo, 2 uds., longitud ajustable para 1/10 RC Crawler Axial SCX10 Traxxas TRX4 D90 TF2 CC01|Partes y accesorios| - AliExpress. (n.d.). Retrieved June 19, 2021, from https://es.aliexpress.com/item/4000214668493.html?spm=a2g0s.9042311.0.0.650963c0fJvg5A

Bolted joint - Wikipedia. (n.d.). Retrieved May 26, 2021, from https://en.wikipedia.org/wiki/Bolted_joint

Bormatec | Ravensburg | Drohnen. (n.d.).

Bruno Borges. (n.d.). *Build Your Own Go Kart: Front Wheel/Steering Assembly | Homemade go kart, Go kart steering, Go kart*. Retrieved June 19, 2021, from https://www.pinterest.es/pin/319544536035342080/

Build your own race car. (2018). *Car Chassis Basics, How-To & Design Tips ~!* https://www.buildyourownracecar.com/race-car-chassis-basics-and-design/

Cálculo de engranajes: ideas esenciales en tus transmisiones mecánicas – Blog CLR. (n.d.). Retrieved April 12, 2021, from https://clr.es/blog/es/calculo-de-engranajes-transmisiones-mecanicas/

Car Chassis Basics, How-To & Design Tips ~ FREE! (n.d.). Retrieved March 3, 2021, from https://www.buildyourownracecar.com/race-car-chassis-basics-and-design/

CLASSES OF MECHANICAL JOINTS - Bearcat. (n.d.). Retrieved May 26, 2021, from https://bearcat.es/en/blog/2020/11/23/classes-of-mechanical-joints/

Decision-matrix method - Wikipedia. (n.d.). Retrieved May 22, 2021, from https://en.wikipedia.org/wiki/Decision-matrix_method

eCalc - propCalc - the most reliable Propeller Calculator on the Web. (n.d.).

eCalc - the most reliable RC Calculators on the Web for electric Motors. (n.d.). Retrieved May 21, 2021, from https://www.ecalc.ch/calcinclude/help/helicalchelp.htm

FlashForge Creator 3. (2018). *Creator 3 Desktop Professional 3D Printer*. www.flashforge.com

Goldman Sachs. (n.d.). *The Drone Market by Sector | Toptal*. Retrieved June 19, 2021, from https://www.toptal.com/finance/market-research-analysts/drone-market

How the steering system works | How a Car Works. (n.d.). Retrieved May 29, 2021, from https://www.howacarworks.com/basics/how-the-steering-system-works

How to Interface GPS Module (NEO-6m) with Arduino - Arduino Project Hub. (n.d.). Retrieved June 2, 2021, from https://create.arduino.cc/projecthub/ruchir1674/how-to-interface-gps-module-neo-6m-with-arduino-8f90ad

How to Weld Aluminum: The Beginner's Guide. (n.d.). Retrieved May 26, 2021, from https://www.uti.edu/blog/welding/aluminum-welding

Kit de frenos de disco para patinete eléctrico, almohadillas de freno para hacer el disco|Piezas y accesorios de scooter| - AliExpress. (n.d.). Retrieved June 19, 2021, from https://es.aliexpress.com/item/1005001926333311.html

Librerías Arduino | Aprendiendo Arduino. (n.d.). Retrieved June 3, 2021, from https://aprendiendoarduino.wordpress.com/2016/11/16/librerias-arduino-2/

Matt Robisnon. (n.d.). *What Actually Is Rack And Pinion Steering?* Retrieved June 19, 2021, from https://www.carthrottle.com/post/what-actually-is-rack-and-pinion-steering/

MG90S Micro Servo Motor Datasheet, Wiring Diagram & Features. (n.d.). Retrieved May 31, 2021, from https://components101.com/motors/mg90s-metal-gear-servo-motor

MG90S servo, Metal gear with one bearing. (n.d.).

North American International Auto Show (NAIAS). (n.d.). *The Car Tech*. Retrieved June 19, 2021, from http://www.thecartech.com/

One Air Company. (n.d.). *One Air Aviación E-ATO 190 | Escuela de Pilotos Autorizada AESA | EASA*. Retrieved June 19, 2021, from https://www.oneair.es/

Qué es Arduino, cómo funciona y qué puedes hacer con uno. (n.d.). Retrieved June 1, 2021, from https://www.xataka.com/basics/que-arduino-como-funciona-que-puedes-hacer-uno

Rack and pinion system with power steering | MOOG. (n.d.). Retrieved May 29, 2021, from https://www.moogparts.eu/blog/rack-and-pinion-system-with-power-steering.html

Rangam Kartik. (2020, October 24). *Types Of Car Chassis Explained | From Ladder To Monocoque!* https://gomechanic.in/blog/types-of-car-chassis/

RC Glider Sailplane Airplane Models TAKEOFF DOLLY 6" Wheels - NEW | eBay. (n.d.). Retrieved June 19, 2021, from https://www.ebay.com/itm/164233999539

Rellenos en impresión 3D. Definen estructura, resistencia y peso. (n.d.). Retrieved May 28, 2021, from https://3dwork.io/rellenos-en-impresion-3d/

Rivet - Wikipedia. (n.d.). Retrieved May 26, 2021, from https://en.wikipedia.org/wiki/Rivet

Starffin Peter. (2019, January 26). *Rellenos en impresión 3D. Definen estructura, resistencia y peso.* 3D Printing Infill Patterns. https://3dwork.io/rellenos-en-impresion-3d/

Tattu Batería LiPo 2300mAh 14.8V 45C 4S para Multicopteros FPV Racing Helicópteros Barcos y Modelos RC Diversos: Amazon.es: Electrónica. (n.d.). Retrieved June 19, 2021, from https://www.amazon.es/Tattu-Batería-Multicopteros-Helicópteros-diversos/dp/B017GRB73S/ref=asc

The Aluminum Advantage | The Aluminum Association. (n.d.). Retrieved June 14, 2021, from https://www.aluminum.org/aluminum-advantage

This is information on a product in full production. LSM303DLHC Ultra-compact high-performance eCompass module: 3D accelerometer and 3D magnetometer Datasheet-production data Features. (2013). www.st.com

Top Model Sailplane Take-off Dolly 1. (n.d.). Retrieved May 18, 2021, from https://alofthobbies.com/top-model-sailplane-take-off-dolly-1.html

Turbofan - Wikipedia. (n.d.). Retrieved June 7, 2021, from https://en.wikipedia.org/wiki/Turbofan

Types of 3D Printers: Complete Guide - SLA, DLP, FDM, SLS, SLM, EBM, LOM, BJ, MJ Printing. (n.d.). Retrieved May 26, 2021, from https://3dinsider.com/3d-printer-types/

Types Of Car Chassis Explained | From Ladder To Monocoque! (n.d.).

US9708077B2 - UAV take-off method and apparatus - Google Patents. (n.d.). Retrieved June 19, 2021, from https://patents.google.com/patent/US9708077

What are Brushless DC Motors | Renesas. (n.d.). Retrieved June 19, 2021, from https://www.renesas.com/us/en/support/engineer-school/brushless-dc-motor-01-overview

What is a Raspberry Pi? (n.d.). Retrieved June 1, 2021, from https://www.raspberrypi.org/help/what- is-a-raspberry-pi/

What Is a Stall Speed and How Does It Affect Airplanes? – Monroe Aerospace News. (n.d.). Retrieved May 21, 2021, from https://monroeaerospace.com/blog/what-is-a-stall-speed-and-how-does-it-affect-airplanes/

What is PLC ? Programmable Logic Controller - Unitronics. (n.d.). Retrieved June 1, 2021, from https://www.unitronicsplc.com/what-is-plc-programmable-logic-controller/

Wheelbase: How Important Is It In Designing The Vehicle? - CarBikeTech. (n.d.). Retrieved May 24, 2021, from https://carbiketech.com/wheelbase/

Wire - ArduWiki. (n.d.). Retrieved June 3, 2021, from https://arduwiki.perut.org/wiki/Wire